

EFFECT OF CROSSLINKING ON ORGANIC SOLVENT NANOFILTRATION
PERFORMANCE OF CELLULOSE MEMBRANES

A THESIS SUBMITTED TO
THE GRADUATE SCHOOL OF NATURE AND APPLIED SCIENCES
OF
MIDDLE EAST TECHNICAL UNIVERSITY

BY
KÜBRA KONCA

IN PARTIAL FULFILLMENT OF THE REQUIREMENTS
FOR
THE DEGREE OF MASTER OF SCIENCE
IN
CHEMICAL ENGINEERING

November 2018

Approval of the thesis:

EFFECT OF CROSSLINKING ON ORGANIC SOLVENT NANOFILTRATION
PERFORMANCE OF CELLULOSE MEMBRANES

submitted by **KÜBRA KONCA** in partial fulfillment of the requirements for the degree of **Master of Science in Chemical Engineering Department, Middle East Technical University** by,

Prof. Dr. Halil Kalıpçılar
Dean, Graduate School of **Natural and Applied Sciences**

Prof. Dr. Pınar Çalık
Head of Department, **Chemical Engineering**

Assoc. Prof. Dr. Zeynep Çulfaz Emecen
Supervisor, **Chemical Engineering Dept.,**

Examining Committee Members:

Prof. Dr. Levent Yılmaz
Chemical Engineering Dept., METU

Assoc. Prof. Dr. Zeynep Çulfaz Emecen
Chemical Engineering Dept., METU

Prof. Dr. Halil Kalıpçılar
Chemical Engineering Dept., METU

Assoc. Prof. Dr. Erhan Bat
Chemical Engineering Dept., METU

Assoc. Prof. Dr. Berna Topuz
Chemical Engineering Dept., Ankara University

Date: 19.11.2018

I hereby declare that all information in this document has been obtained and presented in accordance with academic rules and ethical conduct. I also declare that, as required by these rules and conduct, I have fully cited and referenced all material and results that are not original to this work.

Name, Last name: Kübra Konca

Signature:

ABSTRACT

EFFECT OF CROSSLINKING ON ORGANIC SOLVENT NANOFILTRATION PERFORMANCE OF CELLULOSE MEMBRANES

Konca, Kübra

M.S., Department of Chemical Engineering

Supervisor: Assoc. Prof. Dr. Zeynep Çulfaz Emecen

November 2018, 89 pages

Nanofiltration is a membrane process capable of separation of small molecules and multivalent ions due to their size and/or charge. NF is mainly used in aqueous applications. However, there are many processes that can take advantages of NF in molecules separation dissolved in organic solvents. Main challenge in Organic Solvent Nanofiltration is the limited number of membranes which can withstand a wide range solvents and have stable, predictable separation performance.

Cellulose is an alternative polymer that can be used in OSN membranes as it is stable in many organic solvents due to its inter- and intra- molecular hydrogen bonds. Cellulose membranes were fabricated via phase inversion. Solutes used in tests are Bromothymol Blue (neutral, 624 Da, $\tilde{V}_m=251.1\text{cm}^3/\text{mole}$), Cresol Red (neutral, 382 Da, $\tilde{V}_m=140.1\text{cm}^3/\text{mole}$), Rose Bengal (anionic, 1017 Da, $\tilde{V}_m=241.0\text{cm}^3/\text{mole}$) and Brilliant Blue R (anionic, 826 Da, $\tilde{V}_m=421.3\text{cm}^3/\text{mole}$) and Crystal Violet (cationic, 407 Da, $\tilde{V}_m=253.7\text{cm}^3/\text{mole}$). Membranes were crosslinked using two crosslinking agents: glutaraldehyde and 1,2,3,4-butanetetracarboxylic acid. Cellulose membranes was tested with five different solutes.

Molecular size is a determining factor for separation of neutral dyes since BTB rejection is higher ratio than CR. BTB and CV rejections are quite close to each other while RB is retained much less than these dyes although molecular size of them are similar. GA-crosslinking did not change solvent permeance and solute rejection. After BTCA-crosslinking, CV rejection decreases slightly while RB rejection increases significantly. Amount of sorbed RB during filtration decreases significantly whereas sorbed CV increases, which may explain increased RB rejection, decreased CV rejection.

Keywords: Organic solvent nanofiltration, membrane, cellulose, crosslinking

ÖZ

SELÜLOZ MEMBRANLARIN ORGANİK ÇÖZÜCÜ İLE NANOFİLTASYON PERFORMANSINA ÇAPRAZ BAĞLAMANNIN ETKİSİ

Konca, Kübra

Yüksek Lisans, Kimya Mühendisliği

Tez Danışmanı: Doç.Dr. Zeynep Çulfaz Emecen

November 2018, 89 sayfa

Selüloz moleküler içi ve moleküler arası yapmış olduğu hidrojen bağları sayesinde birçok organik çözücüye karşı direnç göstermektedir. Organik Çözücü ile Nanofiltrasyon uygulamalarında kullanım için selüloz alternatif polimer olabilmektedir. OSN uygulamalarına yönelik olarak selüloz membranlar faz değişim yöntemiyle üretildi. Polimer çözücü olarak 1-etil-3-metilimidazolyum, yardımcı çözücü olarak aseton ve çözmeyen olarak su kullanıldı. Üretilen membranların performansları model moleküllerin ayırma performansı ve geçirgenliği ile nitelendirildi. Filtrasyon testlerinde nötr boya olarak Bromotimol mavisi (BTB,624 Da, $\tilde{V}_m=251.1\text{cm}^3/\text{mol}$) ,Krezol kırmızısı (CR,82 Da, $\tilde{V}_m=140.1\text{cm}^3/\text{mol}$), negatif yüklü boya olarak Bengal pembesi (RB,1017 Da, $\tilde{V}_m=241.0\text{ cm}^3/\text{mol}$), Brilyant Mavisi (BBR,826 Da, $\tilde{V}_m=421.3\text{ cm}^3/\text{mol}$), pozitif boya olarak ise Kristal viyole (CV,407 Da, $\tilde{V}_m=253.7\text{ cm}^3/\text{mol}$) kullanıldı. Membranlar ileri işlem olarak çapraz bağlamaya tabi tutuldular. 1,2,3,4-bütantetrakarboksilik asit ve Glüteraldehit olmak üzere iki çeşit çapraz bağlayıcı kullanıldı.

Moleküler boyutu Krezol kırmızısından büyük olan Bromotimol mavi çözünenin daha yüksek oranda tutulduğu görüldü. Her iki boyanın benzer moleküler yapıya sahip olması ve nötr özellikte olmasından dolayı selüloza olan yatkinliklerinin benzer olduğu, böylece nötr boyaların ayırımında moleküler boyutun belirleyici faktör olduğu söylenebilir. BTB, RB ve CV boyalarının moleküler boyutlarının benzer

olmasına rağmen, yapılan testlerde BTB ve CV benzer oranlarda tutulurken RB boyasının tutulma oranı çok düşüktür. Glüteraldehit ile çapraz bağlama sonucu membranların boyaları tutma oranları ve çözücü geçirgenlik oranlarında değişim gözlemlenmemiştir. BTCA ile çapraz bağlanan membranların RB boyasının tutma oranında artış görülür iken, CV boyasını tutma oranında azalma görüldü. Filtrasyon boyunca membrana sorblanan RB boya miktarında azalma, CV boya miktarında ise artış olmuştur. Bu sonuç artan RB tutma oranına ve azalan CV tutma oranına açıklık getirmektedir.

Anahtar Kelimeler: Organik çözücü ile nanofiltrasyon, membran, selüloz, çapraz bağlama

To My Family and Friends

ACKNOWLEDGEMENT

I would like to express my sincere gratitude to my advisor Assoc. Prof. Dr. Zeynep ulfaz Emecen for her guidance, limitless support, patience and suggestions throughout all my studies. I am very grateful to her for accepting me in her endless membrane world.

I would like to thank to every precious member of ulfaz-Emecen research group. I am very lucky for having such lab mates. I am very grateful to Begüm, Elif, Faqih, Canan, Zeynep, Hazal and Kaan for their amazing friendship and suggestions related to my study.

I would like to extend my deepest gratitude to my dear friends Konüy, Seren and Hande and of course their family for being my family in Ankara. I owe them so much.

I would like to express my deepest appreciation to my family for unconditional support throughout my life and believing me.

I would like also to thank The Scientific and Technological Council of Turkey (TUBITAK) with the grant number 115M520.

TABLE OF CONTENTS

ABSTRACT.....	v
ÖZ.....	vii
TABLE OF CONTENTS.....	xi
LIST OF TABLES.....	xiii
LIST OF FIGURES.....	xiv
LIST OF SYMBOLS.....	xviii
CHAPTERS	
1. INTRODUCTION.....	1
1.1 Nanofiltration.....	4
1.2 Membranes for Organic Solvent Nanofiltration.....	4
1.3 Separation Performance and Mechanism in Organic Solvent Nanofiltration.....	7
1.4 An alternative polymer to Organic Solvent Nanofiltration: Cellulose.....	11
1.5 Post-treatment of Cellulose Membranes.....	13
1.6 Aim of the Study.....	16
2. EXPERIMENTAL METHODS.....	17
2.1 Materials.....	17
2.2 Polymer Dope Solution Preparation.....	17
2.3 Membrane Fabrication.....	18
2.4 Membrane Crosslinking.....	19
2.4.1 Crosslinking with Glutaraldehyde.....	19
2.4.2 Crosslinking with 1,2,3,4-butanetetracarboxylic acid (BTCA).....	20
2.5 Membrane Morphology.....	22
2.6 Nanofiltration Performance Tests.....	22
2.7 Swelling Tests.....	25
2.8 Dye Sorption Tests.....	26

2.9 Fourier Transform Infrared Spectroscopy (FT-IR)	26
2.10 X-Ray Photoelectron Spectroscopy (XPS)	26
2.11 X-Ray Diffraction (XRD)	27
2.12 Mechanical Test	27
3. RESULTS AND DISCUSSION	29
3.1 Membrane Morphology.....	29
3.2 Effect of Post-treatment: Drying	30
3.3 Effect of Transmembrane Pressure	34
3.4 Effect of Solute and Solvent on membrane performance	37
3.5 Effect of Crosslinking on Membrane Performance.....	45
3.5.1 Crosslinking with Glutaraldehyde.....	46
3.5.2 Crosslinking with 1,2,3,4- butanetetracarboxylic acid.....	54
3.6 Solvent stability.....	61
3.7 Crossflow Filtration.....	62
3.8 Effect of Feed Concentration	64
3.9 The Recovery of Homogenous Catalyst.....	66
4. CONCLUSION	69
5. APPENDICES.....	81

LIST OF TABLES

TABLES

Table 1: Membrane Codes	22
Table 2: Probe molecules and their properties	24
Table 3: Resistance values of solvents	44
Table 4: Elemental analysis of KK2D and KK2G membranes based on XPS analysis	47
Table 5: Different Glutaraldehyde crosslinking conditions	49
Table 6: KK2D BTB-Ethanol filtration at different concentration	65

LIST OF FIGURES

FIGURES

Figure 1: Basics of Membrane System	1
Figure 2: Classification of Membrane Processes	2
Figure 3: Schematically drawing of ISA (left one) and TFC (right one) membrane ...	5
Figure 4: Schematic drawing of cellulose chains	13
Figure 5: Formation of cyclic anhydride	14
Figure 6: Crosslinking of cellulose chains	14
Figure 7: Schematic representation of the membrane fabrication process.....	18
Figure 8: Solvent evaporation process	18
Figure 9: Molecular structure of Cellulose	19
Figure 10: Molecular structure of Glutaraldehyde.....	19
Figure 11:(a) Reaction of Glutaraldehyde with one hydroxyl group of cellulose forming a hemiacetal, (b) with another hydroxyl group of cellulose forming an acetal.....	20
Figure 12: Molecular structure of 1,2,3,4-butanetetracarboxylic acid (BTCA).....	21
Figure 13: Crosslinking reaction between Cellulose and BTCA	21
Figure 14: Schematic drawing of dead-end filtration experimental set-up	23
Figure 15: Schematic drawing of crossflow filtration experimental set-up	23
Figure 16: SEM Images of Membrane Cross section	29
Figure 17: SEM Images of top region of membrane cross section	29
Figure 18: Membrane cross section pictures taken after filtration.....	31
Figure 19: Rejection and permeance values of KK2 membrane during the filtration of BTB-ETOH solution	32
Figure 20: Rejection and permeance values of KK2 and KK2D membrane during the filtration of BTB-ETOH solution.....	32
Figure 21: Pure ethanol flux at different trans membrane pressure	34
Figure 22: BTB Rejection by KK2 membrane and sorbed dye amount per membrane area during filtration at different TMP	35

Figure 23: Permeance values of KK2 membrane during the filtration of BTB-ETOH solution at different TMP	35
Figure 24: BTB Rejection by KK2D membrane and sorbed dye amount per membrane area during filtration at different TMP	36
Figure 25: Permeance values of KK2D membrane during the filtration of BTB-ETOH solution at different TMP	36
Figure 26: Rejection values of KK2D membrane during the filtration of different dyes-ethanol solution	38
Figure 27: Sorption coefficient of each solute in ethanol solutions.....	40
Figure 28: Membrane pictures taken before and after dye-ethanol solution (a) Before filtration (b) After Bromothymol Blue-Ethanol filtration (c) After Cresol Red-Ethanol filtration (d) After Brilliant Blue R-Ethanol filtration (e) After Rose Bengal-Ethanol filtration (f) After Crystal Violet-Ethanol filtration	40
Figure 29: Rejection and permeance values of KK2D membrane during the filtration of dye-ethanol solutions and dye-DMSO solutions	41
Figure 30: Sorbed dye amount on/in the membrane surface during the filtration of different dye-solvent solutions.....	42
Figure 31: Sorption coefficient of each solutes in both ethanol and DMSO solutions	42
Figure 32: Membrane pictures taken before and after dye-ethanol solution (a) Before filtration (b) After Bromothymol Blue-Ethanol filtration (c) After Rose Bengal-Ethanol filtration (d) After Crystal Violet-Ethanol filtration (e) After Bromothymol Blue-DMSO filtration (f) After Rose Bengal-DMSO (g) After Crystal Violet-DMSO filtration.....	43
Figure 33: C1s level spectra of KK2D membrane.....	46
Figure 34: C1s level spectra of KK2G membrane	47
Figure 35: FT-IR Spectrum of KK2D and KK2G membranes	48
Figure 36: FT-IR spectrum of crosslinked cellulose membrane at different conditions	49
Figure 37: Elastic modulus values of KK2D and KK2G membranes	50
Figure 38: Tensile strength values of KK2D and KK2G membranes	51
Figure 39: Elongation at break values of KK2D and KK2G membranes.....	51

Figure 40: Rejection and permeance values of KK2D and KK2G membrane during the filtration of dye-ethanol solutions	52
Figure 41: Sorbed dye amount on/in GA crosslinked and uncrosslinked membrane surface during the filtration of different dye-solvent solutions.....	53
Figure 42: Membrane pictures taken after dye-ethanol solution (a) KK2D-After BTB-Ethanol filtration (b) KK2G-After BTB-Ethanol filtration (c) KK2D-After RB-Ethanol filtration (d) KK2G-After RB-Ethanol filtration (e) KK2D-After CV-Ethanol filtration (f) KK2G-After CV-Ethanol	53
Figure 43: FT-IR spectrum of BTCA crosslinked cellulose membrane	54
Figure 44: Elastic modulus of KK2D and KK2B membranes	55
Figure 45: Tensile strength values of KK2D and KK2B membranes.....	55
Figure 46: Elongation at break values of KK2D and KK2B membranes	55
Figure 47: XRD pattern of crosslinked and un crosslinked membranes.....	56
Figure 48: Rejection and permeance values of BTCA-crosslinked and uncrosslinked membrane during the filtration of BTB, RB anc CV from their ethanol solutions....	57
Figure 49: Sorbed dye amount on/in BTCA crosslinked and uncrosslinked membrane surface during the filtration of different dye-solvent solutions.....	58
Figure 50: Rejection and permeance values of BTCA-crosslinked and uncrosslinked membrane during the filtration of BTB, RB anc CV from their DMSO solutions	59
Figure 51: Sorbed dye amount on/in BTCA crosslinked and uncrosslinked membrane surface during the filtration of different dye-DMSO solutions.....	60
Figure 52: Sorption coefficient of each solute in DMSO solutions	60
Figure 53: Comparison of KK2D separation performance during BTB-Ethanol filtration in dead-end and crossflow mode	62
Figure 54: Comparison of KK2D separation performance during RB-Ethanol filtration in dead-end and crossflow mode	63
Figure 55: Comparison of KK2D separation performance during CV-Ethanol filtration in dead-end and crossflow mode	63
Figure 56: KK2D separation performance during filtration of BTB-Ethanol solutions at different concentration	64
Figure 57: KK2D Jacobsen catalyst separation performance from its ethanol solution	67

Figure 58: Calibration curve for Bromothymol Blue-Ethanol solution at 423 nm	81
Figure 59: Calibration curve for Cresol Red-Ethanol solution at 432 nm	81
Figure 60: Calibration curve for Brilliant Blue R-Ethanol solution at 588 nm	82
Figure 61: Calibration curve for Rose Bengal-Ethanol solution at 560 nm.....	82
Figure 62: Calibration curve for Crystal Violet-Ethanol solution at 590 nm	83
Figure 63: Calibration curve for Bromothymol Blue-DMSO solution at 413 nm.....	84
Figure 64: Calibration curve for Crystal Violet-DMSO solution at 308.5 nm	84
Figure 65: Calibration curve for Rose Bengal-DMSO solution at 566 nm.....	85
Figure 66: Calibration curve for Jacobsen-Ethanol solution at 416 nm.....	86
Figure 67: Calibration curve for Jacobsen-DMSO solution at 415 nm	86
Figure 68: KK2B Jacobsen catalyst separation performance from its DMSO solution	89

LIST OF SYMBOLS

SYMBOLS

NF	: Nanofiltration
OSN	: Organic Solvent Nanofiltration
ISA	: Integrally Skinned Asymmetric
TFC	: Thin Film Composite
MMM	: Mixed Matrix Membranes
MWCO	: Molecular Weight Cut Off
[EMIM]OAc	: 1-Ethyl-3-methylimidazolium acetate
PWP	: Pure Water Permeance
TMP	: Transmembrane Pressure
DMSO	: Dimethyl sulfoxide
BTB	: Bromothymol Blue
CR	: Cresol Red
BBR	: Brilliant Blue R
RB	: Rose Bengal
CV	: Crystal Violet
BTCA	: 1,2,3,4-Butanetetra carboxylic acid
GA	: Glutaraldehyde
SEM	: Scanning Electron Microscope
UV	: Ultraviolet
FTIR	: Fourier Transform Infrared Spectroscopy
XPS	: X-Ray Photoelectron Spectroscopy
XRD	: X-ray Diffraction
μm	: Micrometer
nm	: Nanometer

CHAPTER I

INTRODUCTION

Separation processes are essential in the chemical and biochemical industries since it is required to concentrate and purify raw materials and products from their solutions at high purity and yield, and these processes are responsible for 40-70 % of capital and operating costs in a chemical process (1). Therefore, it is quite important to devise efficient and economic separation processes. Traditional separation processes such as distillation, extraction or crystallization are typically used for concentration, purification and fractionation of the products. These processes require a large amount of energy and the use of additional solvents. Membrane process is a feasible alternative to conventional separation processes due to its low energy and chemical consumption, low operating temperature, easy scale-up, installation and possibility of combining with existing processes (1; 2).

A membrane is capable of separating species in a mixture under a driving force. Membrane is a selective barrier that allows one species of a mixture to pass through the membrane faster while hindering transportation of other species. Components passed through the membrane are collected in permeate side while other components restricted by the membrane remain in retentate side (3).

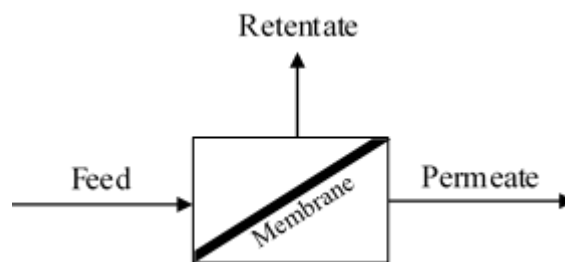


Figure 1: Basics of Membrane System

Membrane processes for separating liquid mixtures under a pressure driving force can be classified into main four group according to the membrane pore size or retained solute size: Microfiltration, Ultrafiltration, Nanofiltration and Reverse Osmosis.

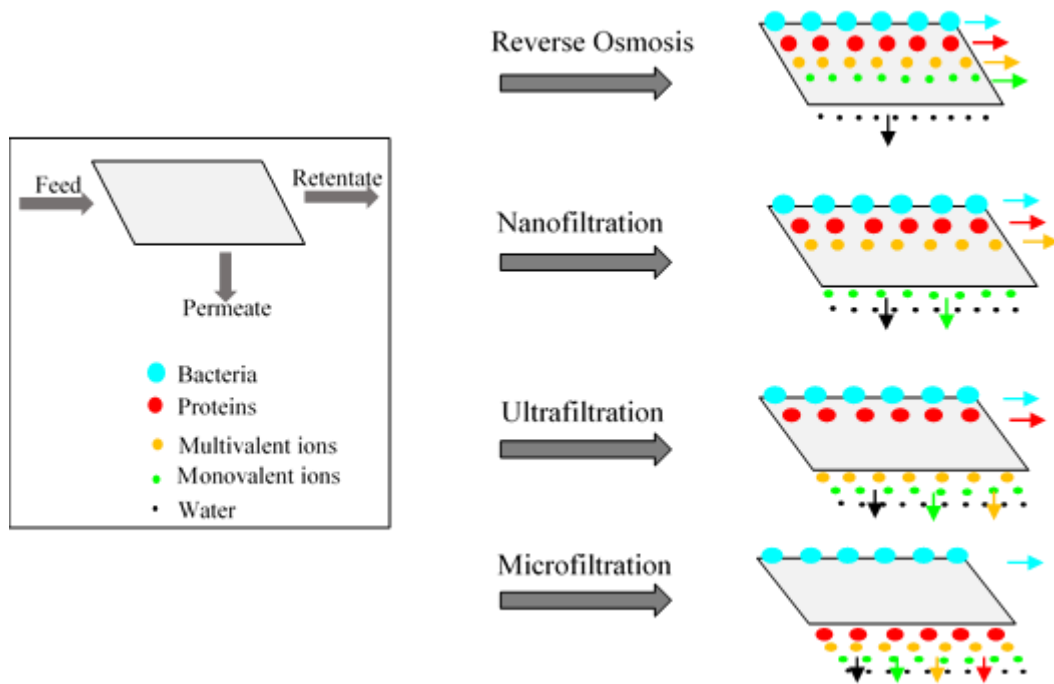


Figure 2: Classification of Membrane Processes

Microfiltration is a membrane process that can efficiently reject species with diameters above $0.1 \mu\text{m}$ such as bacteria, pigments or colloidal particles. Microfiltration membranes are classified as porous membranes and their separation mechanism is characterized by pore flow theory.

Ultrafiltration membranes are finely porous membranes that are capable of efficient separation of molecules within the range of 2-100 nm, and their separation mechanism is characterized by pore flow theory.

Reverse osmosis membranes are non-porous membranes. These membranes permeate only solvent in a mixture and are widely used in desalination process in which membranes are permeable to water but impermeable to salt. Their separation mechanism is classified as solution-diffusion mechanism.

Nanofiltration is a membrane process that can separate molecules smaller than 2 nm. These membranes can be both micro-porous membranes and non-porous membranes, and thereby their separation mechanism are characterized by both pore flow theory and solution-diffusion mechanism. Pore flow theory suggests that transport through the membrane occurs through permanent pores in the structure and this transport occurs because of pressure gradient across the membrane. According to this model, solutes whose diameter is smaller than pores diameter can pass to the permeate side while larger solutes than pores leave at the retentate side. In microporous membranes separation of solutes from feed solution occurs according to screen filtration or depth filtration. Screen filtration provides the separation of solute at the membrane surface due to the existence of pores smaller than the size of solutes at the membrane surface layer. In case of depth filtration solutes are separated from solution within the membrane by capture mechanism.

Solution-diffusion model is based on solubility of solutes in membrane material and diffusivity of solutes through the membrane due to concentration gradient. According to this model, separation is driven by solubility difference of solutes and difference in diffusion rates of solutes from high concentration region to low concentration medium, and fluxes of solute and solvent are independent of each other.

Therefore, membrane separation performance is affected by the interaction between solute, solvent and membrane as well as the size of the solute and solvent that diffuse through the membrane. Following parameters have influence on these interactions.

- sorption of solute in the membrane
- swelling of membrane in solvent, which is a measure of the affinity of the membrane to the solvent
- charges of solute and membrane resulting in repulsion or attraction between each other
- effective pore diameter and effective solute diameter in solvent

1.1 Nanofiltration

Over the years, nanofiltration membranes have been used in many aqueous applications such as treatment of groundwater (4; 5), removal of organics and pesticides from drinking waters supplies (6; 7), water softening (8; 9), cleaning of textile waste water (10) and pretreatment for desalting water process (11).

In recent years, there has been great extension of nanofiltration membranes to applications including organic solvents in their feed solutions. The first study of NF membranes in applications with organic solvents was reported as cellulose acetate membranes for hydrocarbon solvents separation (12), and Sourirajan and colleagues continued to study on the separation performance of these membranes in organic solvent mixtures for years. Later, the separation process with a membrane involving organic solvents was applied in industry by large companies such as oil companies (Exxon and Shell), chemical companies (Union Carbide) (13) and petrochemical companies (MAX-DEWAX) (14). MAX-DEWAX process used for dewaxing of lube oil is the biggest success of Organic Solvent Nanofiltration (OSN) in industrial scale and it still continues to work. OSN is also used in other applications such as concentration and purification of active pharmaceutical ingredients (15), solvent recovery and exchange (16; 17) and homogenous catalyst recovery (18; 19). Today, this interest into OSN applications in both industrial and lab scale is still growing.

1.2 Membranes for Organic Solvent Nanofiltration

The selection of membrane material is one of the most significant parameters that affects membrane performance. For OSN applications, membrane materials must be mechanically, chemically and thermally stable in the wide range of organic solvents (1). Over the years, polymers and ceramic materials have been used for the fabrication of OSN membranes. Ceramic membranes are the most robust membranes because they are usually made of aluminum, titanium or silica oxides (3), and thereby they can preserve their integrity in organic solvents and remain stable against wide range of temperature and pH. However, ceramic membranes are more brittle than polymeric membranes, and their scaling and fabrication is more difficult and expensive. Therefore, the application of ceramic membranes in OSN is less common compared to polymeric membranes (2).

Polymeric membranes are mostly used in OSN applications. There are a wide variety of polymer materials that can be used for the membrane fabrication and their processing and scaling are relatively easier compared to ceramic membranes. There are two main types of polymeric membranes. One of these types is the integrally skinned asymmetric (ISA) membrane comprising of a skin layer and porous sublayer. ISA membranes are generally formed by phase inversion technique which is the precipitation of casting solution by immersion into nonsolvent medium. Phase inversion is the most common technique for the membrane formation because it is the simplest method among other membrane fabrication techniques and it is possible to obtain a wide variety of membrane morphologies by phase inversion. Other type is thin film composite (TFC) membrane which consists of a dense selective layer on top of porous support. TFC membranes are generally fabricated by interfacial polymerization or dip coating.

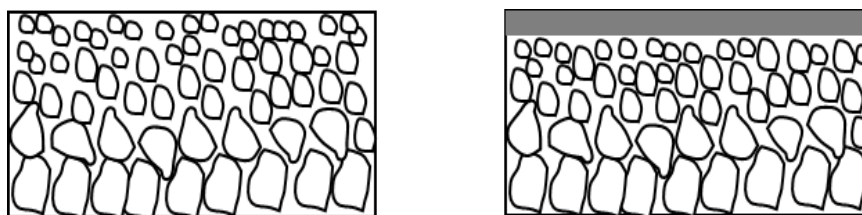


Figure 3: Schematically drawing of ISA (left one) and TFC (right one) membrane

One of the most studied polymer for OSN applications is Polyimide (PI) due to its ability to produce polymer films with good mechanical properties by interfacial polymerization or phase inversion and having thermal and chemical resistance (20). However, these membranes are not stable in some harsh organic solvents such as tetrahydrofuran, n-methyl pyrrolidone, dimethyl formamide and methylene chloride (21; 22). Several crosslinking methods can be used to enhance polymer stability. PI membrane crosslinked via chemical reactions now have resistance to toluene, methylene chloride, tetrahydrofuran, dimethyl formamide and n-methyl pyrrolidone, and good mechanical properties (21; 22). These membranes have stable permeance and good separation performances.

UV radiation is another crosslinking method. These crosslinking methods resulted in increased solvent stability in strong solvents and reorganization of polymer chains, and thereby decline in flux but small increase in selectivity (20). Crosslinked PI membranes are commercially most used membranes and most common ones are Starmem Membranes and DuraMem Membranes (1).

Polyether-ether ketone (PEEK) is another attractive polymer for organic solvent nanofiltration. PEEK polymer remains stable in harsh organic solvents under strong pH conditions and high temperatures and PEEK membrane performance can be tested in THF/DMF solutions (23; 24). Polysulfone (PSf) membrane is commonly used for the filtrations in mild organic solvents such as methanol and isopropanol, and good separation performance in these solvents has been achieved (25; 26). To further improve the membrane separation performance additives with different molecular weights were added into casting solution or PSf was blended with PI in casting solution (27; 28; 29). Polytriazole membranes crosslinked with poly(ethylene glycol) diglycidyl ether (PEGDE) (30), Poly(oxindolebiphenylene) (POXI) membranes crosslinked with di-bromides (31), Poly(ether block amide) membranes coated with Pebax and then crosslinked with Toluene diisocyanate (TDI) (32) and oxidized PASS (O-PASS) membranes (33) are recently studied membranes for separation in organic solvents.

In addition to ceramic and polymeric membranes, there is another membrane type that is produced by the combination of polymeric membrane with inorganic materials and named Mixed Matrix Membranes (MMM). Combining inorganic materials into polymeric membrane can be performed in three different ways which are dispersing the inorganic filler in the polymer solution, in-situ polymerization and the sol-gel method (34). These membranes can be ISA or TFC membranes. Recently, membranes produced using these methods for OSN applications are stable at high temperatures and have reasonable fluxes and resistance to compaction and swelling (34).

Considering literature studies and commercial applications, polymeric membranes are mostly preferred membranes for Organic Solvent Nanofiltration due to existing a wide variety of polymeric materials for the membrane fabrication and having relatively easy processing and scaling. Without any further treatment, polymeric membranes fabricated are generally unstable in harsh organic solvents and have weak mechanical, chemical and thermal resistance. To improve their stability in harsh environment and enhance their separation performances post-treatment of membrane such as chemical crosslinking, thermal annealing and UV curing is required. It is clearly seen that there is an urgent need of OSN membranes which are stable in a wide range of solvents and which have good and repeatable separation performance.

1.3 Separation Performance and Mechanism in Organic Solvent Nanofiltration

In order to predict the separation performance (solvent flux and solute rejection) of OSN membranes the transport mechanism of solute and solvent through membranes should be considered. This separation mechanism can be classified as pore flow mechanism and solution diffusion mechanism considering the membrane structure whether it is porous or dense membrane. According to pore flow mechanism, solvent passes through the membrane pores and the separation of solutes occurred based on sieving. The transport of solute and solvent through the membrane depends on some parameters such as feed viscosity, membrane pore size. On the other hand, many nanofiltration membranes have a nonporous top layer in which transport of solute and solvent occurs in only free volume elements between polymer chains based on the solution diffusion mechanism. In the investigation of transport through OSN membranes, both pore flow mechanism and solution-diffusion mechanism should be taken into consideration due to the fact that not only membrane pore size is related with the transport of solvent and solute, but also the interaction between solvent, solute and membrane also affects the separation performance of dense or microporous membranes (35).

Solutes have different charged groups due to having different functional groups in their own molecular structure and they have different molecular sizes. The separation of solutes from their aqueous solutions depends on both molecular charge and size. If the molecular size of the solute is relatively much smaller than the membrane pores, then these charged groups are the determinant factor that affects the rejection behavior of charged membranes. When the molecular size of the solute is similar with the size of membrane pores, charge effect on the separation mechanism of the membrane becomes less important, in this case sieve effect becomes determining factor in the rejection of solutes (36). It can be said that the rejection behavior of solutes in aqueous solution is much more predictable than that of solutes in organic solvents. Yang et al. observed the lower rejections of Orange II (negatively charged, 350 Da), Safranin O (positively charged, 350 Da) and Solvent Blue (neutral, 350 Da) in organic solvents than water using the same hydrophilic commercial membranes which was attributed to, considering sieve effect, the enlargement in the effective solute size due to the complexation of water molecules with solutes (37). On the other hand, the rejection of Solvent Blue, neutral and hydrophobic dye, is lower than that of Safranin O and Orange II, which are negatively charged dyes in methanol although they have the same molecular weights. Also, the negatively charged dye Orange II and positively charged dye Safranin O were retained at the almost same ratio by both negatively charged (MPF-44) and positively charged (UTC-20) membranes. This indicates that there might be different transport mechanism in organic solvents, and for a better understanding of this separation mechanism the interaction between solute, solvent and membrane should be examined.

Solute transport through the membrane is not only related with the molecular weight of the solute, nor the effective molecular size of the solute. Geens et al. (38) characterized the commercial Desal-5-K and MPF-50 membranes by four different solutes including Victoria Blue (positively charged, 458 Da), Bromothymol Blue (neutral, 624 Da), Vitamin E and Erythrosine B (neutral, 835 Da) and two different solvents like ethanol and methanol. They calculated the effective diameter of all solutes using Wilke Chang equation for the calculation of diffusion coefficient and then Stokes-Einstein equation for stokes diameter calculation, and they observed that all solute effective diameters are greater in methanol than ethanol which explains the higher rejection of these solutes in methanol than ethanol based on size exclusion

model. However, larger solute, higher rejection is not valid for all cases. The rejection of Victoria Blue both in ethanol and methanol is higher than Vitamin E although the molecular size (effective diameter) of Vitamin E is larger than Victoria Blue. They also observed that the rejection of Erythrosine B, which has the highest molecular weight but smallest molecular size, is higher than all solutes. Geens et al. also stated that solute rejections in organic solvent are not only attributed to solute-solvent interactions (effective molecular size) but also solute-membrane (polarity and charge effect) and solvent-membrane (swelling) interaction affect the separation mechanism of OSN membranes.

Soltane et al. (39) studied about the separation mechanism of PDMS membrane using three different dyes (Sudan Blue (neutral, 350 Da), Red 82 (negatively charged, 566 Da) and Alphazurine FG (negatively charged, 766 Da)) and three aliphatic molecules having the similar molecular weights, and several solvents including ethanol, dimethyl carbonate, hexane, heptane and toluene, which have different affinity to the membrane. They observed that the rejection of the same solute shows differences for all solvents which indicates that the solvent has an important effect on the separation of the solutes. The filtration tests with Sudan Blue showed that highest rejection was achieved with the solvent that has highest swelling degree, but lowest rejection was not obtained with the solvent having lowest swelling ratio. Therefore, the rejection of solutes is not directly linked to the solvent-membrane interaction, solute-membrane interaction is another significant decisive parameter. They stated that the rejection of solute increases as the solvent-solute solution becomes more thermodynamically stable because the transport of the solute through the membrane becomes more difficult. In addition to the solvent-solute interaction, the affinity of solute to the membrane together with its diffusion ability is also determining parameter for the transport of the solute.

Bhanushali et al. (40) using six different membranes (hydrophilic and hydrophobic) discussed the solute transport mechanism in organic solvent nanofiltration membranes. Sudan IV (neutral, 384 Da) was used as a solute to understand the solute transport mechanism both in polar solvents (methanol and ethanol) and nonpolar solvent (hexane). Negative rejection of Sudan IV by composite dimethyl silicone NF membrane named membrane D in polar solvents (about -10 % in methanol and about -5 % in ethanol at same pressure) was observed while the rejection of the same solute in hexane by the hydrophobic membrane D was about 25 %. Negative rejections have been observed in literature by other researchers (41; 42; 43). Negative rejection behavior of these membranes can be explained by the sorption of the solute in the membrane (high affinity of the solute to the membrane) and faster permeation than the solvent (44). The hydrophilic polyamide-based charged membrane commercially named YK membrane showed the positive rejection of the dye in both hexane (43%) and methanol (86%). As expected, the permeance of hexane is lower than that of methanol for the hydrophilic YK membrane. In their previous study (45), they observed that the flux of nonpolar solvent through the hydrophilic membrane was lower than that of polar solvent while the flux of nonpolar solvent through the hydrophobic membrane was higher than that of polar solvent. It can be stated that type of membrane material and type of solvent has an important effect on the solute transport.

For the further investigation of negative rejection, other researches done in literature were followed. Volkov et al. (46) worked with PTMSP membrane using two neutral dyes (Solvent Blue 35 (350 Da) and Oil Red O (408 Da) and two negatively charged dyes (Remazol Brilliant Blue R (626 Da) and Orange II (350 Da)) in ethanol solutions. They observed negative rejection of neutral dyes and high rejection of negatively charged dyes by PTMSP membrane. Higher distribution coefficient of neutral dyes resulted in the sorption of these dyes in the membrane and blocking the transport of solvent through the membrane, and thereby lower rejection. This study is another evidence that the affinity of solute to the membrane plays a significant role in determining the separation mechanism of solutes for OSN membranes.

1.4 An alternative polymer to Organic Solvent Nanofiltration: Cellulose

Cellulose, which is the most widely found polymer on earth, is an alternative material that can be used in producing OSN membranes as it is known to be stable in many organic solvents due to its inter- and intra- molecular hydrogen bonds. These strong hydrogen bonds provide cellulose mechanical and chemical strength towards wide range of organic solvents including polar aprotic solvents which dissolve most of polymer types. This feature makes cellulose very good candidate for Organic Solvent Nanofiltration processes.

In the preparation of polymer dope solution using cellulose as polymer, the most common solvents currently used to dissolve cellulose are NaOH/CS₂ which converts cellulose to a derivative, cellulose xanthate, which is later regenerated to cellulose upon coagulation and N-methylmorpholine-N-oxide (NMMO) with thermally unstable feature (47). Recent studies in literature shows the alternative way of dissolving cellulose using ionic liquids. By this way, cellulose membranes can be produced using phase inversion technique which is easy and commonly used way to fabricate most of commercial membranes. Ionic liquids provide cellulose to turn into membrane without derivatization of cellulose into any of its derivatives. Ionic liquids are defined as molten salts having melting points below 100 ° C. Ionic liquids may be seen as a harmless solvent with negligible vapor pressure and recyclability (48).

Li et. al studied about the fabrication of cellulose membranes by phase inversion method using one of ionic liquids, 1-allyl-3-methylimidazolium chloride (AMIMCl) and water as non-solvent. They stated that chemical structure of cellulose does not change and there is a significant decrease in crystallinity of cellulose after the membrane fabrication. Based on SEM images, cellulose membranes with 700 Da molecular weight cut off (MWCO) have the structure with dense and macro void free selective layer. They tested their cellulose membranes with the filtration of three anionic dye in their aqueous solutions and found the rejections of Brilliant Blue R (826 Da) and Congo Red (697 Da) over 95 %, and that of Methyl Orange (327 Da) less than 25 %. They stated that the separation mechanism of these cellulose membranes depends on the molecular size of the solutes since dye having molecular size smaller than 700 Da was not retained at all (49).

Chen et. al worked to fabricate regenerated cellulose membrane using wheat straw with ionic liquid, 1-butyl-3-methylimidazolium chloride ([BMIM]Cl). They reported that regenerated cellulose membranes have good mechanical properties with pure water permeance of 80 L/hm²bar and high rejection of bovine serum albumin about 97 % (50). Ma et. al also observed high bovine serum albumin rejection (99 %) with bamboo pulp hollow fiber membranes using 1-butyl-3-methylimidazolium chloride/dimethyl sulfoxide as solvent (51). In recent studies, Anokhina et. al fabricated cellulose composite membranes using N-methylmorpholine oxide to dissolve cellulose. They tested cellulose membranes by the filtration of anionic dyes-aprotic solvents solution. They observed that the rejection of Orange II (350 Da) was in the range of 15-85 % with the filtration of DMSO, NMP, DMFA, THF and acetone solutions while Remazol Brilliant Blue R (626 Da) retained at about 42-94 %. They noticed that the interaction between solvents and cellulose membranes shows differences for all solvents: membrane swelled in THF at the ratio of 37 % while higher swelling degree of cellulose (230 %) was obtained with DMSO. The highest rejection (≥ 90 %) was obtained with Remazol Brilliant Blue R which is larger molecule and having higher swelling ratio of 100 % in DMSO. They stated that swelling of polymer in these solvents affect the membrane pore structure and thereby the separation performance of the membrane (52). They later studied about the fabrication of cellulose membranes using [EMIM]OAc/DMSO solvent system with different cellulose concentration in polymer dope solution (6 to 16 wt. %). They stated that higher Remazol Brilliant Blue R (82 %) was obtained with higher polymer concentration (16 wt.%) (53).

1.5 Post-treatment of Cellulose Membranes

The molecular structure of cellulose consists of two glucose unit located at C1 and C4 positions and there exists glycosidic bond between them (Figure 4). Hydroxyl groups located at C2, C3 and C6 positions of cellulose units provide cellulose to make possible derivatives. In molecular structure of cellulose, C6 OH group has highest reactivity while C3 OH is the least reactive group due to the existence of hydrogen bond with neighboring oxygen molecule.

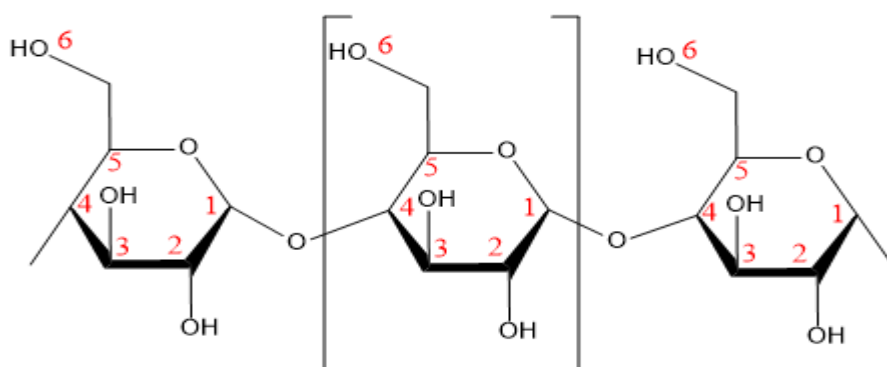


Figure 4: Schematic drawing of cellulose chains

The reactivity of the hydroxyl groups of cellulose offers the crosslinking of these groups with some chemical agents, so by this way polymer chain structure of cellulose may change, and thereby swelling-sorption characteristics, membrane porosity, mechanical strength may show difference.

Zhou et al. worked on the crosslinking mechanism of paper with polycarboxylic acids. They cured papers with polycarboxylic acids in aqueous solution in the presence of NaH_2PO_4 . Crosslinking reactions consist of two reactions shown in.

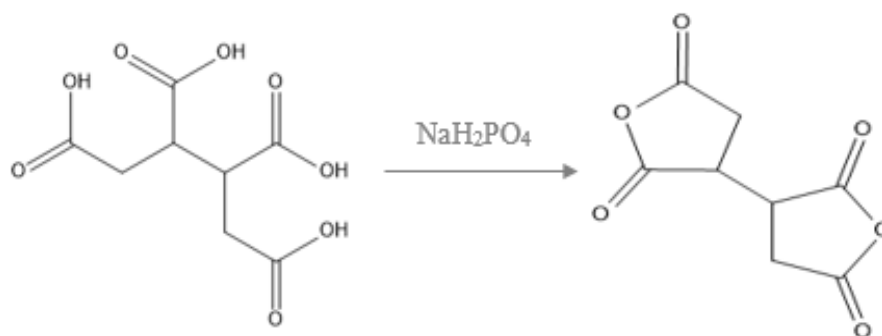


Figure 5: Formation of cyclic anhydride

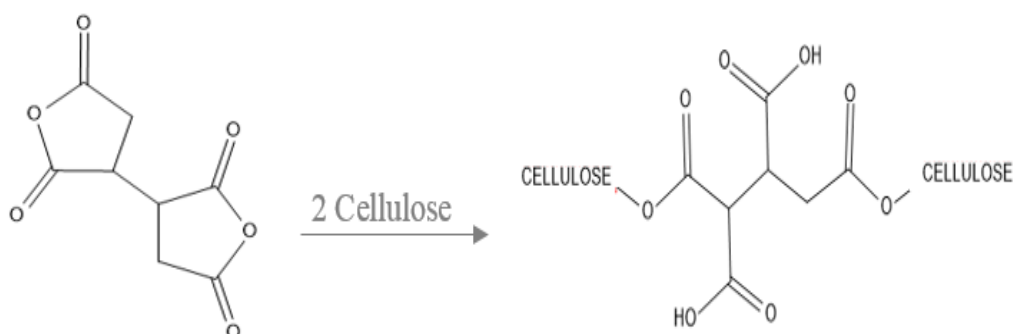


Figure 6: Crosslinking of cellulose chains

First one is the formation of cyclic anhydride in carboxylic acid groups to form ester with hydroxyl groups of cellulose, and last one is crosslinking of cellulose chains via esterification. They stated that carboxylic acid groups prevent the swelling of cellulose chains in wet state by keeping them together and thereby paper strength in the wet conditions increased after crosslinking of papers with carboxylic acids since ester groups can stay stable in water (54). According to Yang and Xu, improving wet performance of wood pulp cellulose such as wet strength, wet stiffness and stability in water is directly related to esterification of cellulose with carboxylic acids (55). In literature, there are lots of studies about the effect of crosslinking of cellulose fibers with polycarboxylic acids on the strength of wet membrane. They all agree about that the wet strength of papers or wood pulp increase as a result of esterification reaction of cellulose fibers with carboxylic acid groups and also 1,2,3,4-butanetetracarboxylic acid over other polycarboxylic acids provide the highest degree of crosslinking of fibers (55; 56; 57).

Literature studies show that glutaraldehyde is one of the chemical agents used to crosslink hydroxyl groups of cellulose, polyvinyl alcohol, chitosan and starch (58). Glutaraldehyde is in the form of hydrate in aqueous solution, which improves its possibility of crosslinking of cellulose. Kim et al. studied about polyvinyl alcohol membranes produced by phase inversion technique and performed the crosslinking reaction with glutaraldehyde. Crosslinking degree of the membranes was controlled by changing crosslinking conditions such as glutaraldehyde concentration in crosslinking solution and crosslinking time.

They observed that PVA membrane crosslinked with glutaraldehyde swells in water less than uncrosslinked one. As crosslinking degree increases degree of swelling in water decreases while degree of swelling in ethanol remains constant at all conditions, and solvent flux and selectivity of water-ethanol mixture decreases with increasing crosslinking degree. Like Kim et al., other researchers as well state that mechanical properties of membrane and its characteristics change with crosslinking treatment of hydroxyl groups with glutaraldehyde. (59; 60; 61).

Organic solvent nanofiltration has been already applied in both lab and industrial scale. There are lots of OSN applications ranging from food applications such as edible oil processing, degumming, deacidification to petrochemical applications like deacidification of crude oil, pharmaceutical applications such as solvent exchange, concentration of pharmaceuticals, catalytic applications like homogenous catalyst recovery. OSN has the potential to be performed in many processes including reactions, recovery and separations instead of traditional processes with high quality of separation performance.

1.6 Aim of the Study

Literature studies show there is an urgent need of OSN membranes which are stable in a wide range of solvents and which have good and stable separation performance. In this study, cellulose is proposed as an alternative polymer to be used in fabricating OSN membranes due to the existence of its inter- and intra-molecular hydrogen bonds. Cellulose membranes were produced by phase inversion using the ionic liquid 1-ethyl-3-methylimidazolium ([EMIM]OAc) as solvent. Fabricated membranes were tested with filtration of different solute-solvent systems. The effect of solute size/charge and solvent type on membrane separation performance was investigated. For further post-treatment, membranes were treated via chemical crosslinking with different crosslinking agents. Crosslinking effects on membrane properties were examined by performing swelling test, sorption tests and filtration tests.

CHAPTER II

EXPERIMENTAL METHODS

2.1 Materials

Cellulose (cotton linters), 1-ethyl-3-methylimidazolium acetate ([EMIM]OAc, 95%), acetone (99%), ethanol (99.9%), toluene (99.5%), hexane (95%), Bromothymol Blue, Cresol Red, Rose Bengal, Brilliant Blue R, 1,2,3,4-butanetetracarboxylic acid (BTCA, 99%), monosodium phosphate (NaH_2PO_4 , 99%), glutaraldehyde (50 wt % in H_2O), sulphuric acid (H_2SO_4) and (R,R)-(-)-N,N'-Bis(3,5-di-tert-butylsalicylidene)-1,2-cyclohexanediaminomanganese(III)chloride (Jacobsen catalyst) were purchased from Sigma Aldrich. Dimethyl sulfoxide (99%), tetrahydrofuran (99%), n-methyl pyrrolidone (99.5%) and Crystal Violet were purchased from Merck, and ethyl acetate was purchased from JT Baker.

Coagulation medium was reverse osmosis water used as non-solvent, and water used for membrane washing after coagulation was also reverse osmosis water. Ultra-pure water was used in crosslinking solutions. All solutes (dyes) and solvents were used as purchased without further purification.

2.2 Polymer Dope Solution Preparation

Cellulose was dried for two days at 80 °C and [EMIM]OAc, which was used to dissolve cellulose, was heated for one hour at 90 °C and then kept at 70°C for three hours to remove volatile impurities prior to use, while acetone, which was used as co-solvent, was used directly from the bottle. Casting solution prepared for membrane fabrication consisted of 12 wt % cellulose, 25 wt % acetone and 63 wt % [EMIM]OAc. Solution was first stirred under magnetic stirrer overnight and then roller mixer for a week at ambient condition.

2.3 Membrane Fabrication

Flat sheet cellulose membranes were cast on glass plate using 250 μm casting bar at room temperature. Cast polymer films were directly put into evaporation bath under nitrogen flow at a rate of 0.6 L/min for 30 minutes to evaporate acetone. Evaporation of acetone aims to increase polymer concentration in the selective layer. After evaporation, polymer films were directly immersed into a coagulation bath including water as non-solvent. After coagulation, membranes were washed by placing into RO water for 24 hours to remove residual solvent and complete coagulation. Membranes were further immersed into ethanol. Membranes were directly used from ethanol or after immersing in ethanol for one hour, they were dried first under nitrogen flow for a while and then kept at ambient condition overnight.

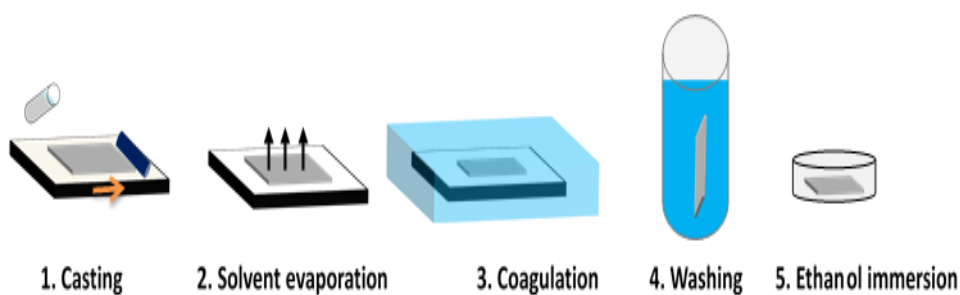


Figure 7: Schematic representation of the membrane fabrication process

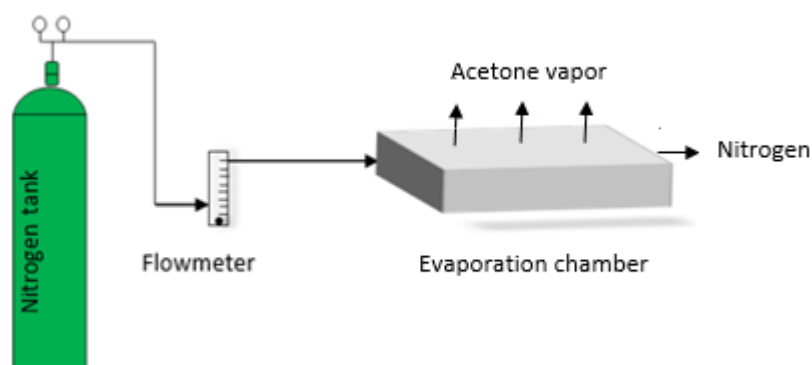


Figure 8: Solvent evaporation process

2.4 Membrane Crosslinking

2.4.1 Crosslinking with Glutaraldehyde

Fabricated membranes were chemically crosslinked with aqueous glutaraldehyde solution. Membranes were immersed into glutaraldehyde crosslinking solution containing 0.5 wt. % glutaraldehyde and 1.0 wt. % sulphuric acid at 40 °C for a period of three hours. After this period, membranes were subsequently washed with water to remove an excess of crosslinking agent. After crosslinking, membranes were put into ethanol for an hour and then dried.

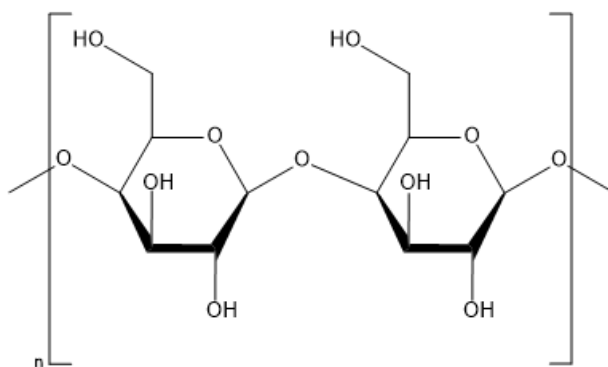


Figure 9: Molecular structure of Cellulose

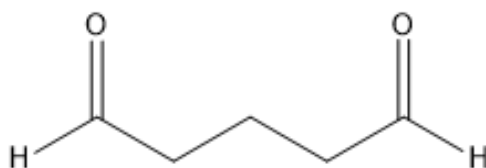


Figure 10: Molecular structure of Glutaraldehyde

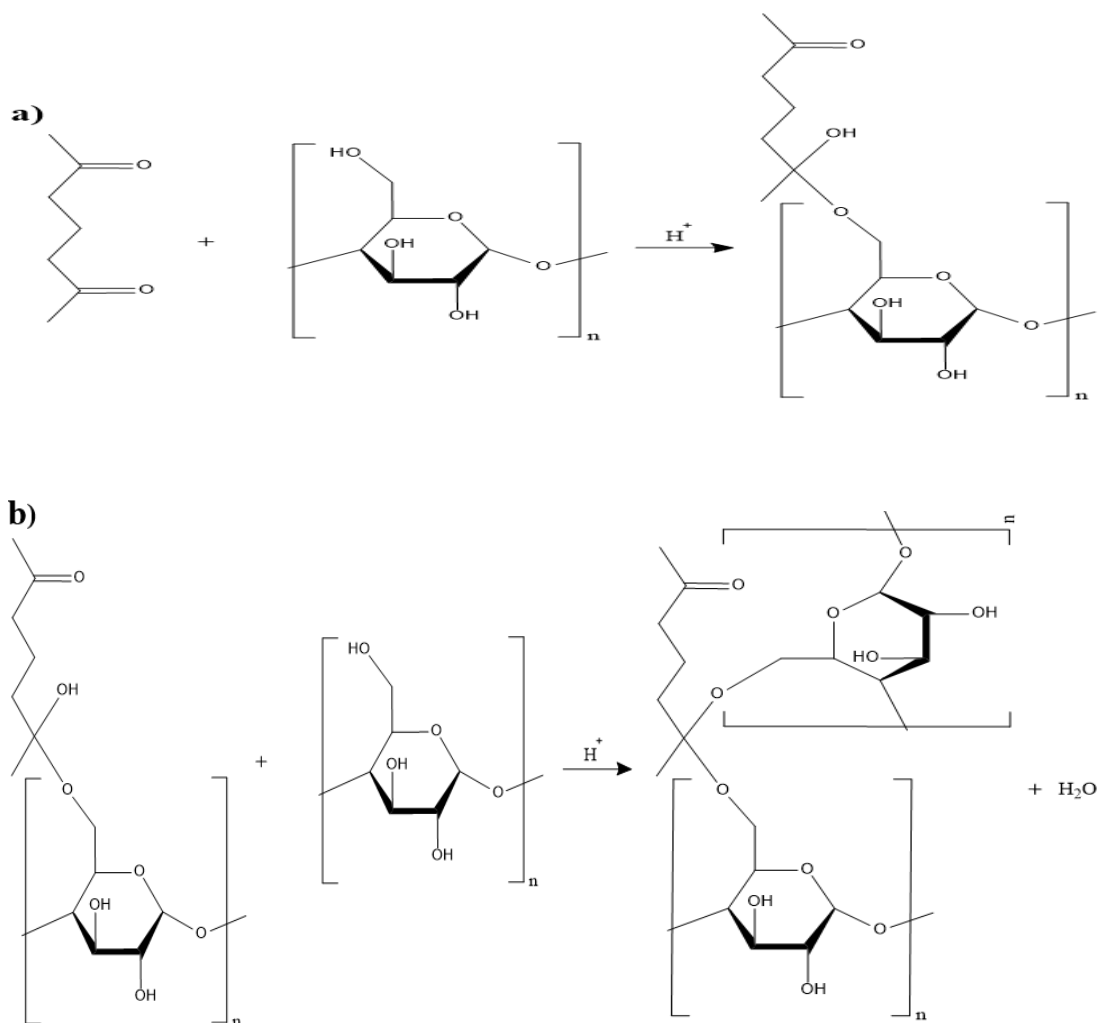


Figure 11:(a) Reaction of Glutaraldehyde with one hydroxyl group of cellulose forming a hemicetal, (b) with another hydroxyl group of cellulose forming an acetal

2.4.2 Crosslinking with 1,2,3,4-butanetetracarboxylic acid (BTCA)

Membranes were also chemically crosslinked with aqueous 1,2,3,4-butanetetracarboxylic acid (BTCA) solution. Membranes were immersed into BTCA crosslinking solution including 2.0 wt % BTCA and 1.0 wt % NaH_2PO_4 at ambient conditions for 15 minutes. After 15 minutes, membranes were directly placed into oven at 80 °C for an hour to be cured. Membranes were further washed with water, then put into ethanol for an hour and dried.

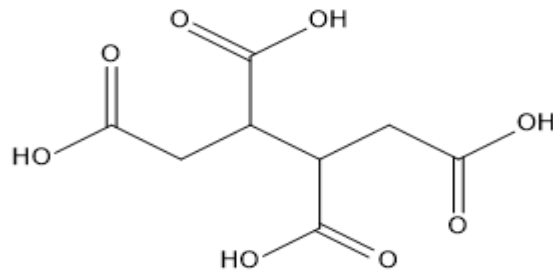


Figure 12: Molecular structure of 1,2,3,4-butanetetracarboxylic acid (BTCA)

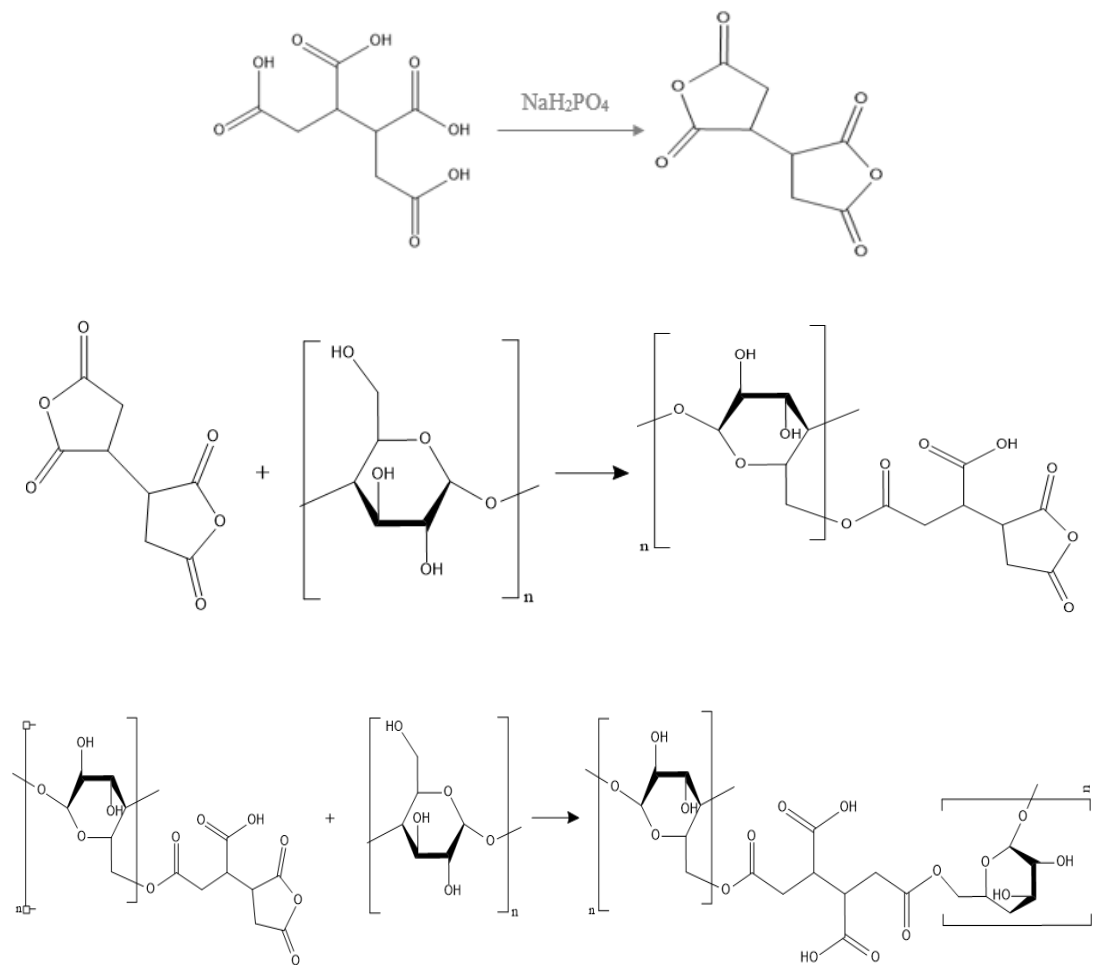


Figure 13: Crosslinking reaction between Cellulose and BTCA

Membrane codes used throughout this thesis were given at Table 1.

Table 1: Membrane Codes

Membrane Code	Drying Procedure	Crosslinking Procedure
KK2	-	-
KK2D	+	-
KK2G	+	Glutaraldehyde
KK2B	+	BTCA

2.5 Membrane Morphology

Membrane morphology was determined by JSM-6400 Scanning Electron Microscopy at Department of Metallurgical and Materials Engineering in METU. Membranes were first dried under vacuum and then broken using liquid nitrogen. Membranes were placed into sample holders and put into vacuum. Membranes were coated with Au-Pd alloy before SEM images were taken.

2.6 Nanofiltration Performance Tests

Nanofiltration tests were conducted in dead-end mode using HP4750 stirred cell of 300 ml volume and cross flow mode using a test module. Dead-end filtrations tests were done at 4 bar transmembrane pressure (TMP) with 250 rpm of stirring and at 10 bar under stirring at 500 rpm to reduce concentration polarization, and the systems were pressurized using nitrogen gas. Cross-flow filtration tests were conducted by setting the operating pressure to 1.8 bar at 30 rpm of cross flow velocity. Schematic representations of both filtration modes are given in Figure 14 and Figure 15.

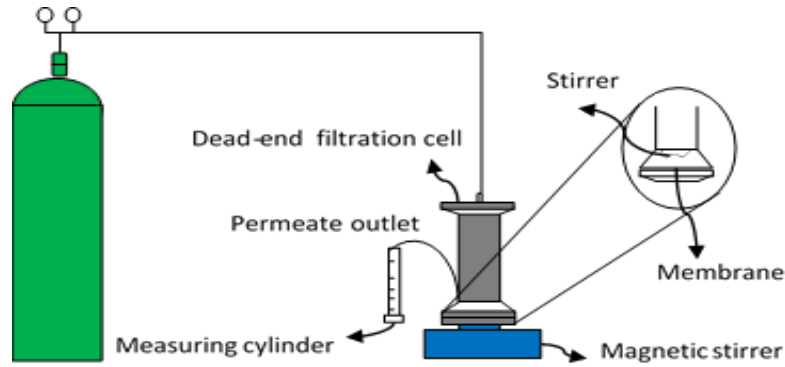


Figure 14: Schematic drawing of dead-end filtration experimental set-up

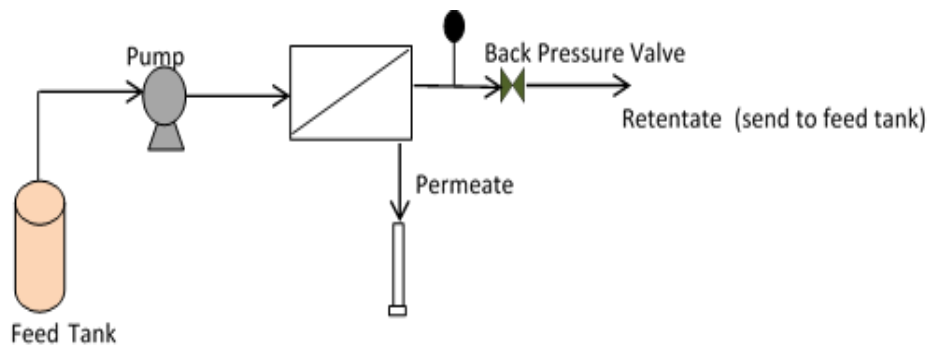


Figure 15: Schematic drawing of crossflow filtration experimental set-up

Filtration tests were continued until dye deposition on the membrane during the filtration calculated by mass balance (eqn.3.1) reached to zero for filtrations at dead-end mode and until constant rejection value was obtained for cross flow filtrations.

$$\text{Sorbed dye in the membrane (mmol)} = C_F \times V_F - \sum_{i=1}^n (C_{P,i} \times V_{P,i}) - C_R \times V_R \quad (3.1)$$

where C_F , C_P and C_R are the dye concentration in feed, permeate and retentate sample, respectively.

Bromothymol Blue, Cresol Red, Rose Bengal, Brilliant Blue R and Crystal Violet were used as solutes in the filtration tests (Table 2). Feed solutions were prepared in ethanol and dimethyl sulfoxide at 0.05 mM dye concentrations, and also to estimate the separation performance of the membrane in a real application Jacobsen catalyst was used in its ethanol and dimethyl sulfoxide solution at same concentrations.

Table 2: Probe molecules and their properties

Solute	Charge	Molar volume, cm ³ /mol	Molecular Weight, Da	Structure
Bromothymol Blue	Neutral	253.1	624	
Cresol Red	Neutral	140.1	382	
Brilliant Blue R	Negative	421.3	824	
Rose Bengal	Negative	241.0	1017	
Crystal Violet	Positive	253.7	407	
Jacobsen Catalyst	Neutral	-	635.2	

Dye concentrations in feed, permeate and retentate samples were measured using UV-1601 M UV-Visible Spectrophotometer. Before filtering feed solutions through the membrane, pure solvent permeance of the membrane was first measured at different operating pressures, and permeance measurement continued until constant solvent flux was achieved at each pressure. After pure solvent permeance, rejection tests were done. Pure solvent permeance and rejection values were calculated as follows:

$$\text{Pure Solvent Permeance (L/hm}^2\text{bar)} = \frac{J}{\text{TMP}} \quad (3.2)$$

where J is the permeate flux (L/hm²) and TMP refers to trans membrane pressure (bar).

$$\text{Rejection \%} = \left(1 - \frac{C_p}{(C_f + C_r)/2} \right) \times 100 \quad (3.3)$$

2.7 Swelling Tests

Fabricated membranes were first cut in the dimension of 2 cm × 3 cm, dried at ambient conditions and then under vacuum until the weight of dried membranes remained constant, and it took a week. After a week, membranes were then immersed into solvents. They were taken out of solvent, wiped with tissue paper to remove excess solvent from the membrane surface and then weighed daily. Membrane weight increases day by day and after a certain time it become constant, which implies that the equilibrium between membrane and solvent is achieved. This immersion of membrane into solvent took two weeks. After swelling, membrane were dried at ambient condition and then in vacuum until the weight of dried membranes remained constant. Swelling ratio of membranes was calculated in the following equation.

$$\text{Swelling Ratio \%} = \left(\frac{W_{\text{wet membrane}} - W_{\text{dry membrane}}}{W_{\text{dry membrane}}} \right) \times 100 \quad (3.4)$$

where $w_{\text{wet membrane}}$ is the mass of the membrane after immersed into solvent while $w_{\text{dry membrane}}$ refers the mass of the membrane dried after swelling.

2.8 Dye Sorption Tests

Wet membranes of 2 cm × 3 cm dimensions were first wiped with tissue paper to remove excess solvent from the membrane surface and then directly immersed into 20 ml of 0.01 mM solutions of selected dye-solvent solutions. To determine the degree of dye sorption on the membrane dye concentration in the solution was measured after a week and then daily measurement was taken until it became constant indicating that the equilibrium between membrane and solute was achieved. The degree of dye sorption was named as sorption coefficient calculated as follows:

$$\text{Sorption Coefficient, } K = \frac{C_{\text{dye,membrane}}}{C_{\text{dye,solution}}} \quad (3.5)$$

$C_{\text{dye,membrane}}$ is the weight fraction of sorbed dye in the membrane and it was calculated as $(m_{\text{dye}})/(m_{\text{dye}}+m_{\text{solvent}}+m_{\text{dry membrane}})$. $C_{\text{dye,solution}}$ is the final dye concentration in the solution in which the membrane was immersed into.

2.9 Fourier Transform Infrared Spectroscopy (FT-IR)

Fourier Transform Infrared Spectroscopy (FT-IR) measurement was done from 500 to 4000 cm^{-1} wavenumber for all membranes (uncrosslinked and crosslinked membranes). Before analysis, BTCA-crosslinked membranes were put into 0.1 M NaOH solution for 5 minutes to transform carboxylic groups into carboxylate anions, and thereby carbonyl groups formed by esterification reaction can be determined by FT-IR analysis. After immersion into NaOH solution, membranes were kept under vacuum for a day to remove solvent from the membrane. FTIR analysis results was given in Results chapter at section 3.4.

2.10 X-Ray Photoelectron Spectroscopy (XPS)

X-ray Photoelectron Spectroscopy (XPS) analysis, which was conducted in METU Central Laboratories, was performed to determine the chemical composition of membranes. After crosslinking, it was expected that some groups of crosslinking

agents were connected to cellulose structure. For glutaraldehyde crosslinking, increase in C-C and C-H bonds was expected if glutaraldehyde was successfully connected to cellulose. On the other hand, for BTCA crosslinking, also new C=O groups expected as a result of successful crosslinking of the membrane with BTCA.

2.11 X-Ray Diffraction (XRD)

Crystallinity of membranes and cellulose powder were measured with Rigaku Ultima-IV X-Ray diffractometer in METU Central Lab to observe the effect of crosslinking on the membrane crystallinity. For cellulose powder, scanning interval is between 3 to 40 degrees while for membranes they were scanned between 5 to 40 degrees.

2.12 Mechanical Test

Mechanical test was performed with Zwick (250 kN) in METU Central Lab to examine the effect of crosslinking on the membrane mechanical properties. Some of crosslinked membranes and un-crosslinked membranes were taken out of ethanol and dried in vacuum before test. Some of them were immersed into DMSO till swelling ratio became constant and then directly tested.

CHAPTER III

RESULTS AND DISCUSSION

3.1 Membrane Morphology

Membrane morphology was measured using SEM. SEM images of membrane cross section were given in Figure 16 and Figure 17 .

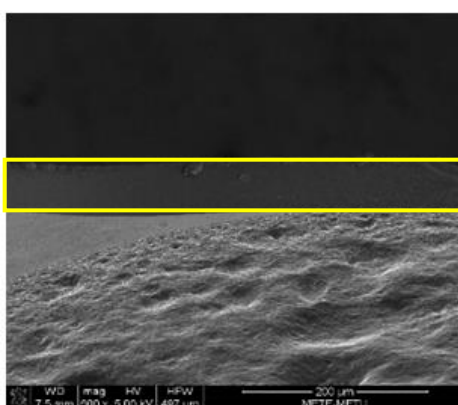


Figure 16: SEM Images of Membrane Cross section

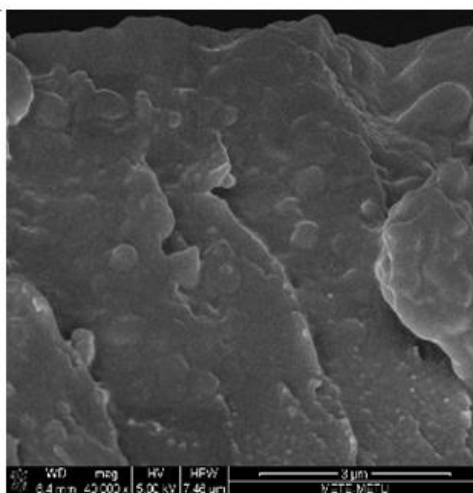


Figure 17: SEM Images of top region of membrane cross section

According to SEM results, fabricated membrane using cellulose as polymer and [EMIM]OAc as solvent have dense structure with no macrovoid formation and no skin layer. Same membrane morphology was obtained by Durmaz et al (62) and

Sukma et al. (63). They worked with the same polymer dope solution and membrane fabrication process.

3.2 Effect of Post-treatment: Drying

The separation performance of all fabricated membranes was determined by pure solvent permeance and rejection tests applied with dead end filtration system at 10 bar transmembrane pressure (TMP) with stirring at 500 rpm. Some of membranes were first dried after coagulation at ambient conditions under Nitrogen flow, which are named dried membrane, while some membranes were directly tested without drying process named non-dried membrane. Performance tests of both membrane (dried and non-dried membranes) were done using Bromothymol Blue (BTB) as the probe molecule and ethanol as solvent. Figure 19 shows the rejection of Bromothymol Blue from its ethanol solution and solution permeance during the filtration test. It was observed that the permeance through the membrane was constant during the filtration and equals to pure ethanol permeance (Figure 19). This implies that fouling and concentration polarization on the membrane were negligible during the tests, there was no accumulation of dyes as cake formation on the membrane surface. It was seen that the membrane became colored after filtration. Both membrane surface and the cross section of the membrane were examined under microscope, and it was observed that the dye was sorbed across the membrane cross section instead of accumulation on the membrane surface (Figure 18). Considering this observation, to eliminate the effect of dye sorption on the rejection of dyes each permeate collected during the filtration and the final retentate concentration, which means the final feed concentration in dead-end filtration, were measured by UV-VIS spectrometer, and back calculation shown in Appendix B was done to find previous retentate concentrations and finally initial feed concentration. It was seen that initial feed concentration found by this back calculation was lower than the original feed concentration prepared at the beginning of filtration with a known concentration, which implies that a certain amount of dye from feed solution was sorbed on the membrane during the filtration.

This sorbed dye amount was calculated by applying material balance. Throughout the text, rejection values calculated from back calculation were taken into consideration since they exclude the dye retained due to sorption in the membrane.

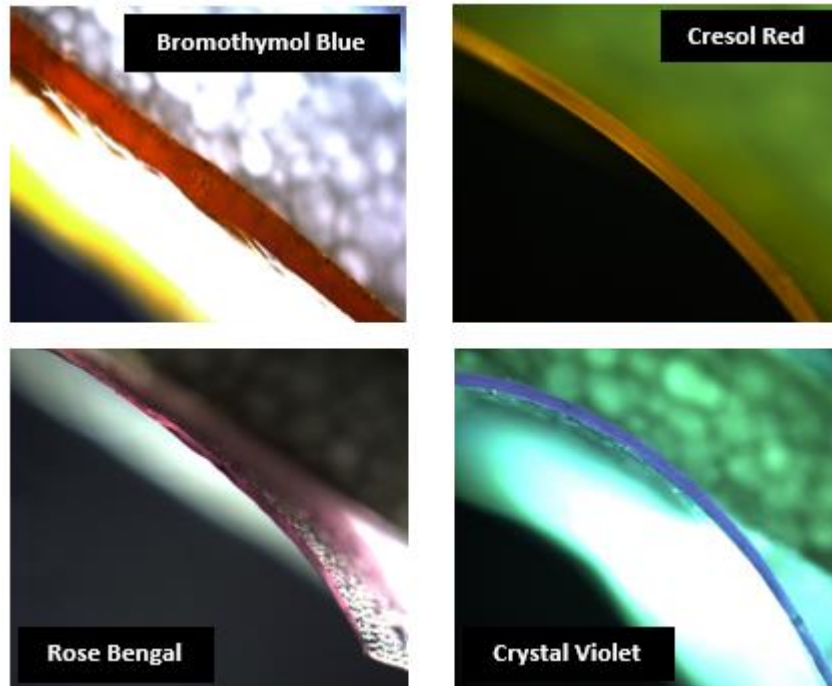


Figure 18: Membrane cross section pictures taken after filtration

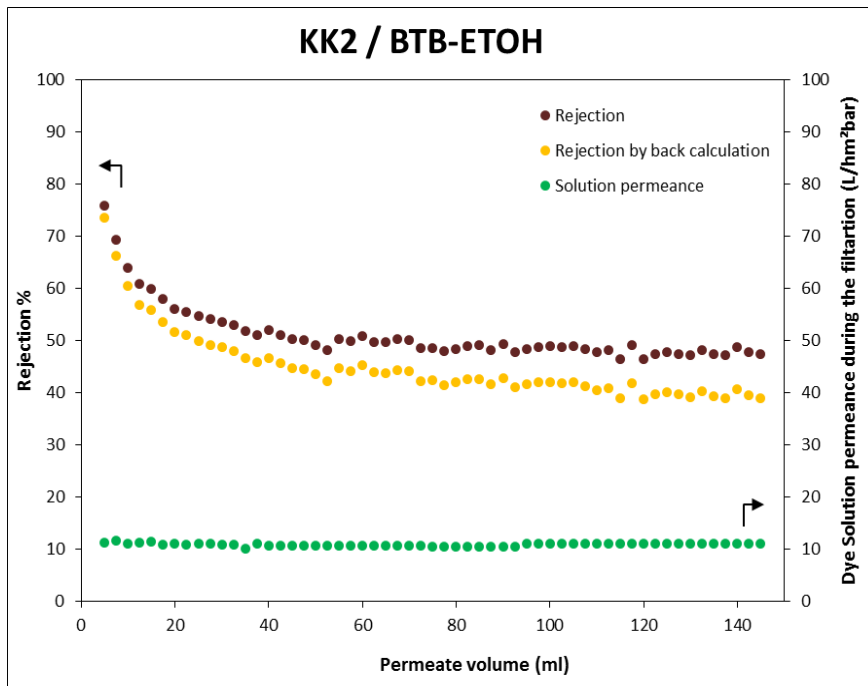


Figure 19: Rejection and permeance values of KK2 membrane during the filtration of BTB-ETOH solution

In Figure 20, rejection values of BTB from its ethanol solution and solution permeance during the filtration for non-dried and dried membrane were given.

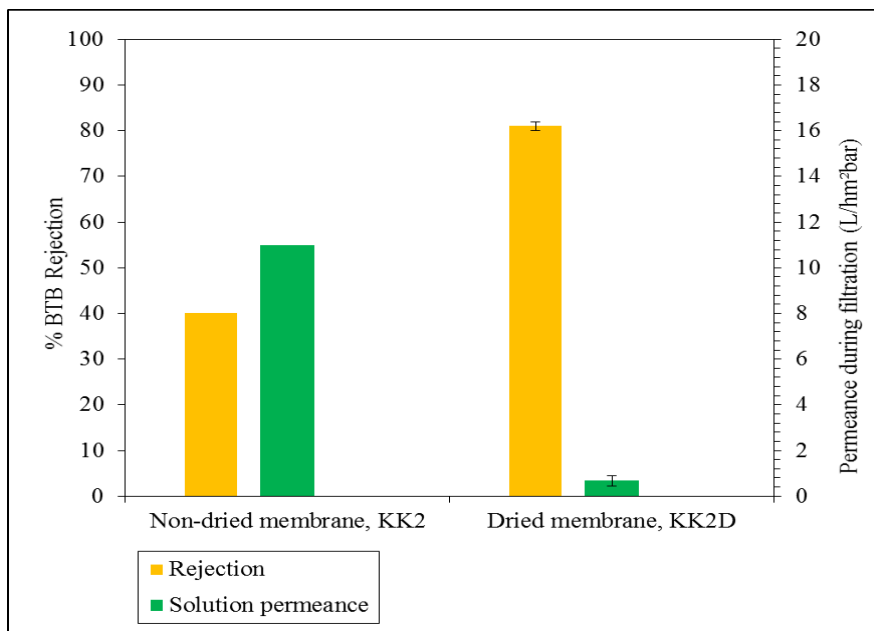


Figure 20: Rejection and permeance values of KK2 and KK2D membrane during the filtration of BTB-ETOH solution

Differences in BTB rejection and solution permeance of membranes were obtained after drying of membranes. The rejection of BTB increased while solution permeance through the membrane decreased with drying process. Permeance of non-dried membrane (KK2) is around 11 L/hm²bar while dried membrane (KK2D) has permeance of 0.47 L/hm²bar. Rejection of BTB increased twofold after drying (40 % to 80 %). Based on this observation, it can be said that porosity existing within the membrane structure is collapsing due to drying post treatment, and the membranes becomes tighter. Similarly, Burgal et al. observed that dried PEEK membranes have higher polystyrene rejection with lower permeance when compared to non-dried membranes (64). They also examined the effect of solvent filling the pores prior to drying and observed that pore structure of the membrane can be controlled by the variation of these solvents, more pores were collapsed when the membrane was soaked into solvent with higher surface tension before drying. In this study, all membranes were immersed into ethanol before drying post treatment.

3.3 Effect of Transmembrane Pressure

Effect of operating pressure on the performance of non-dried (KK2) and dried (KK2D) membranes was assessed using 0.05 mM Bromothymol Blue-ethanol solution as feed solution. From Figure 21, it was observed that the pure solvent flux (ethanol flux in this case) increased proportionally with increasing transmembrane pressure.

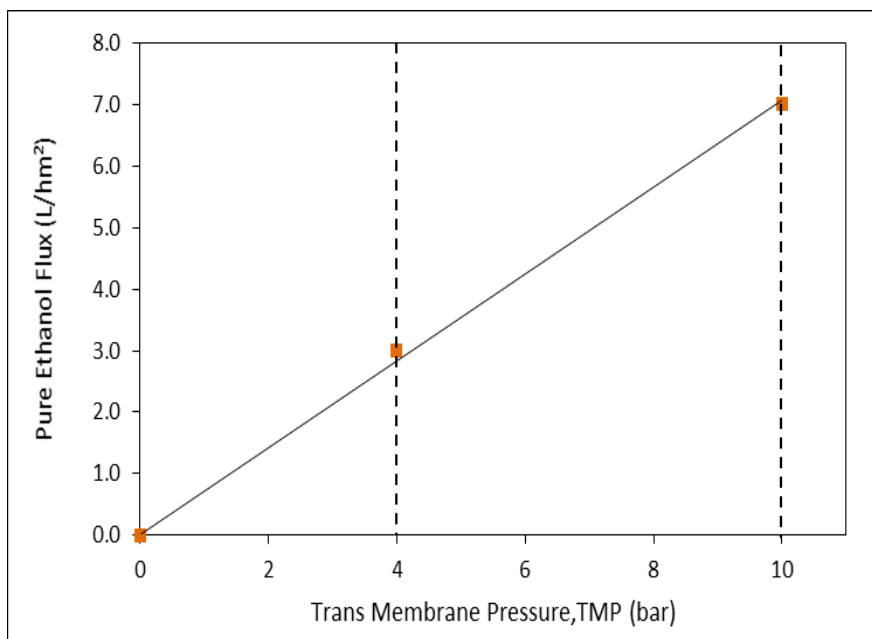


Figure 21: Pure ethanol flux at different trans membrane pressure

This linear relationship between flux and transmembrane pressure results in constant pure solvent (ethanol) permeance with the help of the eqn. 3.2. In Figure 22-Figure 25, it was seen that for both non-dried and dried membrane ethanol permeance of membrane does not significantly change when TMP is changed from 4 bar to 10 bar. Li et al. worked with cellulose membranes under the different operating pressures (2 bar to 6 bar), and they observed the constant water permeance through the membrane and unchanged rejection of Congo Red (99.4-99.8 %) at all pressures (49). Volkov et al. obtained the same relation between system pressure and membrane performance (65).

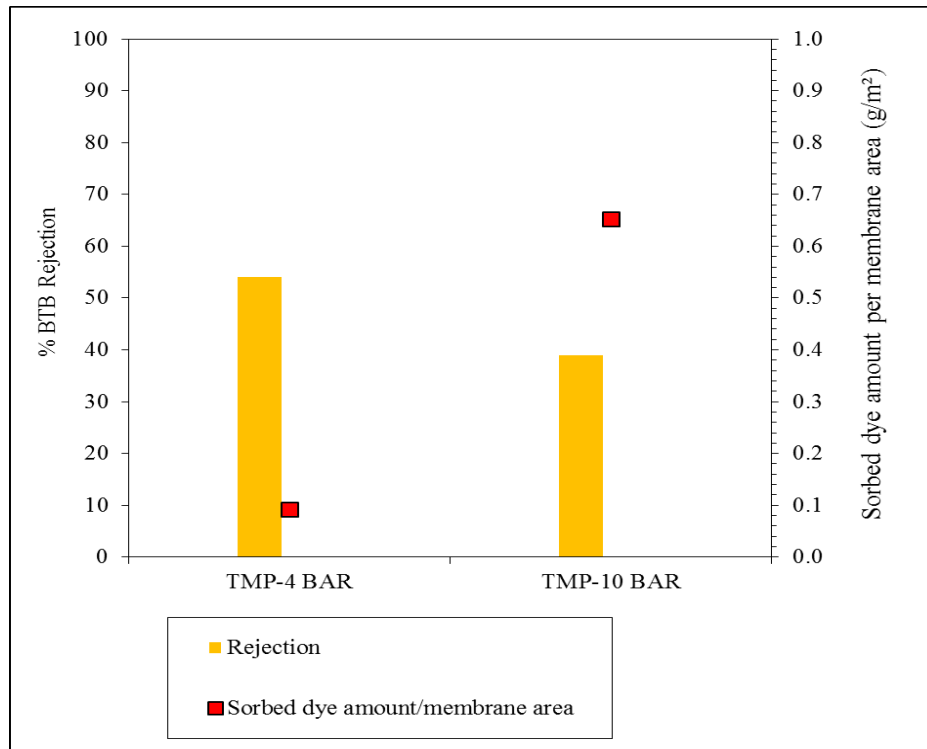


Figure 22: BTB Rejection by KK2 membrane and sorbed dye amount per membrane area during filtration at different TMP

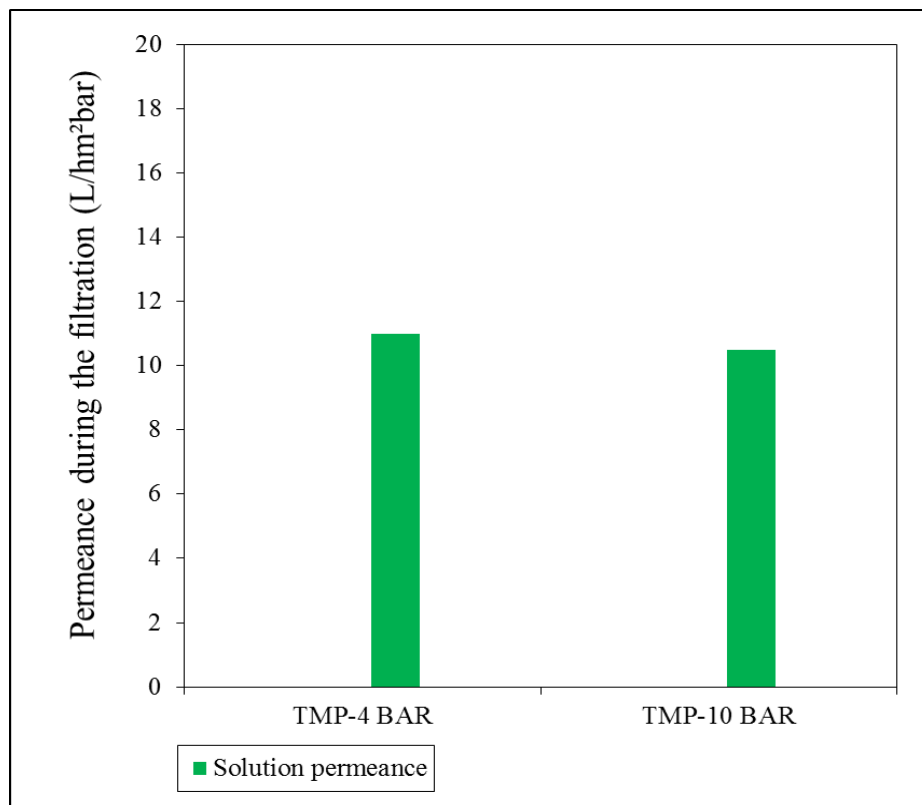


Figure 23: Permeance values of KK2 membrane during the filtration of BTB-ETOH solution at different TMP

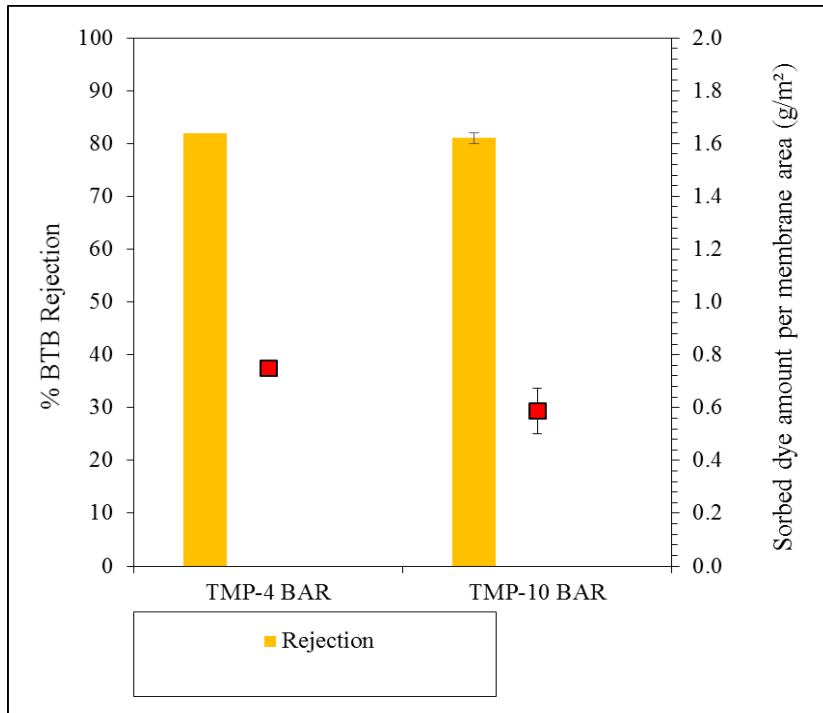


Figure 24: BTB Rejection by KK2D membrane and sorbed dye amount per membrane area during filtration at different TMP

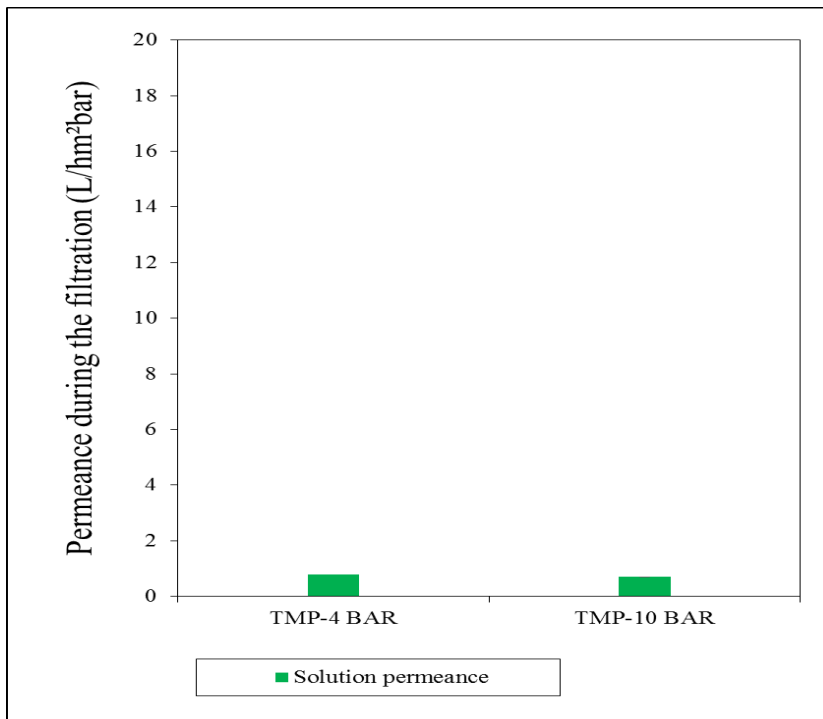


Figure 25: Permeance values of KK2D membrane during the filtration of BTB-ETOH solution at different TMP

It was observed that rejection of BTB of KK2 (non-dried) membrane slightly decreased from 50 % to 40 % with increasing TMP while KK2D (dried) membrane

has the same rejection value of around 80 % at 4 bar and 10 bar (Figure 22, Figure 24). As a result of dead-end filtrations of KK2 membranes conducted at different pressures, it was seen that the amount of solute (dye) sorbed on membrane increased 0.09 to 0.65 g/m² with the increasing transmembrane pressure. This increase in the amount of sorbed dye can be the reason of decrease in BTB rejection of membrane due to the fact that there is much more sorbed dye within membrane structure meaning more solute in permeate stream, which causes less rejection value of BTB compared to less sorbed one. For dried membrane constant rejection of BTB can be attributed to becoming more tighter and dense membrane as a result of pore collapse in the membrane structure with drying, which leads that sorbed amount of solute (BTB) on membrane surface or in pores during the filtration does not increase with the increasing pressure (Figure 24).

3.4 Effect of Solute and Solvent on membrane performance

To predict the separation performance (permeance and rejection) of all obtained membranes the transport mechanism of solute and solvent through membranes should be considered. In the investigation of transport through OSN membranes, both pore flow mechanism and solution-diffusion mechanism should be taken into consideration due to the fact that not only membrane pore size is related with the transport of solvent and solute, but also the interaction between solvent, solute and membrane also affects the separation performance of dense or microporous membranes. Thus, for the characterization of membranes solutes having different molecular size, charge and solvents showing difference in polarity and hydrogen bonding capacity were chosen.

Bromothymol Blue and Cresol Red, which have very similar chemical structure but different molecular size, were chosen as neutral dyes. Crystal Violet was chosen as a positively charged dye which has similar molecular size with Bromothymol Blue and larger than Cresol Red. Rose Bengal, with similar size to Bromothymol Blue and Crystal Violet, and Brilliant Blue R having larger size than all dyes were chosen as negatively charged dyes. These dyes dissolved in two different solvents: ethanol and dimethyl sulfoxide. In Figure 26, the rejections of five dyes by the dried membrane KK2D in ethanol solutions were given.

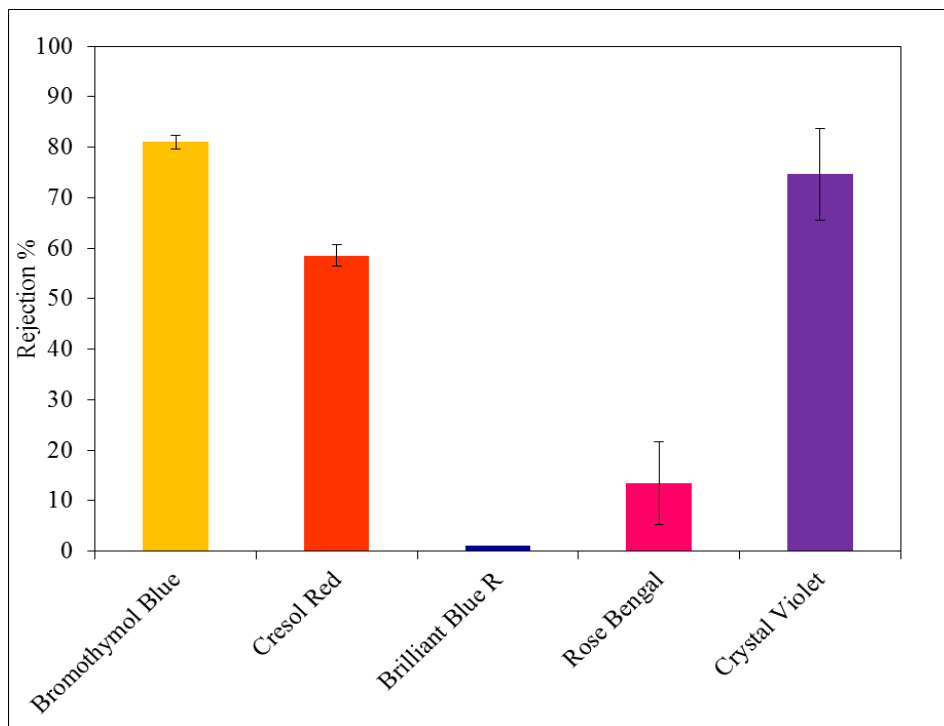


Figure 26: Rejection values of KK2D membrane during the filtration of different dyes-ethanol solution

The Rose Bengal rejection in ethanol was 13 ± 5 % while Brilliant Blue R, which has the largest molecular size, was not rejected at all in its ethanol solution. To predict the extent of the interaction between these solutes sorption coefficients (Figure 27) and membrane the pictures that belongs to the membranes before and after filtrations of BBR and RB in ethanol solutions were considered. From Figure 28, it was seen that both negatively charged dyes were sorbed quite strongly on the membrane, which means having high tendency to membrane. Based on solution-diffusion model these two negatively charged dyes dissolve in cellulose to a higher extent and hence have a higher permeability in the membrane due to the increased solubility, which gives lower rejection values of BBR and RB.

Figure 28 shows that Crystal Violet, which has similar size with RB and smaller size than BBR, was sorbed quite weakly on the membrane, thereby it can be said that it has lower affinity to the membrane than negatively charged dyes. This low interaction between CV and the membrane resulted in higher rejection (75 ± 9 %) than BBR and RB in their ethanol solutions.

It was observed that the rejection of Cresol Red (59 ± 2 %) is lower than that of Bromothymol Blue (81 ± 1 %) in their ethanol solutions. CR and BTB are neutral dyes and have similar chemical structures shown in Table 2. Thus, it can be expected that both dyes show similar affinity to the membrane, which can be supported by the images of the membranes pictured before and after filtrations of CR and BTB in their ethanol solutions (Figure 28). During filtration tests, the neutral dyes CR and BTB were sorbed quite strongly on the membrane like the negatively charged dyes BBR and RB. However, low rejection resulting from high sorption, which was observed during the filtrations of BBR and RB solution through the membrane, is not the case for the neutral dyes. This may be related to the aggregation of CR and BTB dyes in the solution due the presence of aromatic stacking (66). This aggregation of more than one dye results in larger size of solute, thus their permeation rate through the membrane becomes smaller than that of single molecular dye, which means smaller diffusivity through the membrane in the light of information based on solution-diffusion model. Charged dyes may not have tendency to aggregate in ethanol solutions due to their ionized groups, which causes electrostatic repulsion between these groups. In addition to electrostatic repulsion, hydrogen bonding is another factor affecting sorption of dyes (66). High affinity of neutral dyes (BTB, CR) and negatively charged dyes (BBR, RB) to the cellulose membrane can be explained considering hydrogen bonding since they are hydrogen bond acceptors and donors.

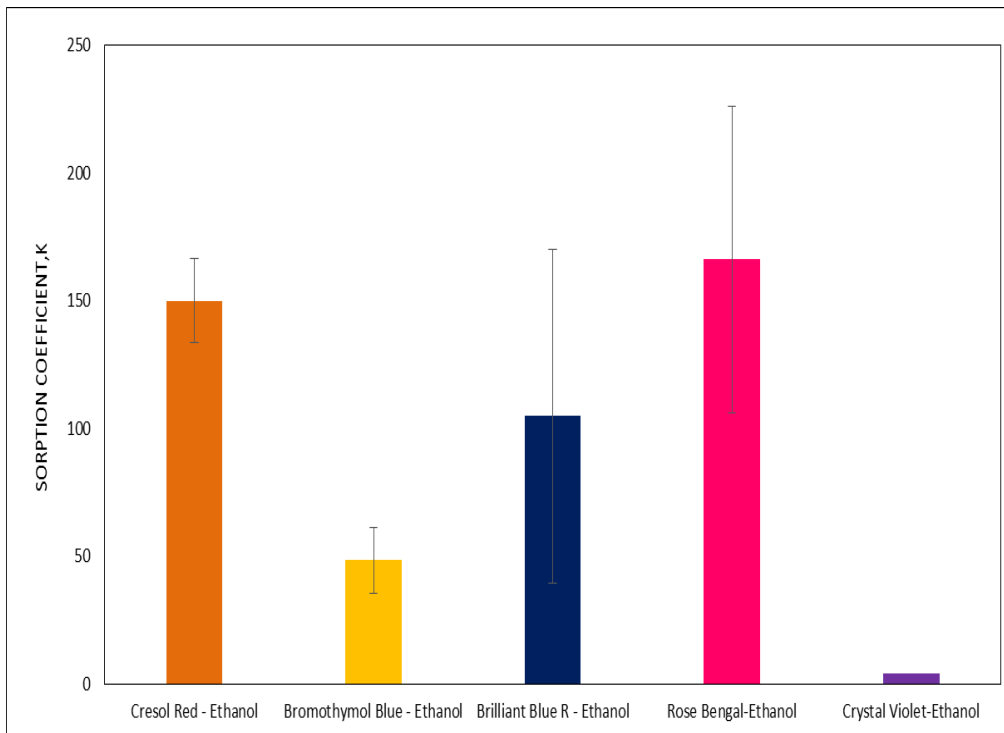


Figure 27: Sorption coefficient of each solute in ethanol solutions

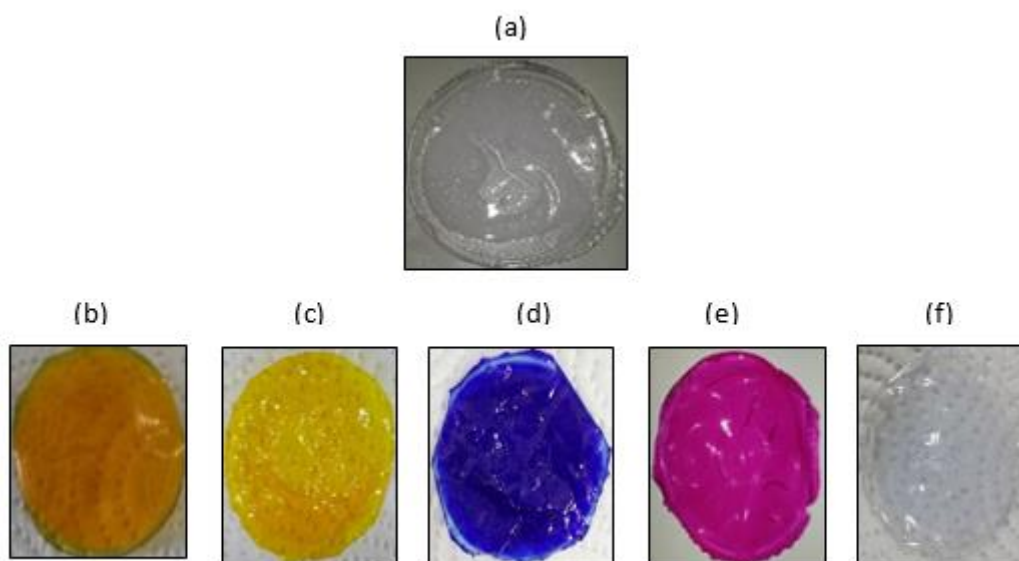


Figure 28: Membrane pictures taken before and after dye-ethanol solution (a) Before filtration (b) After Bromothymol Blue-Ethanol filtration (c) After Cresol Red-Ethanol filtration (d) After Brilliant Blue R-Ethanol filtration (e) After Rose Bengal-Ethanol filtration (f) After Crystal Violet-Ethanol filtration

Next, the rejection of BTB (neutral solute), RB (negatively charged dye) and CV (positively charged dye) in dimethyl sulfoxide was studied. In Figure 29, membrane performance in ethanol and DMSO was compared to each other in terms of rejection and solvent permeance.

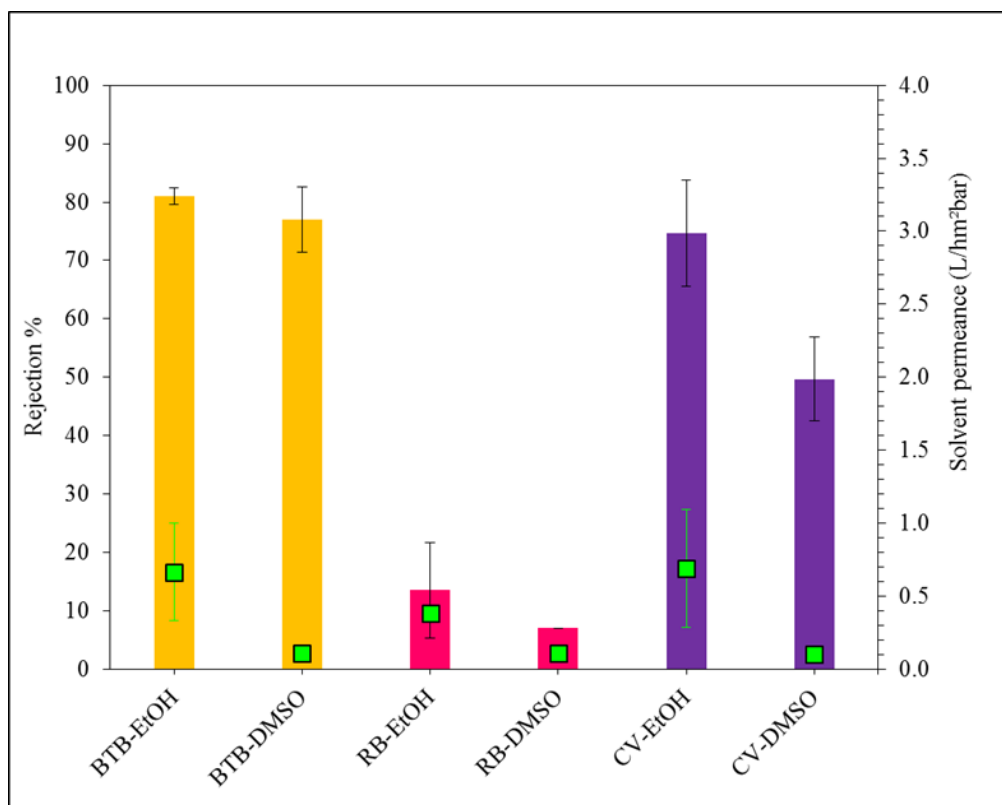


Figure 29: Rejection and permeance values of KK2D membrane during the filtration of dye-ethanol solutions and dye-DMSO solutions

Bromothymol Blue and Rose Bengal were rejected from dimethyl sulfoxide at the same ratio with ethanol while CV rejection decreased when DMSO was used as solvent. It was observed that the amount of BTB and RB sorbed on the membrane during the filtration tests done with DMSO decreased compared to tests done with ethanol while sorbed CV on the membrane increased significantly (Figure 30). Sorption tests were also applied on each solute in both solution system (Figure 31). Results of these tests were found to be similar to change in sorbed amount of solutes during the filtration.

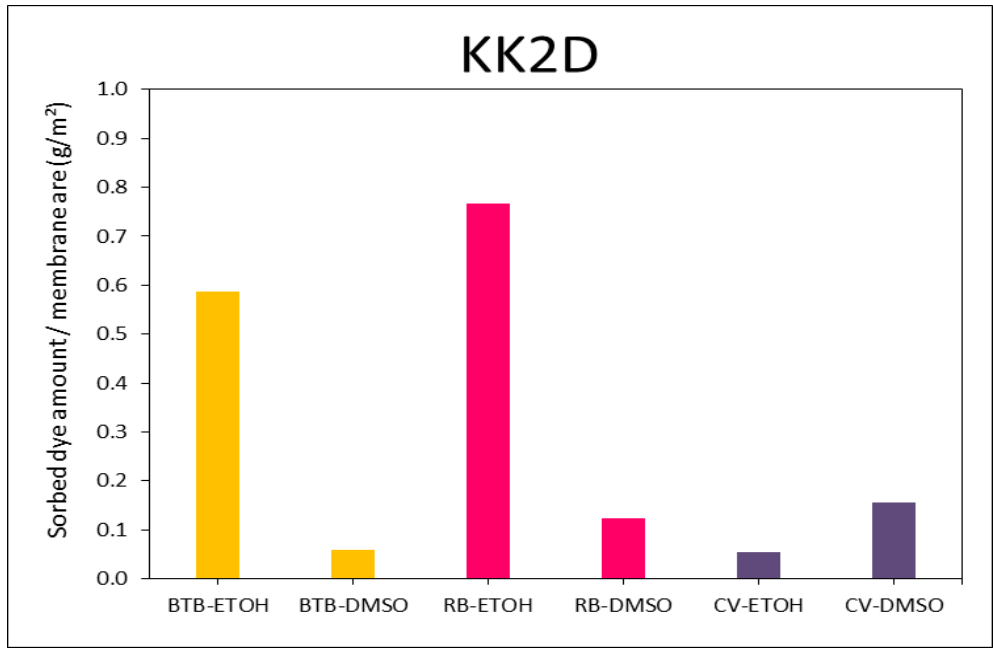


Figure 30: Sorbed dye amount on/in the membrane surface during the filtration of different dye-solvent solutions

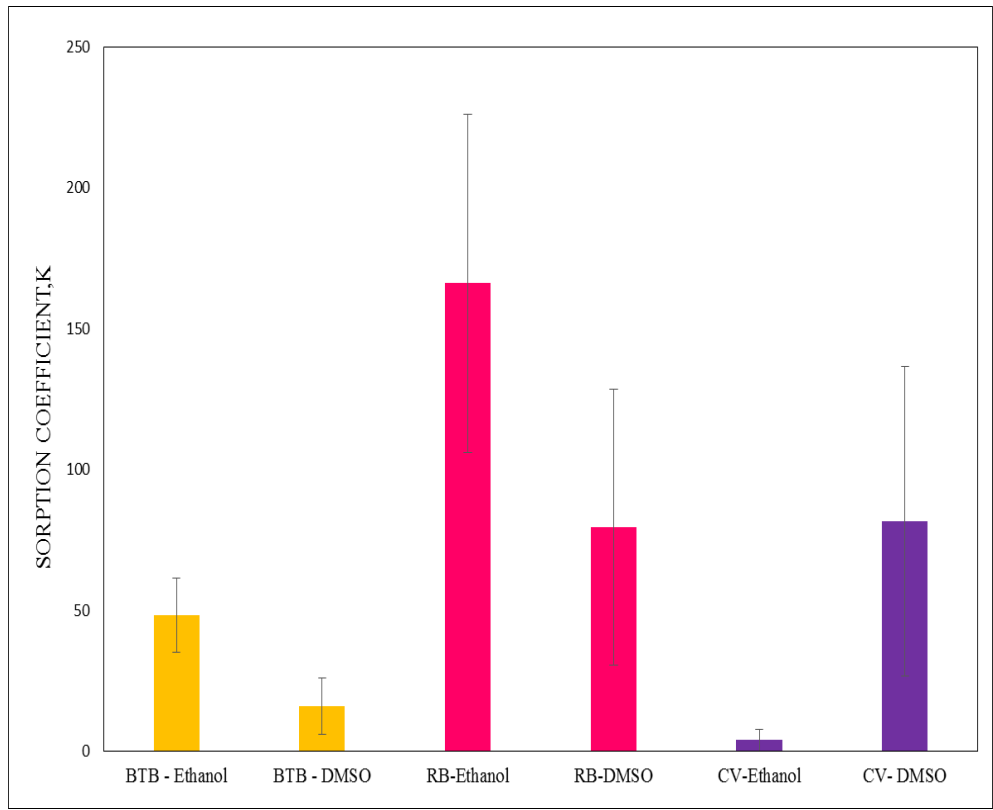


Figure 31: Sorption coefficient of each solutes in both ethanol and DMSO solutions

In Figure 32, the membrane pictures taken before and after filtration tests with both CV-ethanol and CV-DMSO solutions were shown and increase in sorbed solute amount was clearly seen from these pictures.

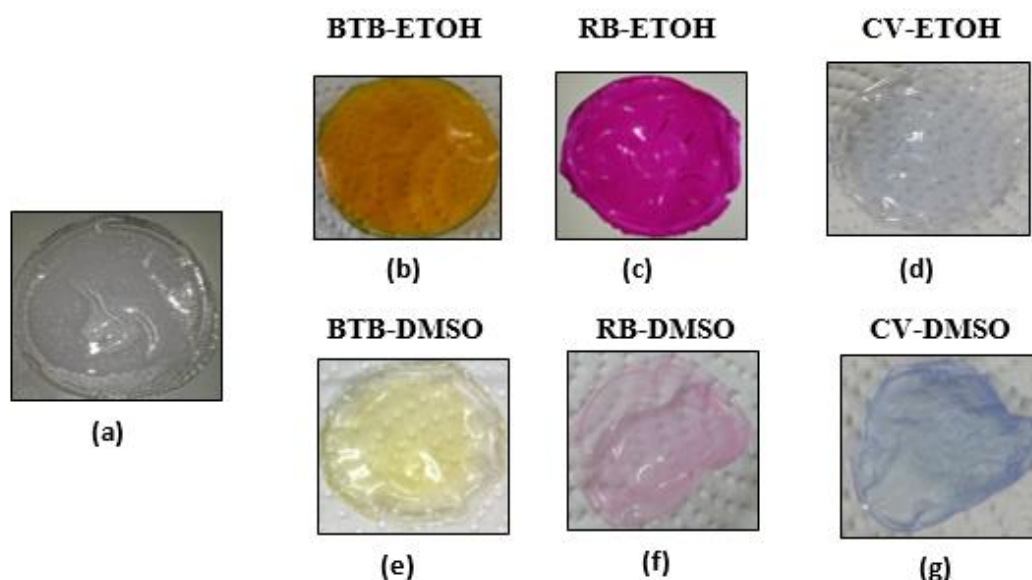


Figure 32: Membrane pictures taken before and after dye-ethanol solution (a) Before filtration (b) After Bromothymol Blue-Ethanol filtration (c) After Rose Bengal-Ethanol filtration (d) After Crystal Violet-Ethanol filtration (e) After Bromothymol Blue-DMSO filtration (f) After Rose Bengal-DMSO (g) After Crystal Violet-DMSO filtration

Ethanol permeance through the membrane was found as 0.47 ± 0.09 L/hm²bar while DMSO permeance was 0.13 ± 0.01 L/hm²bar for all filtration tests. Based on solution-diffusion mechanism diffusivity of solvents through the membrane affects transport rate of them. It is expected that solvents with higher molar volume diffuse slower than those with lower molar volume. Considering this, lower flux for DMSO can be expected since DMSO (71.3 cm³/g) has lower molar volume than ethanol (58.6 cm³/g). Therefore, changing the solvent permeance from 0.47 to 0.13 can be related to higher molar volume of dimethyl sulfoxide than ethanol considering solution-diffusion transport mechanism. Also, higher resistance of DMSO to transport across the membrane due to its higher viscosity may have resulted in lower permeance than ethanol (Table 3).

Table 3: Resistance values of solvents

Solvent	Permeance (P)	Viscosity (η)	Resistance (1/P.η)
Ethanol	0.47	1.07	1.99
DMSO	0.13	2.0	3.85

To get a deeper insight into the interaction between solvent and membrane swelling degree of membrane in ethanol and DMSO was studied. From swelling tests, higher degree of membrane swelling in DMSO (185 %) and a lower degree in ethanol (6 %) was observed, which indicates that cellulose has higher affinity to DMSO than ethanol. Volkov et al. used THF and DMSO as solvents and Remazol Brilliant Blue R as solute in their filtration tests. They observed that DMSO swells cellulose (230%) 6 times more than THF (37%) and a rejection of Remazol Brilliant Blue from DMSO in its solution was higher than from THF (52). They concluded that higher swelling degree of membrane in the solvent leads to improvement in separation performance of membrane since solvent amount in the permeate side increases as affinity of membrane to solvent increases. Likewise, Soltane et al. obtained the negative rejection values of Sudan Blue (-10%) using PDMS membrane with lower degree of membrane swelling in ethanol while higher rejection (99%) was achieved with high amount of swelling in toluene. However, they also studied with Alphazurine using toluene and ethanol feed solutions and observed that the similar rejection values of Alphazurine from these solutions was obtained while toluene swells membrane 20 times more than ethanol. They stated that rejection of solute from its feed solution increases as the affinity between membrane and solute decreases (67). Thus, in addition to the interaction between solvent and membrane, the interaction of solute and membrane in the presence of organic solvent also plays a key role for the separation performance of the membrane due its ability to diffuse through the membrane.

The great extent of swelling of cellulose in DMSO (185 %) may result in the transport of a certain amount of solute with solvent through the opened polymer chains, thereby increase in the amount of solute in permeate side. Thus, rejections of BTB and RB from DMSO, which are the similar for both filtrations of ethanol and DMSO solution although sorbed amount of solutes decreased compared to filtrations

done with ethanol, can be attributed to the high extent swelling of membrane in DMSO. Robinson et al. studied about separation performance of dense PDMS membrane using heptane and xylene as organic solvent and poly-nuclear aromatics and organometallics as solutes. They observed that rejection changed with solvent type and lower rejections were obtained with highly swollen membrane because of the fact that swelling degree of membrane in solvents affects the pore size of membrane and membrane porosity (68). Transport mechanism of solute and solvent through the membrane may not follow solution-diffusion model anymore due to formation of large pore in membrane structure depending on swelling degree. At this point pore flow mechanism was also determinant on transporting of substances. Due to high degree of swelling cellulose membranes lose their highly ordered polymer chain structure, and then solutes are retained by the size exclusion rather than solution-diffusion.

3.5 Effect of Crosslinking on Membrane Performance

Cross-linking is in general used to increase the separation performance of the membrane and to increase their long-term stability. Different cross-linking methods can be used for polymeric membranes such as thermal cross-linking, UV cross-linking and chemical crosslinking.

Figure 4 schematically shows the cellulose chain. Cellulose provides various possibilities for functionalization reactions due to the presence of the hydroxyl groups at positions 2 (the less reactive), 3 (the weakest reactive due to the formation of hydrogen bond with the neighboring oxygen molecule) and 6 (the most reactive due to being linked to a primary carbon) of the glycol groups (58).

In this study, considering the reactivity of the hydroxyl groups of cellulose, chemical crosslinking of cellulose was studied with the aim of transforming OH groups, in order to see the effect of hydrogen bond and electrostatic interactions on solute rejection. Dialdehydes provide thermal stability and increase the resilience and the mechanical strength of cellulose fibers (69). In the scope of this study, glutaraldehyde with high thermal stability (58), and 1,2,3,4-butanetetracarboxylic acid (BTCA), which is capable of forming higher reactive cyclic anhydrides (57),

were used as cross-linking agents for the chemical cross-linking of –OH groups of cellulose.

3.5.1 Crosslinking with Glutaraldehyde

Cellulose membrane was first cross-linked with glutaraldehyde following the process mentioned in section 2.4.1. First of all, the chemical composition of functional groups in the membrane surface was analyzed by XPS. XPS measurements were partially done for both GA-crosslinked and un-crosslinked membrane. To examine functional groups of both membrane carbon bonds were quantitatively analyzed by fitting C1s curve (Figure 33, Figure 34). The binding energy of C-H groups, C-C groups and C-O groups are at 284.8, 286.0 and 288.0 eV, respectively (71).

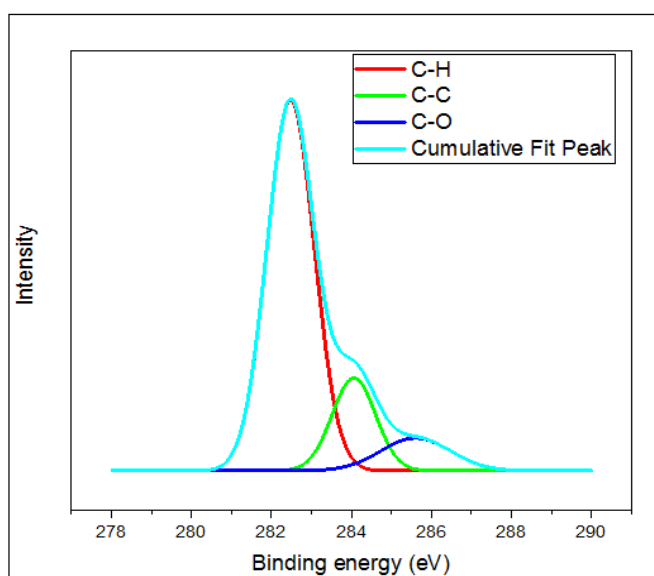


Figure 33: C1s level spectra of KK2D membrane

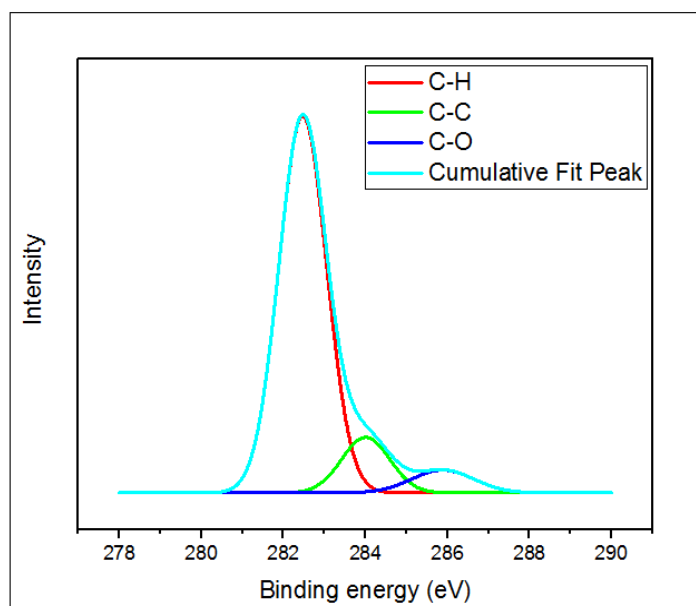


Figure 34: C1s level spectra of KK2G membrane

In Figure 33 and Figure 34, blue lines represent cumulative peak, which was drawn by fitting it into all three peaks for both membrane.

Table 4: Elemental analysis of KK2D and KK2G membranes based on XPS analysis

Peak	Binding energy		Percentage, %	
	KK2D	KK2G	KK2D	KK2G
C-H	282.5	282.5	73.5	83.1
C-C	284.1	284.0	16.9	12.4
C-O	285.6	285.9	9.6	4.5

Table 4 shows the examined binding energies of different carbon groups for both membranes, and also their compositions were calculated by using the area under each curve, which is related to the amount of corresponding group. It was found that there were some changes in the chemical composition of the membrane as a result of crosslinking. For crosslinked membrane, increased amount of C-H bond and thereby decreased amount of other groups when compared to un-crosslinked membrane may indicate the attachment of glutaraldehyde groups to membrane surface.

FT-IR spectra of both un-crosslinked (KK2D) and GA crosslinked (KK2G) membrane were measured to identify chemical bonds in these membranes, which are presented in Figure 35.

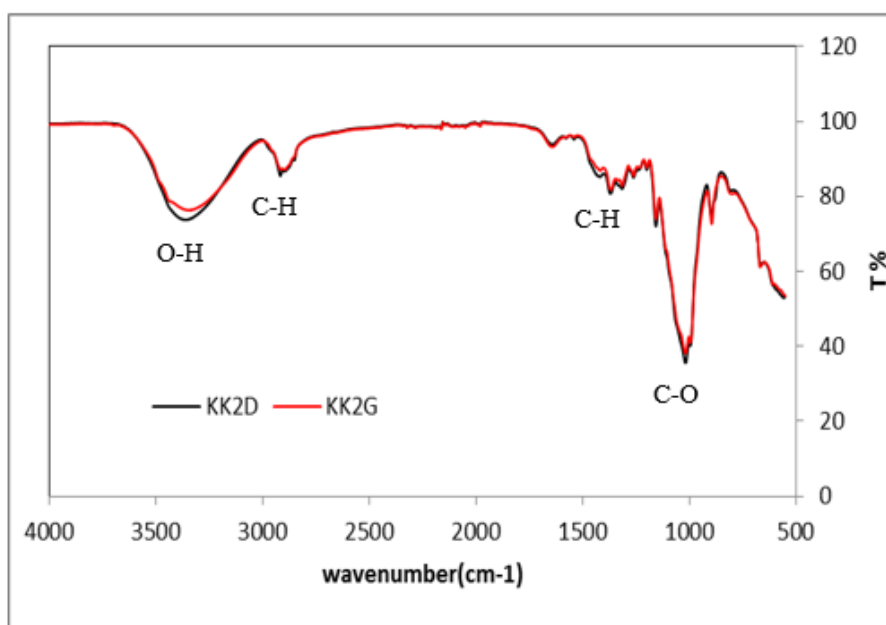


Figure 35: FT-IR Spectrum of KK2D and KK2G membranes

In the typical cellulose pattern represented as black line in Figure 35, a broad band around 3400 cm^{-1} related to O-H stretching, peaks at 2900 cm^{-1} due to stretching of methylene groups and another band at 1090 cm^{-1} corresponding to C-O stretching are represent (18). These peaks with the same distribution were also confirmed for the membrane cross-linked with GA (red line). Considering the GA cross-linking reaction (Figure 11), during GA crosslinking one C-O bond is consumed and new one is created, which indicates that there is no new peak formation in the chemical structure of membrane after the cross-linking reaction. On the other hand, decrease in the O-H stretching band is expected at around 3400 cm^{-1} due to replacing some C-O-H groups with C-O-C groups as a result of the reaction. It is known that glutaraldehyde has two aldehyde groups and connecting of two cellulose chain to these two aldehyde groups was expected during the crosslinking reaction. However, if it was not so, if only one aldehyde group crosslinked with cellulose chain and the other one did not, then in the FT-IR spectrum new peak formation at around 1700

cm⁻¹ can be expected. Wang et al stated that to observe the aldehyde peak in FT-IR spectrum the concentration of glutaraldehyde in its aqueous solution should be higher than 8 % (58). Based on this information, cellulose membranes were crosslinked with different crosslinking conditions shown in Table 5, and their FT-IR analysis was performed Figure 36.

Table 5: Different Glutaraldehyde crosslinking conditions

Glutaraldehyde : H ₂ SO ₄ (%)	Crosslinking medium temperature, °C
0.5 : 1.0	40
1.0 : 2.0	40
2.0 : 4.0	40
1.0 : 1.0	40
2.0 : 1.0	40
8.0 : 1.0	40
0.5 : 1.0	60

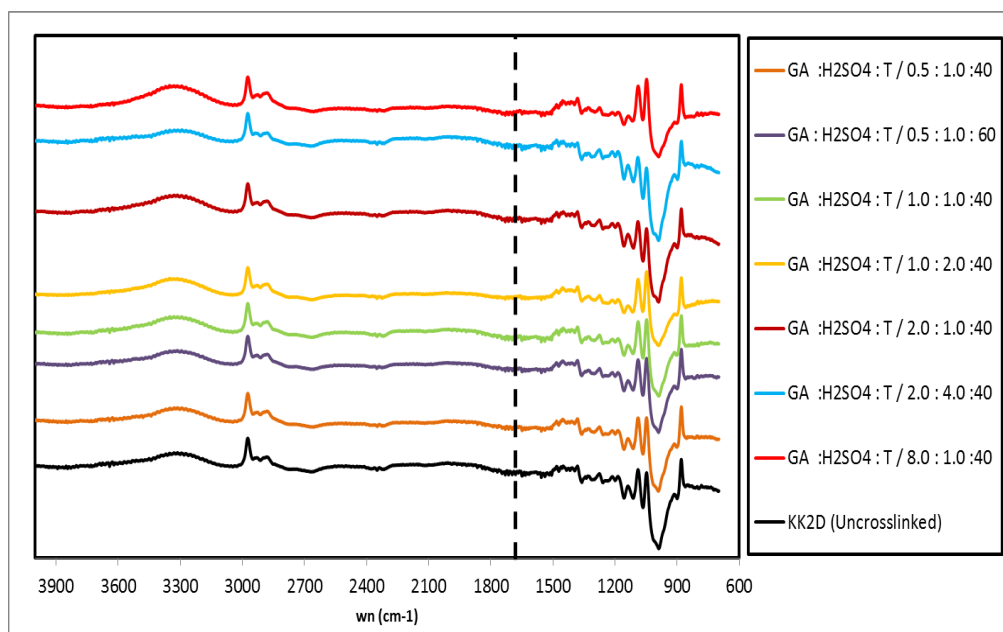


Figure 36: FT-IR spectrum of crosslinked cellulose membrane at different conditions

No new peak formation due to the presence of the aldehyde groups was observed from FT-IR analysis at different crosslinking conditions. Thus, membranes were crosslinked with initial glutaraldehyde crosslinking conditions, which is 0.5 wt % GA, 1.0 wt % H₂SO₄ in aqueous solution at 40 °C. Brown et al. have seen that there is no new peak formation or change in peak positions in the FTIR spectra of crosslinked fibrins with glutaraldehyde indicating that crosslinking was not achieved. On the other hand, they observed that there are significant changes in the mechanical properties of GA-crosslinked fibrins (higher strain and lower creeping) when compared to un-crosslinked one (61).

To examine the effect of crosslinking on mechanical properties of GA-crosslinked and un-crosslinked membrane mechanical test was applied to membranes (Figure 37- Figure 39).

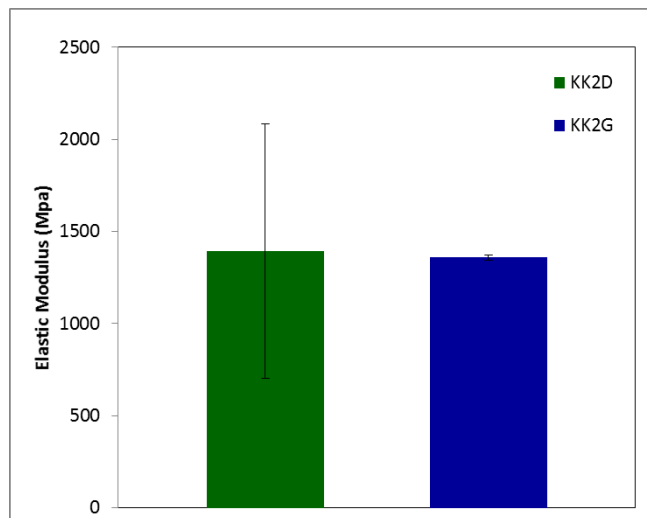


Figure 37: Elastic modulus values of KK2D and KK2G membranes

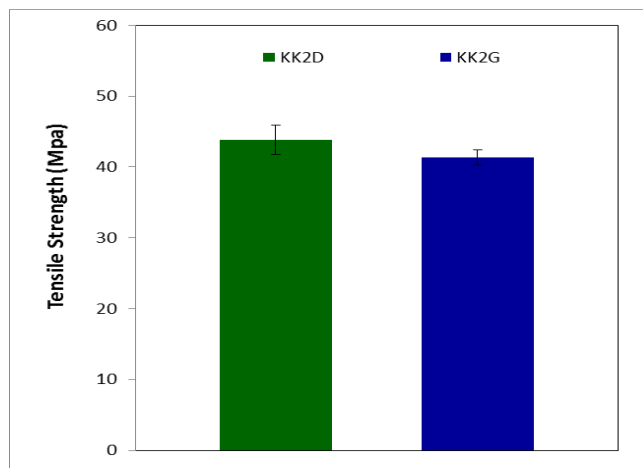


Figure 38: Tensile strength values of KK2D and KK2G membranes

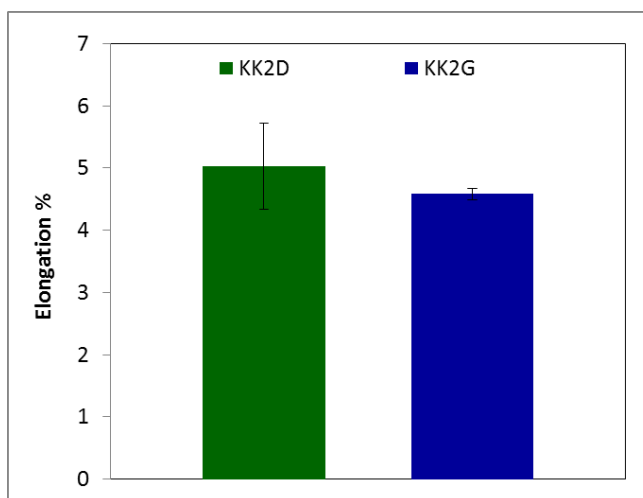


Figure 39: Elongation at break values of KK2D and KK2G membranes

It was observed that the degree of the strain at break and degree of creeping of GA-crosslinked membrane were similar to un-crosslinked membrane indicating that no change in the mechanical properties of cellulose chain after crosslinking.

Performance tests of both membranes (KK2D and KK2G) were done using Bromothymol Blue (BTB), Cresol Red (CR), Rose Bengal (RB) and Crystal Violet (CV) as probe molecule and ethanol as solvent. In Figure 40, rejection values of these solutes in ethanol and ethanol permeance were given.

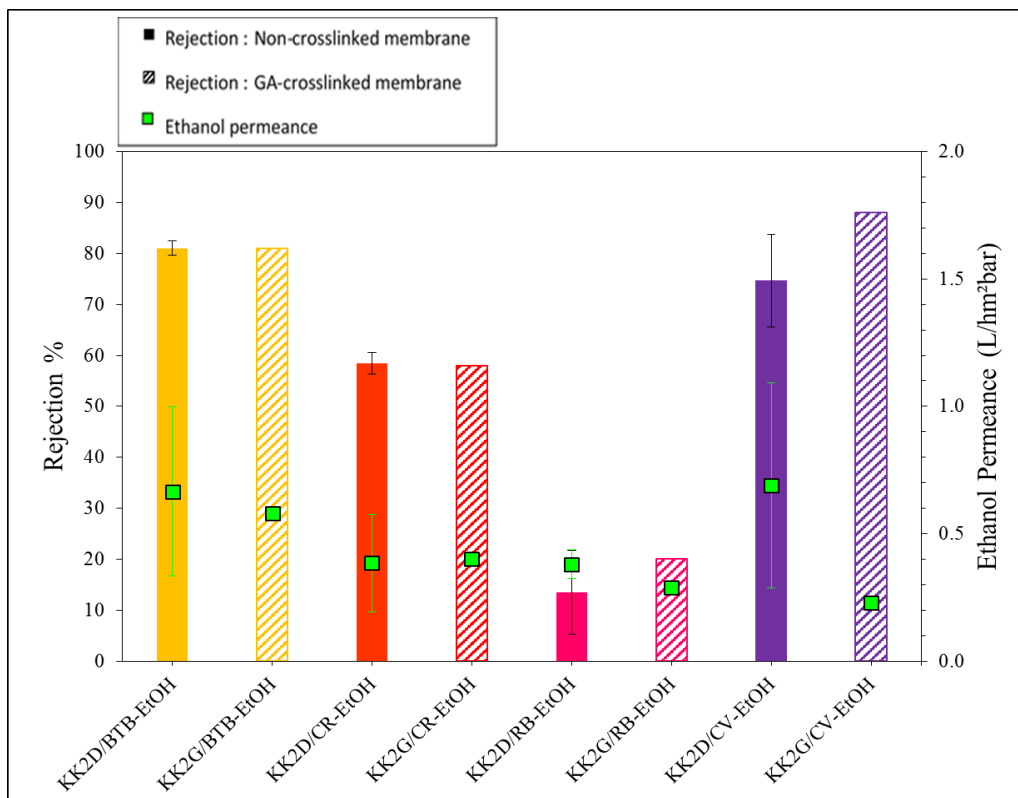


Figure 40: Rejection and permeance values of KK2D and KK2G membrane during the filtration of dye-ethanol solutions

All dyes were rejected from their ethanol solutions at the same ratio by both KK2D and KK2G membranes. From Figure 41, it can be said that after crosslinking of membranes with glutaraldehyde there is no major change in the amount of sorbed dye on the membrane during the filtration, which can be supported by the pictures of membranes taken before and after filtration tests (Figure 42). This indicates that both membranes have the similar affinity to the solutes.

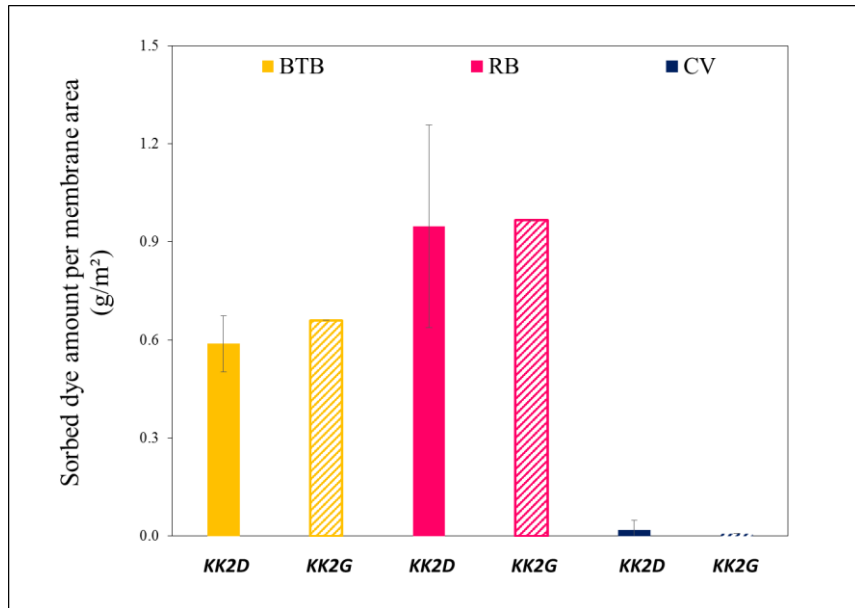


Figure 41: Sorbed dye amount on/in GA crosslinked and uncrosslinked membrane surface during the filtration of different dye-solvent solutions

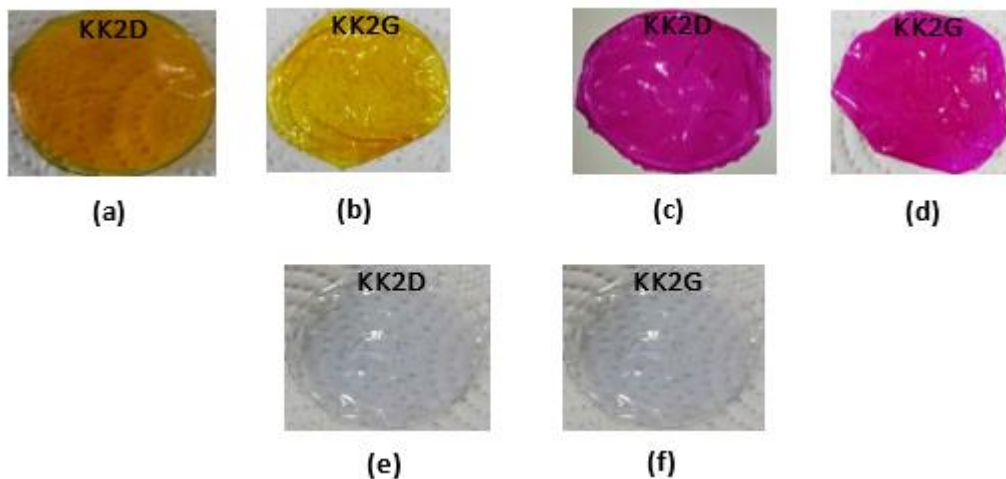


Figure 42: Membrane pictures taken after dye-ethanol solution (a) KK2D-After BTB-Ethanol filtration (b) KK2G-After BTB-Ethanol filtration (c) KK2D-After RB-Ethanol filtration (d) KK2G-After RB-Ethanol filtration (e) KK2D-After CV-Ethanol filtration (f) KK2G-After CV-Ethanol

3.5.2 Crosslinking with 1,2,3,4- butanetetracarboxylic acid

Cellulose membrane was also cross-linked with one of the polycarboxylic acids, which is 1,2,3,4-butanetetracarboxylic acid (BTCA), following the process mentioned in section 2.4.2. FT-IR spectra of both un-crosslinked (KK2D) and BTCA crosslinked (KK2B) membrane are given in Figure 43.

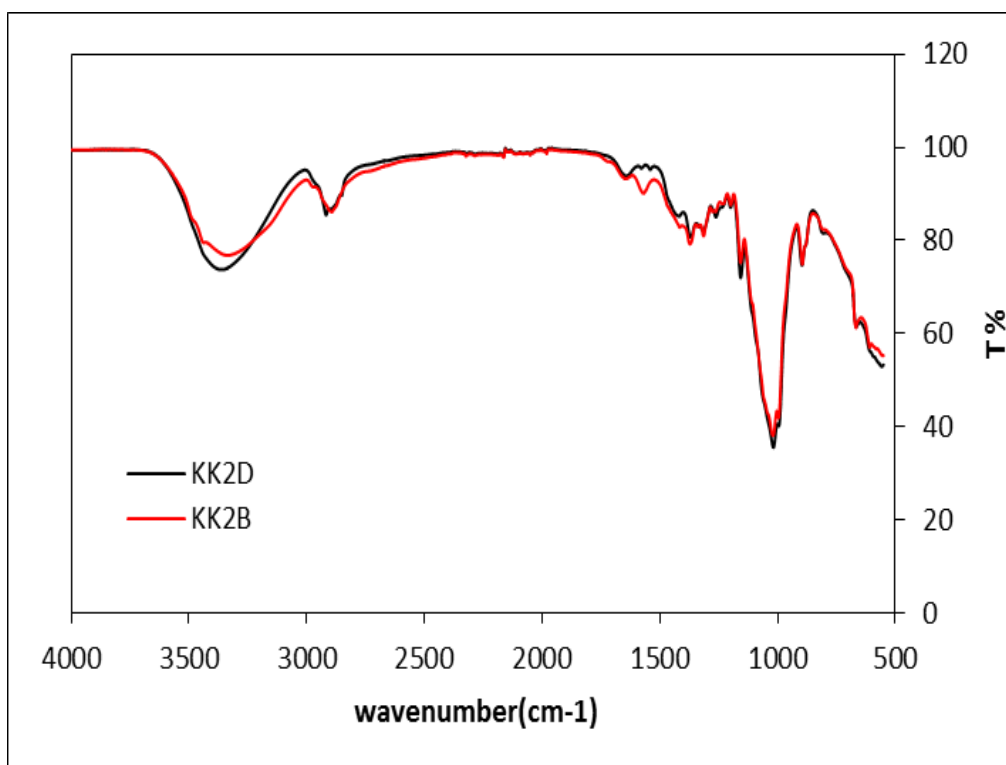


Figure 43: FT-IR spectrum of BTCA crosslinked cellulose membrane

In the FTIR spectra of BTCA-crosslinked membrane KK2B (red line), a new peak formation was observed at around 1500-1600 cm^{-1} when compared to typical cellulose pattern KK2D (black line). It is known that a peak at 1600-1800 cm^{-1} is due to the presence of C=O bond of carboxylic acid (54). With the light of this information, it can be said that this peak, which is different from the un-crosslinked membrane, belongs to the C = O bond in the BTCA crosslinked membrane.

To examine the effect of crosslinking on membrane mechanical properties mechanical test was applied to both dried membranes and membrane immersed into DMSO (wet) (Figure 46-Figure 44).

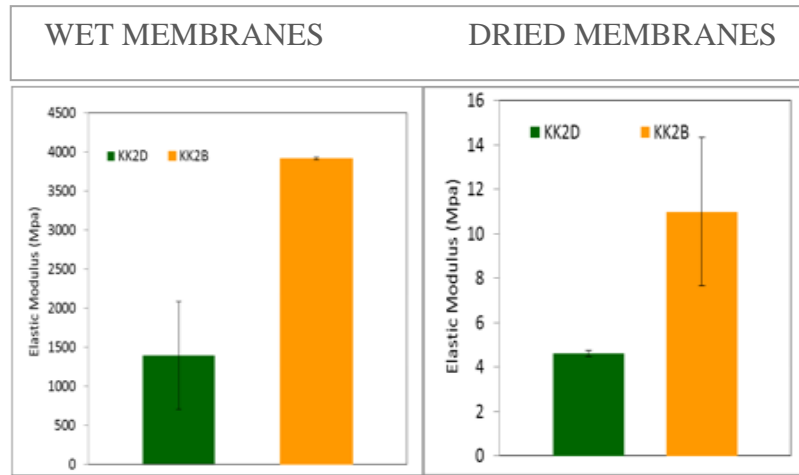


Figure 44: Elastic modulus of KK2D and KK2B membranes

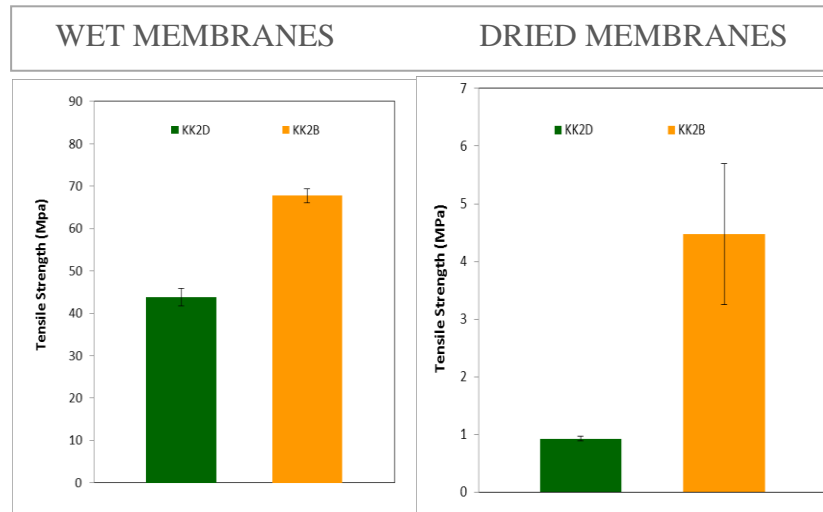


Figure 45: Tensile strength values of KK2D and KK2B membranes

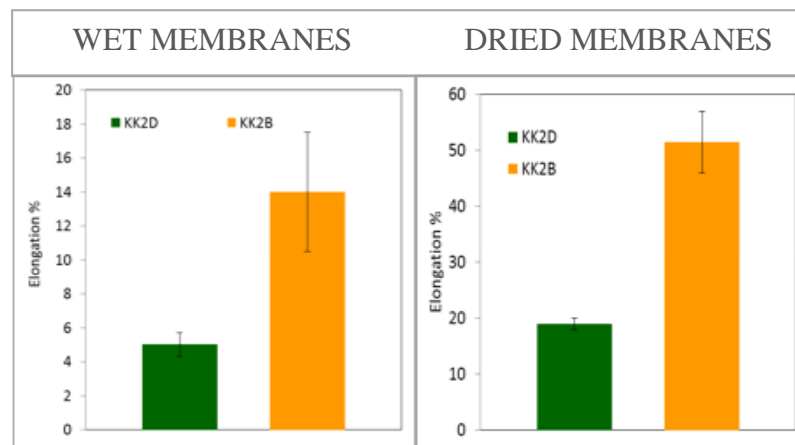


Figure 46: Elongation at break values of KK2D and KK2B membranes

For both cases (dried and wet membrane testing) BTCA-crosslinked membrane has higher elastic modulus than un-crosslinked membrane. Increased elastic modulus, tensile strength and elongation of the membranes after crosslinking reaction with BTCA is the evidence that the reaction between BTCA and cellulose occurs at a certain degree.

XRD patterns of un-crosslinked, GA crosslinked and BTCA crosslinked membranes are given in Figure 47, in which x-axis showing data of 2θ degree was kept at the same scale for all membranes while intensity data on y-axis were shifted away. To compare the crystallinities of membranes the peak heights at 12.3° were considered since it was known that the peak at around 20° is seen for amorphous materials. Comparing heights of peaks at 12.3° , un-crosslinked (KK2D) and GA crosslinked membrane (KK2G) have nearly the same depths at 12.3° , which indicates that membranes have similar structure in terms of crystallinity. On the other hand, BTCA crosslinked membrane has higher depth at 12.3° , and it can be said that crystallinity of membrane increased as a result of crosslinking with BTCA when compared to un-crosslinked membrane.

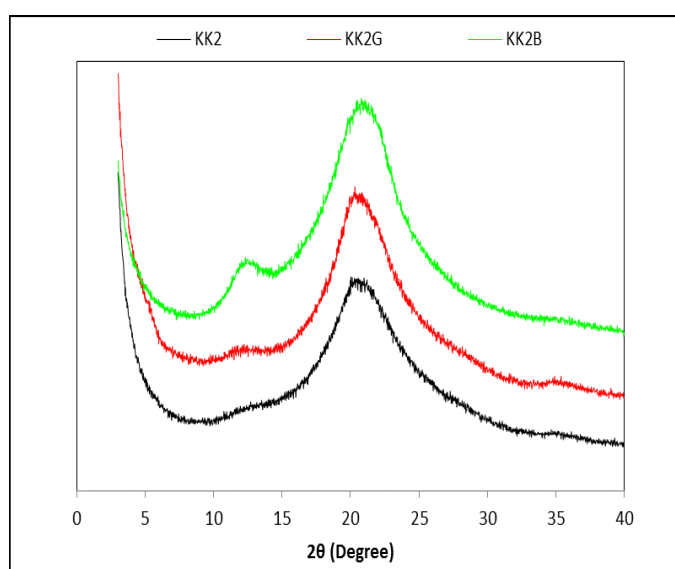


Figure 47: XRD pattern of crosslinked and un crosslinked membranes

Performance tests of both membrane (KK2D and KK2B) were done using Bromothymol Blue (BTB), Rose Bengal (RB) and Crystal Violet (CV) as probe molecule, ethanol and dimethyl sulfoxide as solvent. In Figure 48, rejection values of these solutes in ethanol and ethanol permeance were shown.

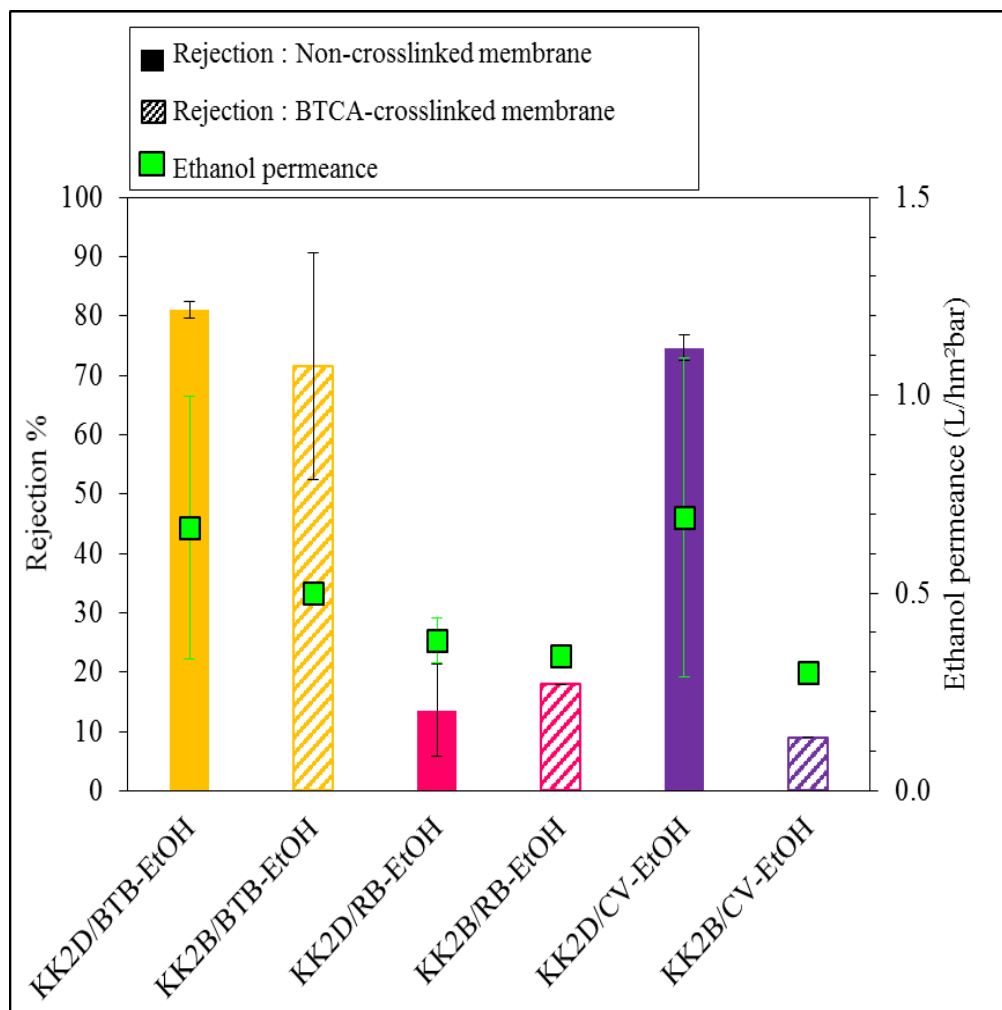


Figure 48: Rejection and permeance values of BTCA-crosslinked and uncrosslinked membrane during the filtration of BTB, RB and CV from their ethanol solutions

It was observed that there is no major change after crosslinking of membranes with BTCA in neither rejection of BTB and RB from their ethanol solutions nor ethanol permeance of membranes while the rejection of CV by the membrane KK2B was lower than that of CV by the membrane KK2D, the rejection decreased significantly after crosslinking. From the swelling test, it was observed that swelling ratio of the BTCA-crosslinked membrane in ethanol was as low as the swelling ratio of un-

crosslinked membrane while BTCA-crosslinked membrane swelled less in DMSO when compared to un-crosslinked membrane, which indicates that the affinity of the membrane to DMSO decreases after crosslinking with BTCA. In section 3.3, it was concluded that less amount of sorbed CV on the membrane and high rejection of CV by KK2D membrane indicates that cellulose membrane (un-crosslinked) has low affinity to a positively charged dye CV. Decrease in the rejection of CV by the membrane and increased amount of sorbed CV on the membrane after BTCA cross-linking (Figure 49) indicates that the affinity of the membrane to CV increased significantly implying increased the interaction between the membrane and positively charged dye.

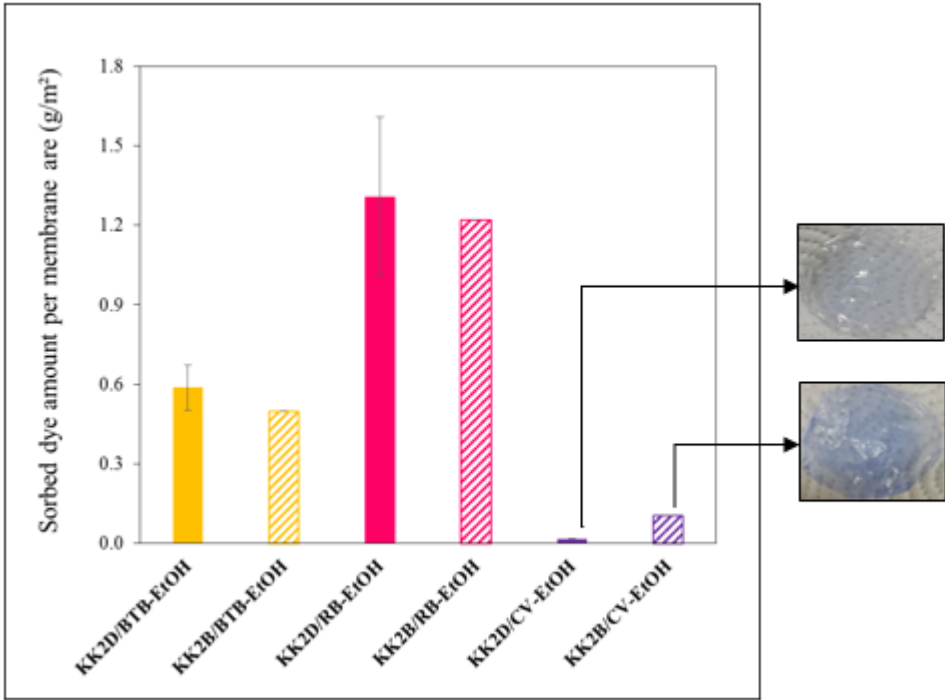


Figure 49: Sorbed dye amount on/in BTCA crosslinked and uncrosslinked membrane surface during the filtration of different dye-solvent solutions

In Figure 50, rejection values of solutes in DMSO and DMSO permeance were shown.

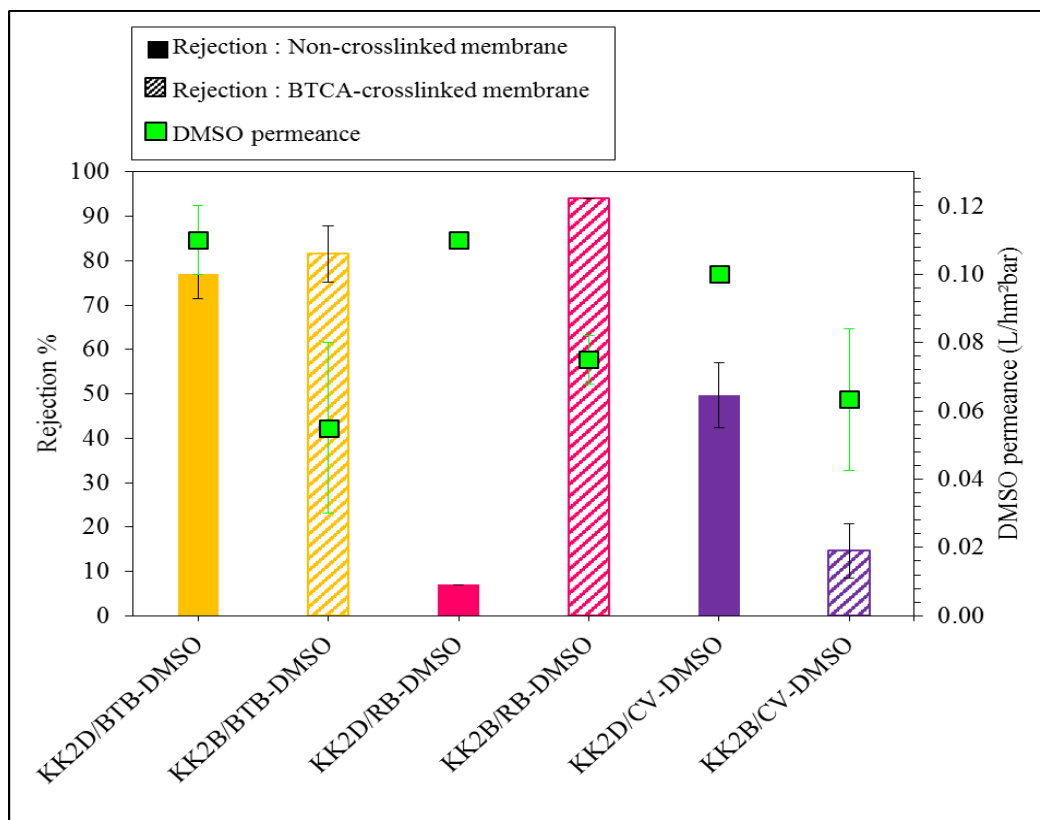


Figure 50: Rejection and permeance values of BTCA-crosslinked and uncrosslinked membrane during the filtration of BTB, RB and CV from their DMSO solutions

It was observed that the rejections of BTB from its DMSO solution by both membrane are quite close to each other. RB rejection of membrane crosslinked with BTCA increases significantly while CV rejection decreases slightly. Changes in rejection of charged dyes from their DMSO solutions and the amount of sorbed dye in membrane during filtration show that the affinity between dye and membrane is changing after crosslinking of membranes with BTCA.

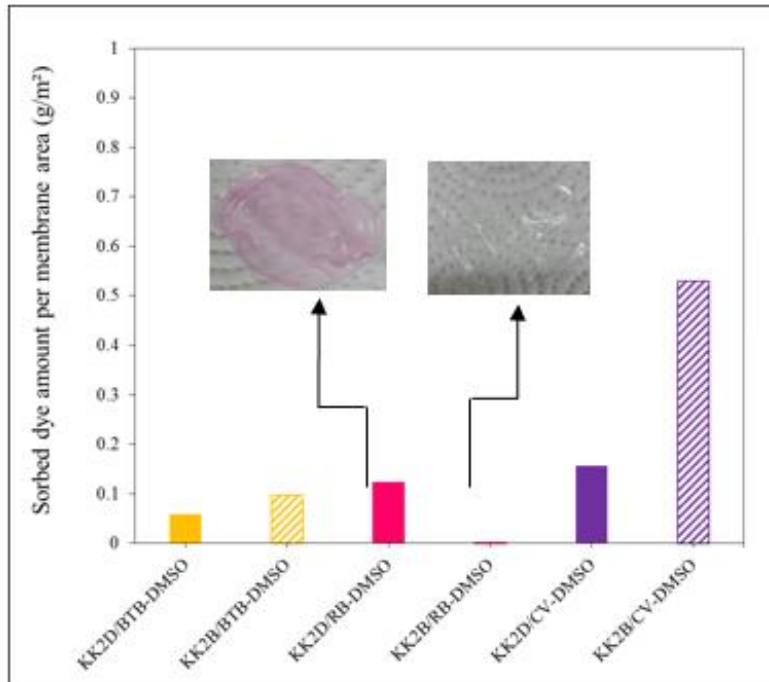


Figure 51: Sorbed dye amount on/in BTCA crosslinked and uncrosslinked membrane surface during the filtration of different dye-DMSO solutions

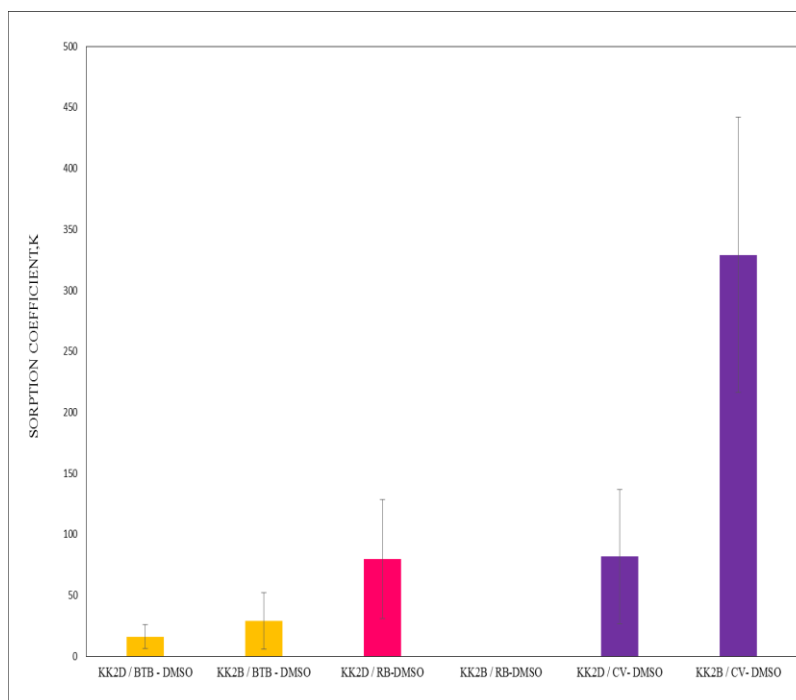


Figure 52: Sorption coefficient of each solute in DMSO solutions

From Figure 51 and Figure 52, it was seen that the amount of sorbed RB in BTCA-crosslinked membranes during both filtration and sorption test decreases significantly whereas sorbed CV amount in crosslinked membrane increases compared to uncross-linked membrane, which may explain the increased RB rejections and decreased CV rejection. It is known that there are four –COOH groups in BTCA chemical structure and crosslinking reaction occurs between these COOH groups and –OH groups of cellulose. During the reaction, binding of all –COOH groups in BTCA to cellulose may not occur, and if it so, after crosslinking cellulose now contains unreacted –COOH groups. These unreacted groups may have caused cellulose to be charged with negative charge, and thereby considering electrostatic repulsion-attraction negatively charged membrane may have resulted in higher rejection of negatively charged dye RB and lower rejection of positively charged dye CV.

3.6 Solvent stability

Within the scope of this study, the performance of cellulose membranes was tested in ethanol and dimethyl sulfoxide solutions. From these tests, it was observed that cellulose membranes were stable with unchanged performance in ethanol and DMSO, which is an aggressive organic solvent, for up to at least 10 days after swelling of membrane in solvents remains constant. To predict the stability of the membranes in different harsh organic solvents, membranes were soaked in acetone, ethyl acetate, hexane, tetra-hydrofuran, N-methyl-2-pyrrolidone and toluene for a month. After this period, dried membrane weight before soaking the membrane in solvent and wet membrane weight were compared and swelling ratios of membranes in all these organic solvents were measured as lower than 1 %. Membranes were observed to swell at very low degree like ethanol, which is a promising performance for application of cellulose membranes in harsh aprotic solvents.

3.7 Crossflow Filtration

As mentioned in Chapter 1, membranes are performed in two type of filtration modes: dead-end filtration and cross-flow filtration. In this study, cellulose membranes produced in lab-scale first were tested in dead-end filtration due to easy installation and to be comparable to other studies in the literature performed at lab-scale setups in dead-end filtration. In industrial applications, the membrane applications are generally studied in cross-flow mode, thus the filtration tests of produced cellulose membranes were also carried out at cross-flow mode to be comparable to real-life applications.

In cross-flow mode, dried membrane (KK2D) performance was tested with the filtration tests in which BTB, RB and CV were used as solute and ethanol used as organic solvent (Figure 53-Figure 55).

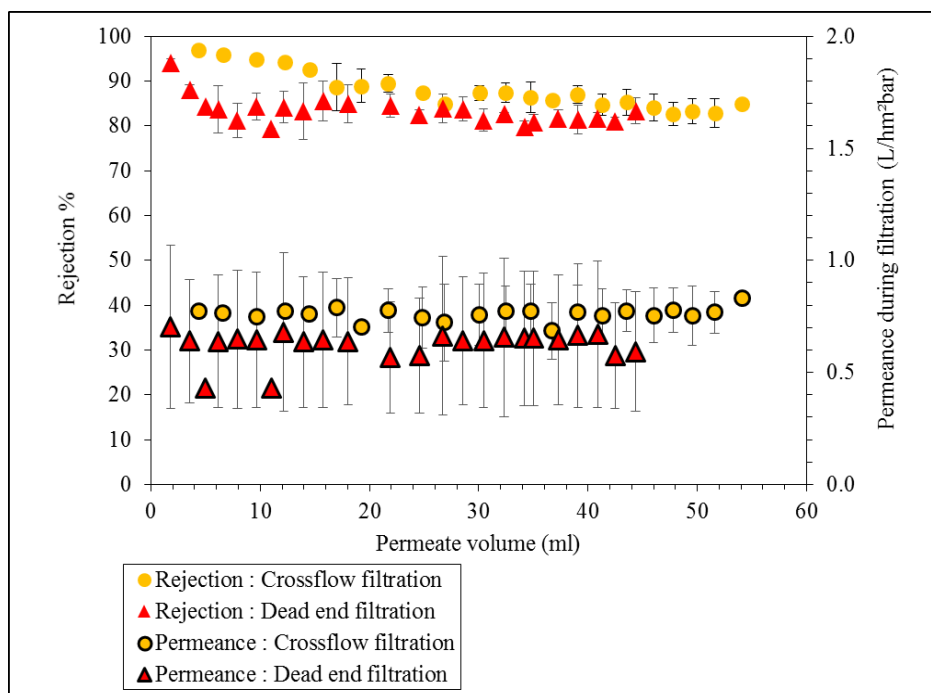


Figure 53: Comparison of KK2D separation performance during BTB-Ethanol filtration in dead-end and crossflow mode

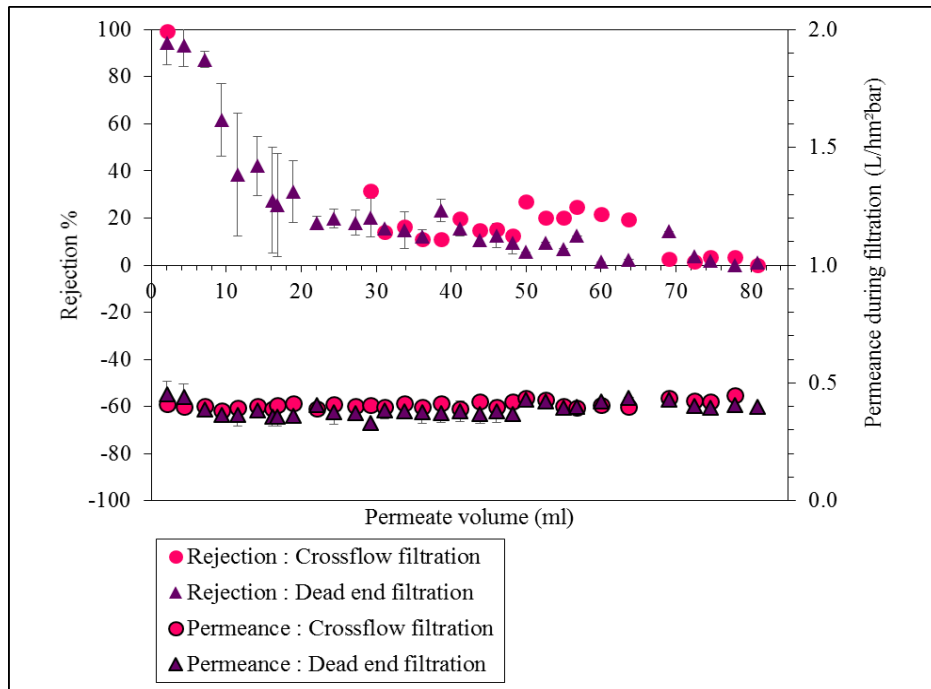


Figure 54: Comparison of KK2D separation performance during RB-Ethanol filtration in dead-end and crossflow mode

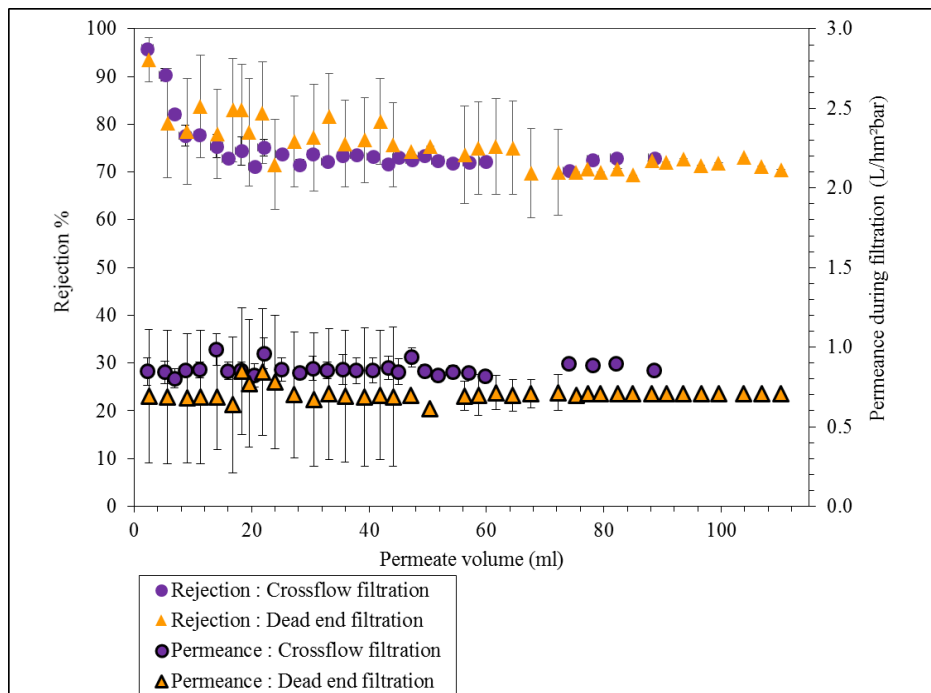


Figure 55: Comparison of KK2D separation performance during CV-Ethanol filtration in dead-end and crossflow mode

In dead-end filtration of cellulose membranes, it was observed that Bromothymol Blue ($81\pm 1\%$) and Crystal Violet ($75\pm 9\%$) were rejected from their ethanol solution at a moderate degree by the membrane KK2D while for both KK2D and KK2B membrane the rejection of Rose Bengal ($13\pm 5\%$) from its ethanol solution was very low. Membranes showed the same performance in cross-flow filtration mode with all solute-solvent solutions, which indicates that membranes done in lab scale have reproducible performance at both filtration modes, thereby promising real-life applications in industrial scale.

3.8 Effect of Feed Concentration

The separation performance of membranes was investigated with the filtration of different solute-solvent solutions at constant concentration, which is 0.05 mM. To illustrate the effect of the feed concentration on the separation performance of membranes (KK2D) different feed concentrations of Bromothymol Blue-ethanol solution were studied in cross-flow filtration mode (Figure 56 and Table 6).

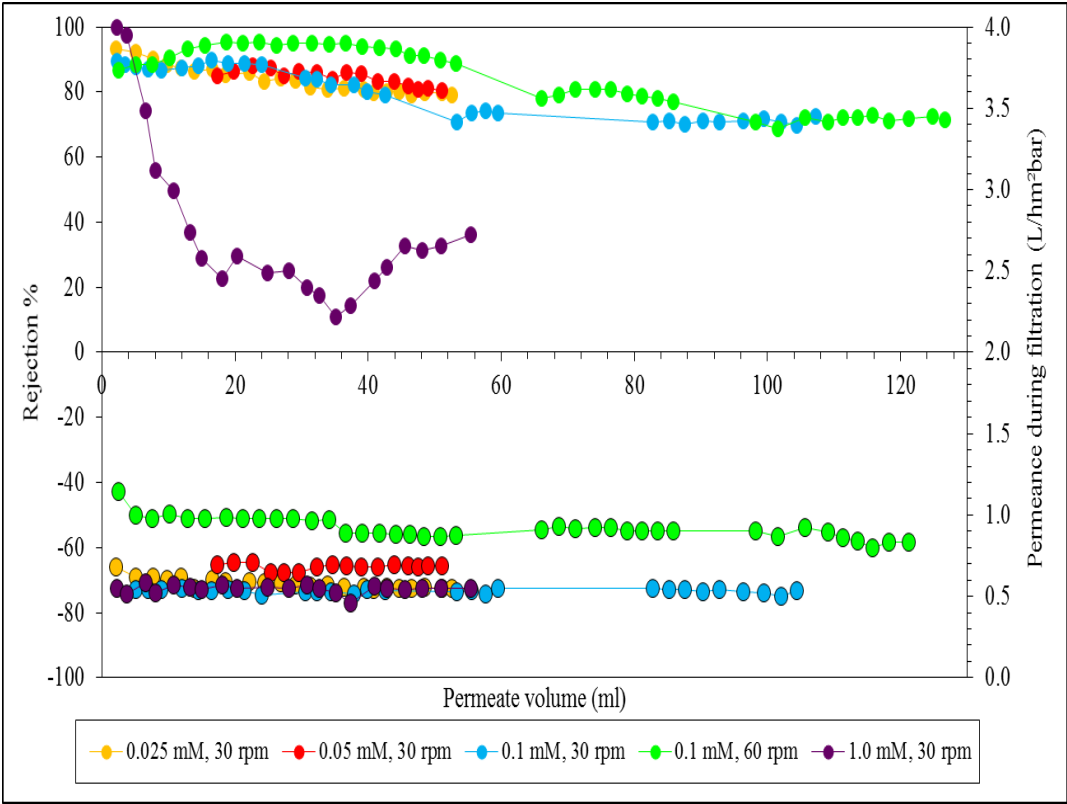


Figure 56: KK2D separation performance during filtration of BTB-Ethanol solutions at different concentration

Table 6: KK2D BTB-Ethanol filtration at different concentration

	Feed Concentration (mM)	Crossflow Velocity (rpm)	Rejection %	Permeance (L/hm²bar)
KK2D	0.025	30	81	0.50
	0.05	30	81	0.55
	0.10	30	70	0.50
	0.10	60	70	0.80
	1.00	30	<40	0.50

Firstly, 0.025 mM BTB-solution was filtrated through the membrane (yellow line). The rejection of BTB from its 0.025 mM ethanol solution was found as 81 ± 1 % while permeance of the membrane was around 0.5 L/hm²bar and remained constant during the filtration. The membrane showed the same separation performance with both 0.025 mM and 0.05 mM feed concentration. After these filtrations, the membrane was performed at higher feed concentration than 0.05 mM. Blue line shows the rejection and permeance of the membrane during the filtration of 0.1 mM BTB-ethanol solution. Permeance of the membrane was found as 0.5 L/hm²bar while the rejection of BTB from its ethanol solution decreased to 70 %. Compared to filtration tests performed at lower concentration than 0.1 mM, this decline in BTB rejection from 80 % to 70 % may be resulted from the accumulation of solutes at the membrane surfaces due to increased feed concentration, and this causes concentration polarization. Considering this possibility cross flow velocity, which is the determining parameter of mass transfer, increased to 60 rpm to examine whether concentration polarization occurs at membrane surface or not. If it is so, increasing cross flow velocity is aimed to reduce concentration polarization by increasing shear force, which is sweeping solutes away from the membrane surface.

Green line shows the rejection and permeance of KK2D membrane during the filtration of 0.1 mM BTB-ethanol solution at 60 rpm. At constant TMP, increasing cross flow velocity to 60 rpm resulted in increase of the solvent and/or solution flux, thereby increase in the permeance compared to the velocity of 30 rpm. The rejection of BTB from its ethanol solution decreased down to 70 %, which is similar with the filtration of 0.1 mM BTB-ethanol solution at 30 rpm. Therefore, it can be said that

decreasing rejection with increasing feed concentration was not related to concentration polarization since there is no difference (increase) in the rejection of solute with increasing cross-flow velocity. This filtration took 3 days, and after 100 ml permeate filtrated through the membrane, the rejection remained constant at the value of 70 %.

Crossflow filtration tests were performed until constant rejection values achieved. Filtration time and permeate volume required the constant rejection were not the same for all BTB-Ethanol filtrations. For the filtration of 0.05 mM BTB-ethanol solution, both filtration time and permeate volume (<60 ml) are lower than the one with 0.10 mM feed solution (>100 ml). Increasing feed concentration (increasing the amount of solute in feed solution) may cause an increase in the amount of solute (BTB) sorbed on the membrane surface/pore walls during the filtration and hence hindering the transport of solvent based on solution-diffusion mechanism.

To see the result of further increasing feed concentration it is significantly increased to 1.0 mM (purple line). It was observed that the permeance of solvent remained constant while the rejection of solute significantly decreased with further increasing feed concentration possibly due to excess sorbed solute on membrane. In this study, the highest rejection of BTB from its ethanol solution achieved with 0.05 mM feed concentration.

3.9 The Recovery of Homogenous Catalyst

In many processes including catalytic reactions such as pharmaceutical production, epoxidation of olefins the recovery of homogenous catalyst from reaction medium is a major problem including the extensive and destructive separation mechanism. Nowadays, there is new interest in the solvent resistant nanofiltration membranes for the efficient separation of homogenous catalysis from the medium with organic solution (13). In one of the recent studies, Scarpello et al. investigated a study about the nanofiltration of homogenous catalysts commonly used in commercial organic synthesis, which are the Jacobsen catalyst, the Wilkinson catalyst and Pd-BINAP, from a series of organic solvents, which are ethyl acetate, tetrahydrofuran and dichloromethane, using OSN membranes (18). They observed that 95 % rejection of catalyst from their organic solutions with 50 l/m²bar fluxes at 2.0 MPa, which imply

that the membrane technology has considerable potential in the recovery of homogenous catalysts. In this study, the separation of Jacobsen catalyst from its ethanol solution was studied using cellulose membranes in dead-end cell under 10 bar. In Figure 57, the rejection of Jacobsen catalyst and solution permeance during the filtration were given.

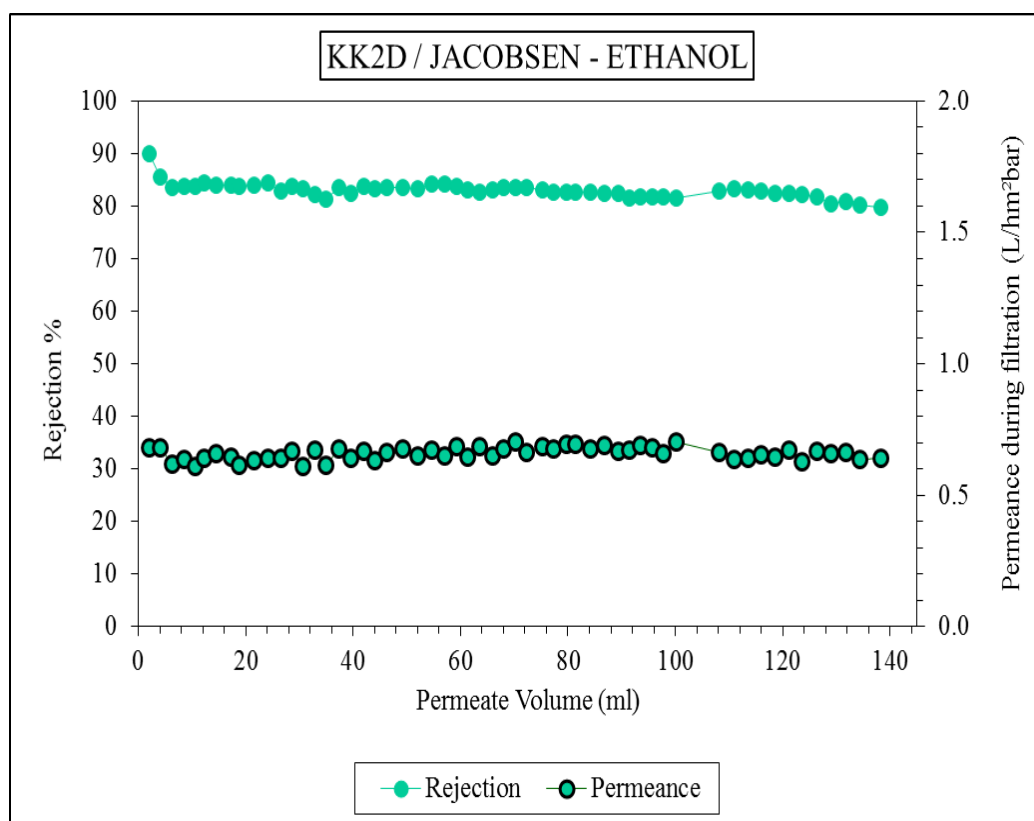


Figure 57: KK2D Jacobsen catalyst separation performance from its ethanol solution

Jacobsen catalyst was retained by KK2D membrane at the ratio of 80 % with the permeance around 0.6 L/hm²bar, and membrane was stable with unchanged performance in ethanol from the beginning of the filtration. To achieve higher recovery of the catalyst from its ethanol solution this single filtration stage can be arranged in multistage membrane cascades, thereby catalyst can be recovered with the highest ratio.

CHAPTER IV

CONCLUSION

In this study, cellulose was used as an alternative polymer to Organic Solvent Nanofiltration for being stable in many organic solvents due to its inter- and intra-molecular hydrogen bonds. Cellulose membranes were fabricated via phase inversion using 1-ethyl-3-methylimidazolium ([EMIM]OAc) as ionic liquid to dissolve cellulose. Acetone was used as cosolvent and water as nonsolvent. To investigate the separation mechanism of solutes through cellulose membrane five probe molecules showing difference in both molecular size and molecular charge were selected. Two of them are neutral dye such as Bromothymol Blue (BTB, 624 Da, $\tilde{V}_m=251.1\text{cm}^3/\text{mole}$) and Cresol Red (CR, 382 Da, $\tilde{V}_m=140.1\text{cm}^3/\text{mole}$), another two of these solutes are negatively charged dye like Bengal (RB, 1017 Da, $\tilde{V}_m=241.0\text{cm}^3/\text{mole}$) and Brilliant Blue R (BBR, 826 Da, $\tilde{V}_m=421.3\text{cm}^3/\text{mole}$) and last of them is a positively charged dye, Crystal Violet (CV, 407 Da, $\tilde{V}_m=253.7\text{cm}^3/\text{mole}$). Type of solvent was also studied, ethanol was used as a polar solvent and dimethyl sulfoxide was chosen as an aprotic solvent. Cellulose membranes in pristine and crosslinked form were tested with the filtration of five different probe molecules from their solutions in ethanol and DMSO.

All cellulose membranes were cast from the same polymer dope solution, and thereby the polymer concentration in dope solution is not a parameter that affect the separation performance of cellulose membranes fabricated within the scope of this study. The effect of drying post treatment after coagulation was examined. As a result of drying process, the rejection of BTB increased from 40 % to 80 % while solution permeance through the membrane decreased from 11 L/hm²bar to 0.47 L/hm²bar. Drying post treatment causes collapsing the porosity existing within the membrane structure and thereby the membranes becomes tighter. It was observed that solution permeance was not changed during the filtration test and its value was equal to pure solvent permeance value. This indicated that there was no cake formation and dye accumulation on the membrane surface, and thereby fouling and

concentration polarization on the membrane were negligible. Colored membrane and their microscope images taken after filtrations tests show that dyes can be sorbed across the cross section of the membrane instead of accumulation on the membrane surface. Both non-dried membrane and dried membrane were tested at two different operating pressures, 4 and 10 bar, using 0.05 mM BTB-ethanol solution. Dried membrane has the same rejection value of around 80 % at 4 bar and 10 bar while rejection of BTB of non-dried membrane slightly decreased from 50 % to 40 % and the amount of sorbed dye on membrane increased 0.09 to 0.65 g/m² indicating that sorbed dye within the membrane pores and thereby in permeate side increases with increasing operating pressure. Drying post treatment contributed to denser and tighter membrane structure, and thus leads to more stable separation performance of cellulose membrane.

Using five different solutes varying in both molecular size and charge, separation mechanism of cellulose membranes was investigated. Rejection of BTB from its ethanol solution in higher ratio than CR shows that molecular size is a determining factor for the separation of neutral dyes. On the other hand, the similar rejection of BTB and CV by the membrane were obtained while RB was retained at lowest ratio although these three dyes have similar molecular size. This indicates that not only molecules' size is linked to solvent-solute transport through the membrane, but also solute-solvent-membrane interaction is a determinant factor for the separation performance of cellulose membranes. Cellulose membranes were crosslinked with glutaraldehyde solution at different crosslinking conditions for further post treatment. Both solvent permeance and separation of solutes by the membrane did not change as a result of GA crosslinking. Membranes were also crosslinked with BTCA solution, and these membranes were tested with solute-DMSO solution. As a result of BTCA crosslinking, rejection of CV by the membrane decreases slightly while RB rejection increases significantly, which may be resulted from electrostatic repulsion-attraction between charged solute due to unreacted -COOH groups of BTCA causing negatively charged membrane. Both solute rejections in DMSO and sorbed dye amount within the membrane changed, implying that the affinity between solute and membrane is changing after BTCA crosslinking. The amount of sorbed CV in membranes crosslinked with BTCA during filtration increases whereas sorbed RB amount in crosslinked membrane decreases significantly compared to un-crosslinked

membrane, which may explain decreased CV rejection and the increased RB rejections.

Changes in membrane structure and properties after crosslinking were also examined using FT-IR, XRD, mechanical test and swelling test. According to mechanical test, less elastic membranes were obtained while tensile stress of the membranes increased after BTCA crosslinking, which implies that BTCA crosslinking has occurred in the membranes. Cellulose membranes were stable with unchanged performance in ethanol and DMSO, which is an aggressive organic solvent, for up to 10 days. All membranes (crosslinked and un-crosslinked) were also immersed into acetone, ethyl acetate, hexane, tetra-hydrofuran, toluene and NMP for a month. In these solvents, all of membranes swelled in the value of lower than 1 %, which is a promising performance for application of cellulose membranes in harsh aprotic solvents.

All filtration tests were conducted in dead-end filtration. Filtration tests of some of the cellulose membranes were also performed at cross-flow mode to be comparable to real-life applications. Membranes showed the same performance in cross-flow filtration mode with all solute-solvent solutions tested, which indicates that performance tests done in lab scale have reproducible performance at both filtration modes, thereby promising real-life applications in industrial scale.

KK2D membranes were tested with different feed concentrations of BTB-ethanol solutions in cross-flow filtration mode to observe the effect of feed concentration. The membrane showed the same separation performance at both 0.025 mM and 0.05 mM feed concentration. However, when feed concentration was increased to 0.1 mM, rejection of BTB decreased to 70 % with the unchanged solvent permeance at different crossflow velocity. To see the result of further increasing feed concentration BTB concentration in feed solution is significantly increased to 1.0 mM, and with further increasing feed concentration the permeance of solvent remained constant while the rejection of solute significantly decreased possibly because of excess sorbed solute on membrane. The filtration of Jacobsen catalyst from its ethanol solution was performed using cellulose membranes in dead-end mode. Jacobsen catalyst was retained at the ratio of 80 % with the permeance around 0.6 L/hm²bar, and membrane remains stable with unchanged performance in ethanol from the

beginning of the filtration. To achieve higher recovery of the catalyst from its ethanol solution this single filtration stage can be arranged in multistage membrane cascades, thereby catalyst can be recovered with the highest ratio.

REFERENCES

1. Marchetti, P., Jimenez Solomon, M. F., Szekely, G., & Livingston, A. G. (2014). Molecular separation with organic solvent nanofiltration: A critical review. *Chemical Reviews*, 114(21), 10735–10806.
2. P. Vandezande, L.E.M Gevers, I.F.J Vankelecom, Solvent resistant Nanofiltration: Separating on a molecular level, *Chem. Soc. Rev.*, 37 (2008) .
3. Baker, R. W. (2004). *Membrane Technology and Applications*. Membrane Technology.
4. Van der Bruggen, B., Schaep, J., Maes, W., Wilms, D., & Vandecasteele, C. (1998). Nanofiltration as a treatment method for the removal of pesticides from ground waters. *Desalination*, 117(1-3), 139-147.
5. Application of nanofiltration for removal of pesticides, nitrate and hardness from ground water: rejection properties and economic evaluation. (2001). *Journal of Membrane Science*, 193(2), 239-248.
6. Montovay, T., Assenmacher, M., and Frimmel, F. H. (1996). Elimination of pesticides from aqueous solution by nanofiltration. *Magyar Kemiai Folyoirat* 102(5), 241–247.
7. Berg, P., Hagemeyer, G., & Gimbel, R. (1997). Removal of pesticides and other micropollutants by nanofiltration. *Desalination*, 113(2-3), 205-208.
8. Schaep, J., Van der Bruggen, B., Uytterhoeven, S., Croux, R., Vandecasteele, C., Wilms, D., Vanlerberghe, F. (1998). Removal of hardness from groundwater by nanofiltration. *Desalination*, 119(1-3), 295-301.
9. Sombekke, H., Voorhoeve, D., & Hiemstra, P. (1997). Environmental impact assessment of groundwater treatment with nanofiltration. *Desalination*, 113(2-3), 293-296.
10. Tang, C., & Chen, V. (2002). Nanofiltration of textile wastewater for water reuse. *Desalination*, 143(1), 11-20.

11. Mohsen, M. S., Jaber, J. O., & Afonso, M. D. (2003). Desalination of brackish water by nanofiltration and reverse osmosis. *Desalination*, 157(1-3), 167.
12. SOURIRAJAN, S. (1964). Separation of Hydrocarbon Liquids by Flow Under Pressure Through Porous Membranes. *Nature*, 203(4952), 1348-1349.
13. Priske, M., Lazar, M., Schnitzer, C., & Baumgarten, G. (2016). Recent Applications of Organic Solvent Nanofiltration. *Chemie Ingenieur Technik*, 88(1-2), 39–49.
14. Gould, R. M., White, L. S., & Wildemuth, C. R. (2001). Membrane separation in solvent lube dewaxing. *Environmental Progress*, 20(1), 12-16.
15. Geens, J., De Witte, B., & Van der Bruggen, B. (2007). Removal of APIs (Active Pharmaceutical Ingredients) from Organic Solvents by Nanofiltration. *Separation Science and Technology*, 42(11), 2435-2449.
16. Sereewatthanawut, I., Lim, F. W., Bhole, Y. S., Ormerod, D., Horvath, A., Boam, A. T., & Livingston, A. G. (2010). Demonstration of Molecular Purification in Polar Aprotic Solvents by Organic Solvent Nanofiltration. *Organic Process Research & Development*, 14(3), 600-611.
17. Sheth, J. P., Qin, Y., Sirkar, K. K., & Baltzis, B. C. (2003). Nanofiltration-based diafiltration process for solvent exchange in pharmaceutical manufacturing. *Journal of Membrane Science*, 211(2), 251-261.
18. Scarpello, J. T., Nair, D., Freitas Dos Santos, L. M., White, L. S., & Livingston, A. G. (2002). The separation of homogeneous organometallic catalysts using solvent resistant nanofiltration. *Journal of Membrane Science*, 203(1-2), 71–85.
19. Dreimann, J., Vorholt, A. J., Skiborowski, M., & Behr, A. (2016). Removal of Homogeneous Precious Metal Catalysts via Organic Solvent Nanofiltration. *Chemical Engineering Transactions*, 47, 343–348.
20. Vanherck, K., Koeckelberghs, G., & Vankelecom, I. F. J. (2013). Crosslinking polyimides for membrane applications: A review. *Progress in Polymer Science*, 38(6), 874–896.

21. See Toh, Y. H., Lim, F. W., & Livingston, A. G. (2007). Polymeric membranes for nanofiltration in polar aprotic solvents. *Journal of Membrane Science*, 301(1-2), 3–10.
22. Dutczak, S. M., Cuperus, F. P., Wessling, M., & Stamatialis, D. F. (2013). New crosslinking method of polyamide-imide membranes for potential application in harsh polar aprotic solvents. *Separation and Purification Technology*, 102, 142–146.
23. Hendrix, K., Koeckelberghs, G., & Vankelecom, I. F. J. (2014). Study of phase inversion parameters for PEEK-based nanofiltration membranes. *Journal of Membrane Science*, 452, 241–252.
24. da Silva Burgal, J., Peeva, L. G., Kumbharkar, S., & Livingston, A. (2015). Organic solvent resistant poly(ether-ether-ketone) nanofiltration membranes. *Journal of Membrane Science*, 479, 105–116.
25. Holda, A. K., Aernouts, B., Saeys, W., & Vankelecom, I. F. J. (2013). Study of polymer concentration and evaporation time as phase inversion parameters for polysulfone-based SRNF membranes. *Journal of Membrane Science*, 442, 196–205.
26. Darvishmanesh, S., Jansen, J. C., Tasselli, F., Tocci, E., Luis, P., Degrève, J., Van der Bruggen, B. (2011). Novel polyphenylsulfone membrane for potential use in solvent nanofiltration. *Journal of Membrane Science*, 379(1-2), 60–68.
27. Hołda, A. K., & Vankelecom, I. F. J. (2014). Integrally skinned PSf-based SRNF-membranes prepared via phase inversion-Part A: Influence of low molecular weight additives. *Journal of Membrane Science*, 450, 499–511.
28. Hołda, A. K., & Vankelecom, I. F. J. (2014). Integrally skinned PSf-based SRNF-membranes prepared via phase inversion-Part B: Influence of low molecular weight additives. *Journal of Membrane Science*, 450, 499–511.
29. Jansen, J. C., Darvishmanesh, S., Tasselli, F., Bazzarelli, F., Bernardo, P., Tocci, E., Van der Bruggen, B. (2013). Influence of the blend composition on the properties and separation performance of novel solvent resistant polyphenylsulfone/polyimide. nanofiltration membranes. *Journal of Membrane Science*, 447, 107–118.

30. Chisca, S., Falca, G., Musteata, V. E., Boi, C., & Nunes, S. P. (2017). Crosslinked polytriazole membranes for organophilic filtration. *Journal of Membrane Science*, 528(October 2016), 264–272.
31. Pulido, B. A., Waldron, C., Zolotukhin, M. G., & Nunes, S. P. (2017). Porous polymeric membranes with thermal and solvent resistance. *Journal of Membrane Science*, 539(April), 187–196.
32. Aburabie, J., & Peinemann, K. V. (2017). Crosslinked poly(ether block amide) composite membranes for organic solvent nanofiltration applications. *Journal of Membrane Science*, 523(August 2016), 264–272.
33. Yuan, S., Wang, J., Li, X., Zhu, J., Volodine, A., Wang, X., ... Van der Bruggen, B. (2018). New promising polymer for organic solvent nanofiltration: Oxidized poly(arylene sulfide sulfone). *Journal of Membrane Science*, 549(October 2017), 438–445.
34. Siddique, H., Rundquist, E., Bhole, Y., Peeva, L. G., & Livingston, A. G. (2014). Mixed matrix membranes for organic solvent nanofiltration. *Journal of Membrane Science*, 452, 354–366.
35. Patterson, D. A., Havill, A., Costello, S., See-Toh, Y. H., Livingston, A. G., & Turner, A. (2009). Membrane characterisation by SEM, TEM and ESEM: The implications of dry and wetted microstructure on mass transfer through integrally skinned polyimide. nanofiltration membranes. *Separation and Purification Technology*, 66(1), 90-97.
36. Van Der Bruggen, B., Schaep, J., Wilms, D., & Vandecasteele, C. (1999). Influence of molecular size, polarity and charge on the retention of organic molecules by nanofiltration. *Journal of Membrane Science*, 156(1), 29–41.
37. Yang, X. J., Livingston, A. G., & Freitas Dos Santos, L. (2001). Experimental observations of nanofiltration with organic solvents. *Journal of Membrane Science*, 190(1), 45–55.

38. Geens, J., Hillen, A., Bettens, B., Van der Bruggen, B., & Vandecasteele, C. (2005). Solute transport in non-aqueous nanofiltration: Effect of membrane material. *Journal of Chemical Technology and Biotechnology*, 80(12), 1371–1377.
39. Ben Soltane, H., Roizard, D., & Favre, E. (2016). Study of the rejection of various solutes in OSN by a composite polydimethylsiloxane membrane: Investigation of the role of solute affinity. *Separation and Purification Technology*, 161, 193–201.
40. Bhanushali, D., Kloos, S., & Bhattacharyya, D. (2002). Solute transport in solvent-resistant nanofiltration membranes for non-aqueous systems: experimental results and the role of solute-solvent coupling. *Journal of Membrane Science*, 208, 343–359.
41. Darvishmanesh, S., Degrève, J., & Van der Bruggen, B. (2010). Mechanisms of solute rejection in solvent resistant nanofiltration: the effect of solvent on solute rejection. *Physical Chemistry Chemical Physics*, 12(40), 13333.
42. Zeidler, S., Kätzel, U., & Kreis, P. (2013). Systematic investigation on the influence of solutes on the separation behavior of a PDMS membrane in organic solvent nanofiltration. *Journal of Membrane Science*, 429, 295–303.
43. Postel, S., Spalding, G., Chirnside, M., & Wessling, M. (2013). On negative retentions in organic solvent nanofiltration. *Journal of Membrane Science*, 447, 57–65.
44. Marchetti, P., Peeva, L., & Livingston, A. (2017). The Selectivity Challenge in Organic Solvent Nanofiltration: Membrane and Process Solutions. *Annual Review of Chemical and Biomolecular Engineering*, 8(1), 473–497.
45. Bhanushali, D., Kloos, S., Kurth, C., & Bhattacharyya, D. (2001). Performance of solvent-resistant membranes for non-aqueous systems: Solvent permeation results and modeling. *Journal of Membrane Science*, 189(1), 1–21.
46. Volkov, A., Yushkin, A., Kachula, Y., Khotimsky, V., & Volkov, V. (2014). Application of negative retention in organic solvent nanofiltration for solutes fractionation. *Separation and Purification Technology*, 124, 43–48.

47. Liebert, T., 2010, "Cellulose solvents-remarkable history, bright future", ACS Symposium Series, 1033, 3-54.
48. Pinkert, A., Marsh, K., Pang, S., & Staiger, M. (2009). Ionic Liquids and Their Interaction with Cellulose. *Chemical Reviews*, 109(12), 6712-6728.
49. X. L. Li, L. P. Zhu, B. K. Zhu, and Y. Y. Xu, "High-flux and anti-fouling cellulose nanofiltration membranes prepared via phase inversion with ionic liquid as solvent," *Sep. Purif. Technol.*, vol. 83, no. 1, pp. 66–73, 2011.
50. Chen, H., Wang, N., & Liu, L. (2012). Regenerated cellulose membrane prepared with ionic liquid 1-butyl-3-methylimidazolium chloride as solvent using wheat straw. *Journal of Chemical Technology & Biotechnology*, 87(12), 1634-1640.
51. Ma, B., Qin, A., Li, X., & He, C. (2013). Preparation of Cellulose Hollow Fiber Membrane from Bamboo Pulp/1-Butyl-3-Methylimidazolium Chloride/Dimethylsulfoxide System. *Industrial & Engineering Chemistry Research*, 52(27), 9417-9421.
52. Anokhina, T. S., Yushkin, A. A., Makarov, I. S., Ignatenko, V. Y., Kostyuk, A. V., Antonov, S. V., & Volkov, A. V. (2016). Cellulose composite membranes for nanofiltration of aprotic solvents. *Petroleum Chemistry*, 56(11), 1085-1092.
53. Anokhina, T. S., Yushkin, A. A., Makarov, I. S., Ignatenko, V. Y., Antonov, S. V., & Volkov, A. V. (2017). Fabrication of composite nanofiltration membranes from cellulose solutions in a [EMIM]OAc-DMSO mixture, *Petroleum Chemistry*, 57(6), 477-482.
54. Zhou, Y. J., Luner, P., & Caluwe, P. (1995). Mechanism of crosslinking of papers with polyfunctional carboxylic acids. *Journal of Applied Polymer Science*, 58(9), 1523-1534.
55. Yang, C. Q., & Xu, Y. (1998). Paper wet performance and ester crosslinking of wood pulp cellulose by poly(carboxylic acid)s. *Journal of Applied Polymer Science*, 67(4), 649-658.].

56. Li, W., Xu, X., Chen, S., Zhou, X., Li, L., Chen, D., Wang, X., 2008, "Esterification crosslinking structures of rayon fibers with 1,2,3,4-butanetetracarboxylic acid and their water-responsive properties", *Carbohydrate Polymers*, 71 (4), 574-582.
57. Lund, K., Brelid, H., 2013, "Kinetics of cross-linking softwood kraft pulp with 1,2,3,4- butanetetracarboxylic acid", *Industrial and Engineering Chemistry Research*, 52 (33), 11502-11509.
58. Wang Y., Hsiegh YL. Cellulose functionalization by glutaraldehyde, 42(1), 2001, 520-1.
59. Kim, K., Lee, S., & Han, N. W. (1993). Effects of the Degree of Crosslinking on Properties of Poly(vinyl alcohol) Membranes. *Polym J*, 25(12), 1295-1302.
60. Kim, K., Lee, S., & Han, N. (1994). Kinetics of crosslinking reaction of PVA membrane with glutaraldehyde. *Korean Journal of Chemical Engineering*, 11(1), 41-47.
61. Brown, E. E., Laborie, M. G., & Zhang, J. (2011). Glutaraldehyde treatment of bacterial cellulose/fibrin composites: impact on morphology, tensile and viscoelastic properties. *Cellulose*, 19(1), 127-137.
62. Durmaz, E. N., & Zeynep Çulfaz-Emecen, P. (2018). Cellulose-based membranes via phase inversion using [EMIM]OAc-DMSO mixtures as solvent. *Chemical Engineering Science*, 178, 93-103.
63. Sukma, F., & Çulfaz-Emecen, P. (2018). Cellulose membranes for organic solvent nanofiltration. *Journal of Membrane Science*, 545, 329-336.
64. Da Silva Burgal, J., Peeva, L., Marchetti, P., & Livingston, A. (2015). Controlling molecular weight cut-off of PEEK nanofiltration membranes using a drying method. *Journal of Membrane Science*, 493, 524-538.
65. Volkov, A., Stamatialis, D., Khotimsky, V., Volkov, V., Wessling, M., & Plate, N. (2006). Poly[1-(trimethylsilyl)-1-propyne] as a solvent resistance nanofiltration membrane material. *Journal of Membrane Science*, 281(1-2), 351-357.

66. Newcomb, L. F., & Gellman, S. H. (1994). Aromatic Stacking Interactions in Aqueous Solution: Evidence That neither Classical Hydrophobic Effects nor Dispersion Forces Are Important. *Journal of the American Chemical Society*, 116(11), 4993-4994.
67. Ben Soltane, H., Roizard, D., & Favre, E. (2016). Study of the rejection of various solutes in OSN by a composite polydimethylsiloxane membrane: Investigation of the role of solute affinity. *Separation and Purification Technology*, 161, 193-201.
68. Robinson, J. P., Tarleton, E. S., Millington, C. R., & Nijmeijer, A. (2004). Evidence for swelling-induced pore structure in dense PDMS nanofiltration membranes. *Filtration*, 4(1), 50-56.
69. Xu, GG., Young C., Deng Y. (2004). Combination of bifunctional aldehydes and poly(vinyl alcohol) as the crosslinking systems to improve paper weat strength. *Journal Applied Polymer Science*, 93(4), 1673-80.
70. NIST XPS Database, Spectrum Search Menu. (2012, September 15).
71. Priske, M., Lazar, M., Schnitzer, C., & Baumgarten, G. (2015). Recent Applications of Organic Solvent Nanofiltration. *Chemie Ingenieur Technik*, 88(1-2), 39-49.

APPENDICES

APPENDIX A

CALIBRATION CURVES

A. CALIBRATIONS OF DYE-ETHANOL SOLUTION

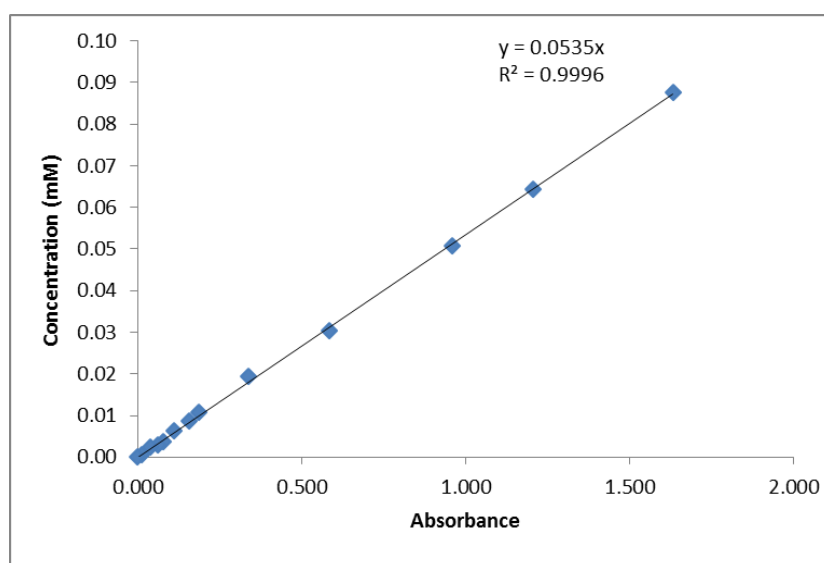


Figure 58: Calibration curve for Bromothymol Blue-Ethanol solution at 423 nm

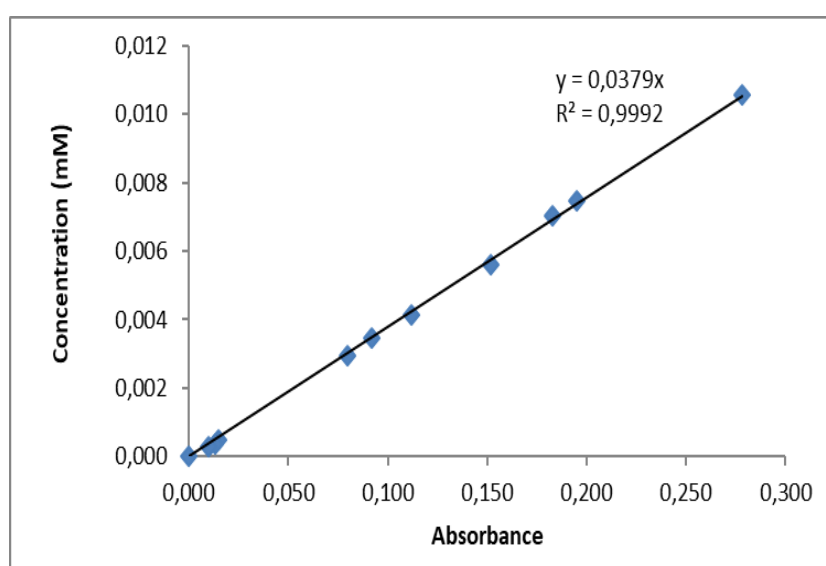


Figure 59: Calibration curve for Cresol Red-Ethanol solution at 432 nm

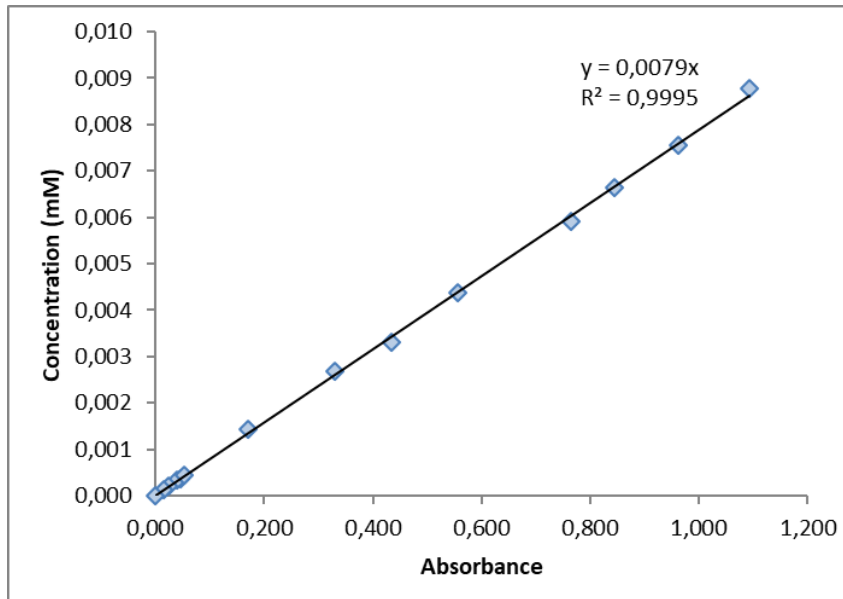


Figure 60: Calibration curve for Brilliant Blue R-Ethanol solution at 588 nm

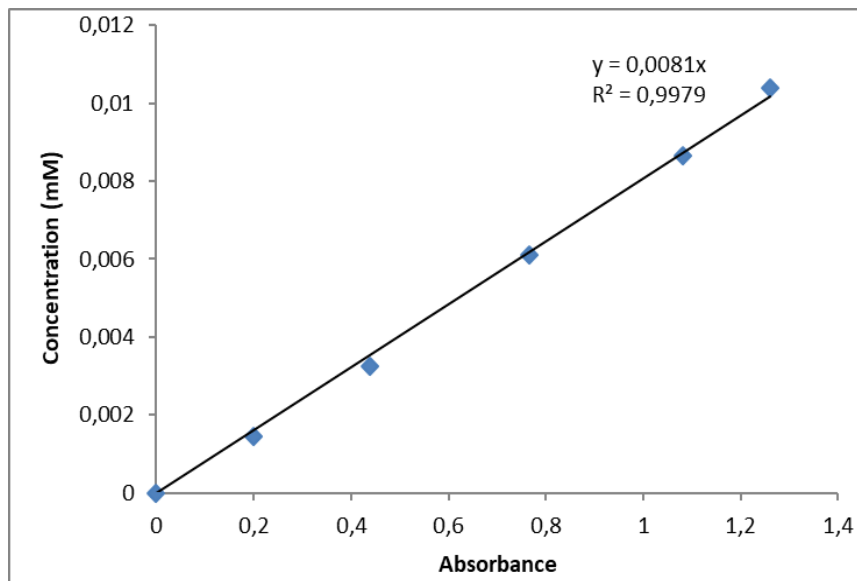


Figure 61: Calibration curve for Rose Bengal-Ethanol solution at 560 nm

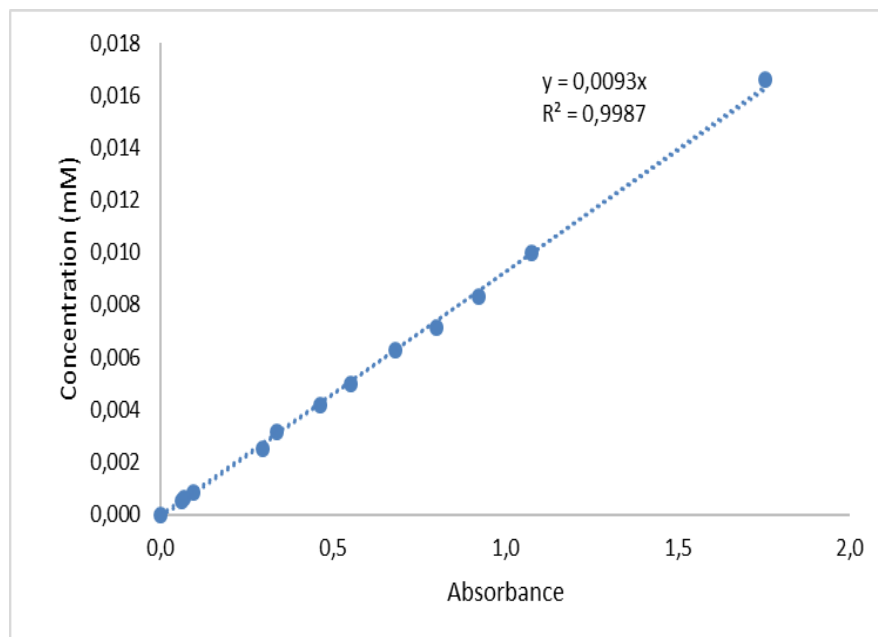


Figure 62: Calibration curve for Crystal Violet-Ethanol solution at 590 nm

B. CALIBRATIONS OF DYE-DMSO SOLUTION

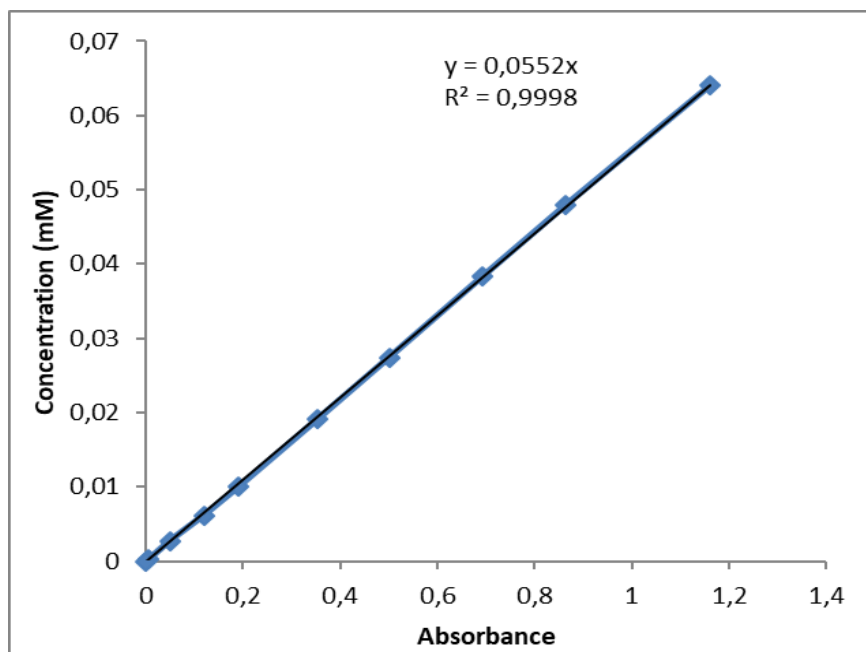


Figure 63: Calibration curve for Bromothymol Blue-DMSO solution at 413 nm

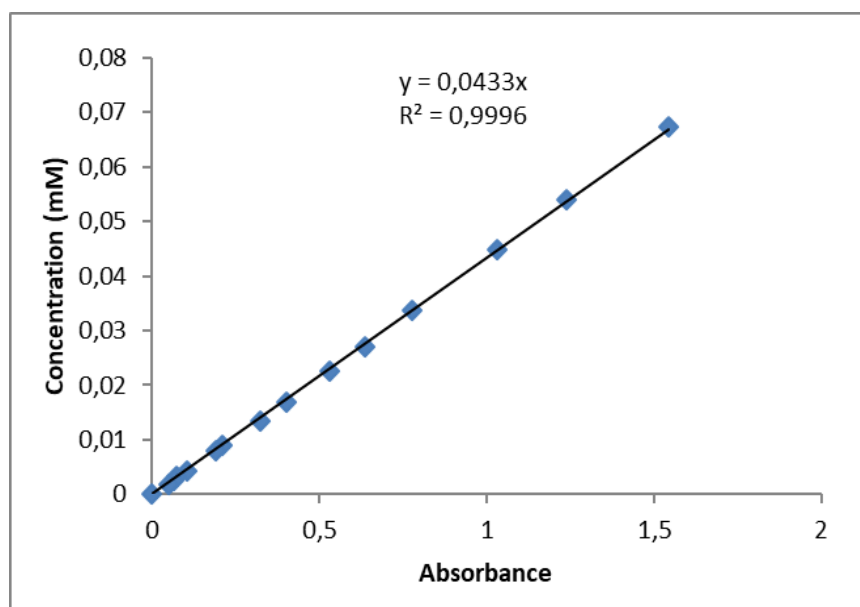


Figure 64: Calibration curve for Crystal Violet-DMSO solution at 308.5 nm

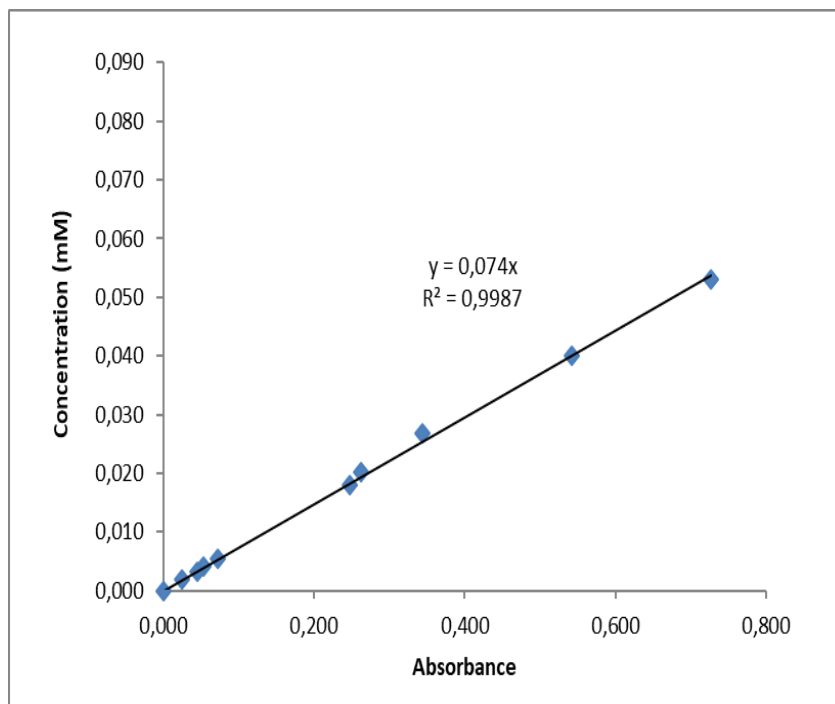


Figure 65: Calibration curve for Rose Bengal-DMSO solution at 566 nm

C. CALIBRATIONS OF JACOBSEN-SOLVENT SOLUTIONS

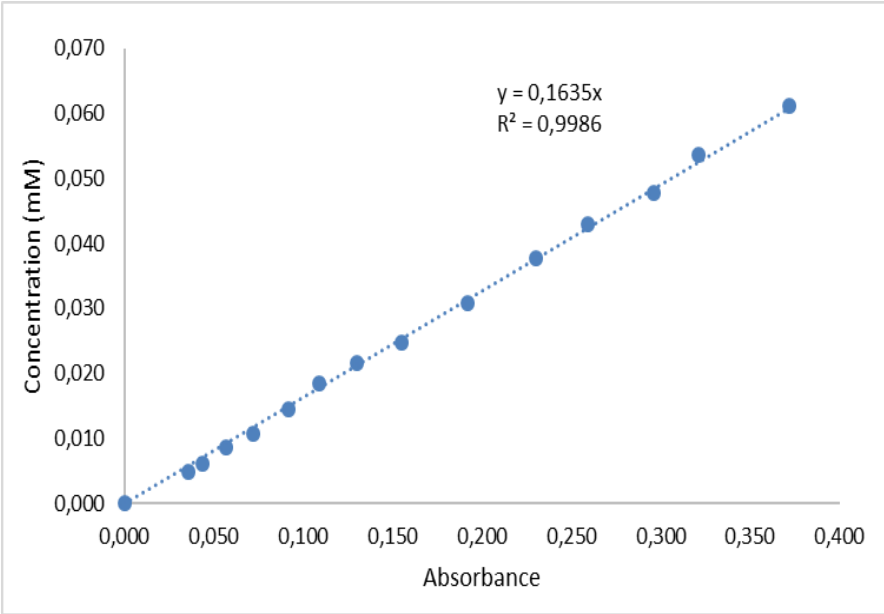


Figure 66: Calibration curve for Jacobsen-Ethanol solution at 416 nm

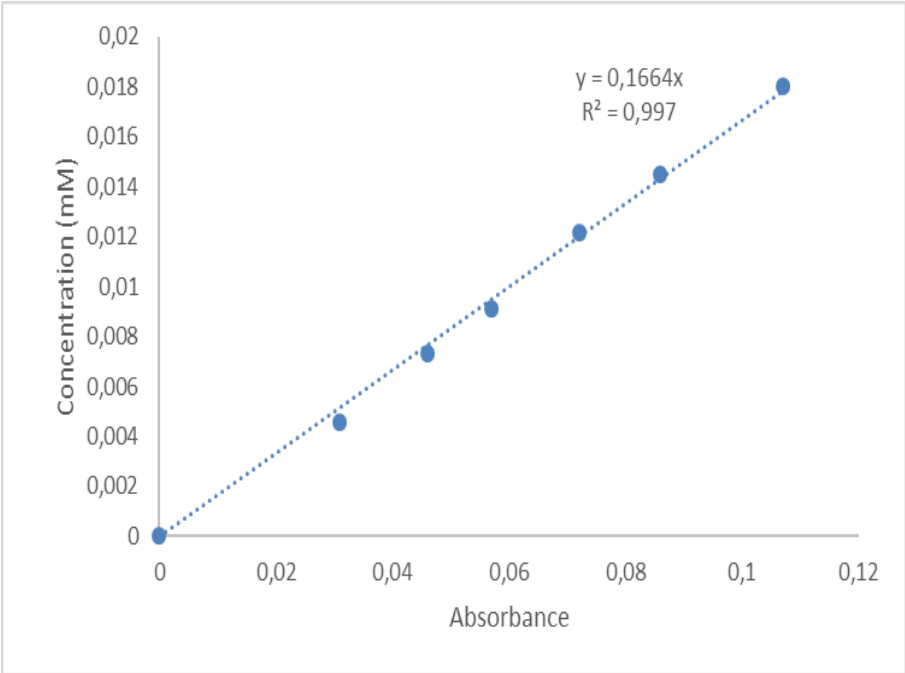


Figure 67: Calibration curve for Jacobsen-DMSO solution at 415 nm

APPENDIX B

REJECTION CALCULATION

Material balance:

$$C_{(F,1)} \times V_{(F,1)} - C_{(P,1)} \times V_{(P,1)} - C_{(R,1)} \times V_{(R,1)} = 0$$

$\checkmark \quad \checkmark \quad \checkmark \quad \checkmark \quad \checkmark$

$$C_{(F,2)} \times V_{(F,2)} - C_{(P,2)} \times V_{(P,2)} - C_{(R,2)} \times V_{(R,2)} = 0$$

$\checkmark \quad \checkmark \quad \checkmark \quad \checkmark \quad \checkmark$

.

.

$$C_{(F,f)} \times V_{(F,f)} - C_{(P,f)} \times V_{(P,f)} - C_{(R,f)} \times V_{(R,f)} = 0$$

$\checkmark \quad \checkmark \quad \checkmark \quad \checkmark \quad \checkmark$

- If, $C_{(R,f)}$ (calculated) < $C_{(R,f)}$ (found by UV)

Sorption on the membrane surface still continues, then another set is done.

- If, $C_{(R,f)}$ (calculated) \cong $C_{(R,f)}$ (found by UV), then sorption reached zero.

In dead-end mode filtration, retentate concentration cannot measure instantaneously, it is measured at the end of the filtration for once. Therefore, for rejection calculation this way mentioned above was followed. The amount of initial feed, permeate and remaining retentate were known. Concentrations of this initial feed and all permeate were also measured by UV, so retentate concentration can be obtained from material balance, and this retentate is going to be our next feed. At the end of filtration final retentate concentration was measured by UV and it was calculated from material balance. For first runs of filtration, these concentrations are not equal to each other, mostly calculated one was smaller than measured by UV which implies that there is accumulation/sorption of dye on membrane. This amount of sorbed dye in membrane was calculated from material balances with known concentrations and amounts.

The amount of dye sorbed in membrane = $C_F \times V_F - \sum(C_P \times V_P) - C_R \times V_R$

Filtrations were performed until the amount of sorbed in membrane reached zero. To obtain the actual rejection values back calculation was done which means calculation from last known retentate concentration to feed concentration was done. By this way, the sorption effect on membrane was eliminated.

APPENDIX C

CROSS-FLOW FILTRATION OF JACOBSEN-DMSO SOLUTION WITH BTCA CROSSLINKED MEMBRANE

The separation performance of BTCA crosslinked membrane was studied with Jacobsen-DMSO solution in crossflow filtration at 1.8 bar, 30 rpm (Figure 68).

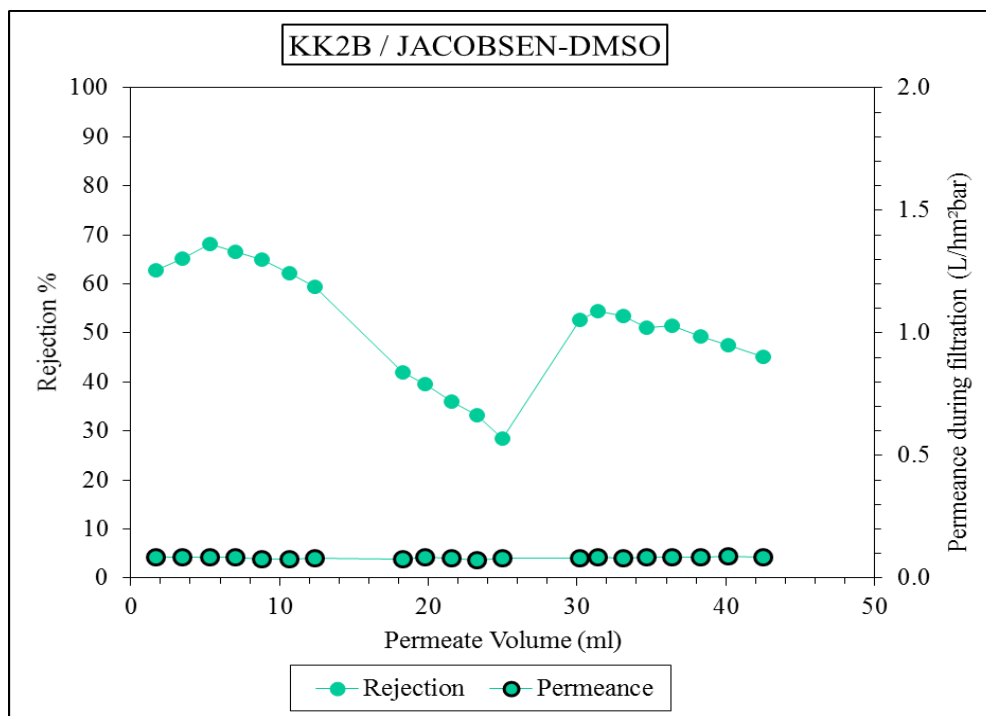


Figure 68: KK2B Jacobsen catalyst separation performance from its DMSO solution

This filtration took three days to achieve constant rejection value of catalyst with the constant permeance of the membrane. The rejection continued to decrease during the filtration and at the end of third day constant rejection was not achieved. Low rejection of the catalyst from its DMSO solution can be attributed the high extent swelling of membrane in DMSO. It was known that produced cellulose membranes were stable at different harsh organic solvents and have very low swelling degree in these solvents like ethanol. Therefore, the recovery of the homogenous catalyst from other harsh solvents at the high ratio can be promising.

